AD-A172 692 CHARACTERIZATION OF INFRARED PROPERTIES OF LAYER SEMICONDUCTORS(U) CALIFORNIA UNIV LOS ANGELES DEPT OF PHYSICS R BRAUNSTEIN 08 AUG 86 AFOSR-TR-86-0861 1/2

UNCLASSIFIED AFOSR-83-0169 F/G 7/4 NL

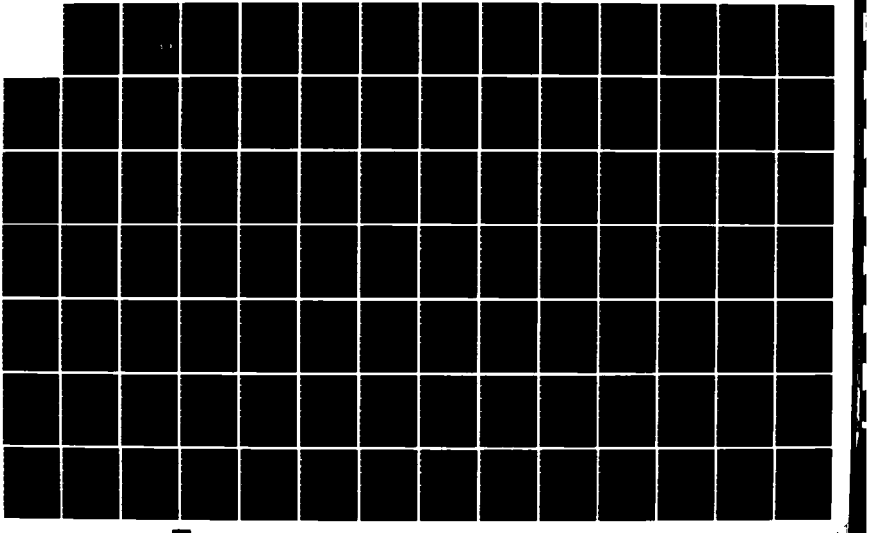

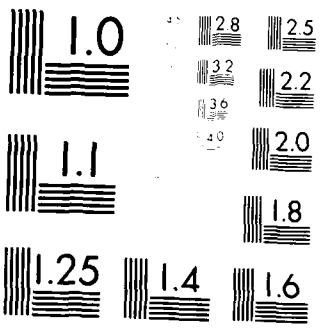

SECURITY CLASSIFICATION OF THIS PAGE (When Data Entered)

REPORT DOCUMENTATION PAGE		READ INSTRUCTIONS BEFORE COMPLETING FORM
1. REPORT NUMBER AFOSR-TR. 86-0861 Annual Scientific Report	2. GOVT ACCESSION NO.	3. RECIPIENT'S CATALOG NUMBER
4. TITLE (and Subtitle) Characterization of Infrared Properties of Layer Semiconductors		5. TYPE OF REPORT & PERIOD COVERED Annual Scientific Report 5/1/84 - 8/31/85
		6. PERFORMING ORG. REPORT NUMBER
7. AUTHOR(s) Rubin Braunstein		8. CONTRACT OR GRANT NUMBER(s) AFOSR 83-0169
9. PERFORMING ORGANIZATION NAME AND ADDRESS Department of Physics University of California, Los Angeles, 90024		10. PROGRAM ELEMENT, PROJECT, TASK AREA & WORK UNIT NUMBERS 61102F 2306/B1
11. CONTROLLING OFFICE NAME AND ADDRESS Air Force Office of Scientific Research, Bolling Air Force Base, D.C. 20332		12. REPORT DATE 8/8/86
		13. NUMBER OF PAGES 126
14. MONITORING AGENCY NAME & ADDRESS(if different from Controlling Office) Same as 11 NE		15. SECURITY CLASS. (of this report)
		15a. DECLASSIFICATION/DOWNGRADING SCHEDULE

16. DISTRIBUTION STATEMENT (of this Report)

Approved for public release; distribution unlimited.

17. DISTRIBUTION STATEMENT (of the abstract entered in Block 20, if different from Report)

Approved for public release; distribution unlimited.

18. SUPPLEMENTARY NOTES

19. KEY WORDS (Continue on reverse side if necessary and identify by block number)

GaAs
Infrared Wavelength Modulation
Photo-Induced Transients
Raman Scattering
Photo-Mixing
Deep Levels
Depletion Layers
High Field Mobility

20. ABSTRACT (Continue on reverse side if necessary and identify by block number)

Infrared wavelength modulation absorption spectroscopy was employed in the spectral range of 0.3-1.45 eV to study deep level impurities in undoped semi-insulating GaAs grown by the liquid encapsulated Czochralski technique. The sensitivity of the measurements allow us to give credence to changes in absorption at levels of $10^{-3}cm^{-1}$. The measurements reveal two resonant type peaks with fine structures near 0.39 and 0.40 eV as well as plateaus and thresholds at higher energy. The absorption band at

DD FORM 1 JAN 73 1473

SECURITY CLASSIFICATION OF THIS PAGE (When Data Entered)

0.37 eV is interpreted as due to the intra-center transition between levels of accidental iron impurity. The absorption band near 0.40 eV can be annealed out by heat treatment and is characterized as belonging to a structural multi-level defect complex. Photo-induced-transient-spectroscopy technique also reveal out annealable level at 0.42 eV. Raman backscattering was employed to measure the shift in the frequency of unscreened and screened phonon-plasma mode in GaAs in a study of the change in the surface depletion layer widths due to various surface treatments. A technique of photo-mixing was employed to measure the drift velocities in the hot carrier small distance regimes in GaAs.

Characterization of Infrared Properties of Layer Semiconductors

Contract: AFOSR 83-0169

Annual Scientific Report

for Period: 5/1/84 - 8/31/85

Submitted to:

Air Force Office of Scientific Research

Bolling Air Force Base, D.C. 20332

Prepared by:

Rubin Braunstein

Department of Physics

University of California at Los Angeles

Table of Contents

I. OBJECTIVES OF PROGRAM

The broad objectives of this program are to extend our understanding of the electrical properties of layered semiconductors of interest to low noise amplification, generation, and detection of high frequency radiation utilizing GaAs, InP, and III-V alloys in large scale integrated technologies. The present program is concerned with the development and utilization of non-contract methods for the assessment of impurities, defects, homogeneity of doping, and characterization of surfaces and interfaces employing electromagnetic and electronic techniques. The experimental and theoretical approaches of this research program utilizes the techniques of infrared wavelength modulation, photo-induced-transient spectroscopy, photo-mixing, and Raman backscattering to investigate a number of closely related areas of semiconductor physics to characterize compound semiconductor and heterostructures which are relevant to high frequency and low noise device application. The interactions studied have a direct bearing on dimensionally confined structures that will determine the properties of ultra-small electronic devices.

The following are specific areas of research that were emphasized during this period:

A. Wavelength modulation techniques are employed to study deep levels in semiconductors.

B. Photo-induced-transient spectroscopy techniques for studying deep levels.

C. Raman scattering measurements were performed to determine surface strain and carrier concentration and surface space charge layers.

D. Photo-mixing techniques were employed to study hot-carriers drift velocities.

II. STATUS OF RESEARCH

During this reporting period, we have continued to study the semiconductor physics of deep levels and interfaces of GaAs relevant to high-frequency low-noise devices. The techniques of infrared wavelength modulation absorption, photo-induced-transient spectroscopy, Raman scattering, and photo-mixing techniques were employed at the appropriate stages of programmatic developments. In the following discussion of the status of the research, we shall use the format of presenting the problem and indicate what progress has been made.

A. Deep Levels Derivative Absorption Spectroscopy

Problem:

The detection and characterization of deep levels in GaAs and other compound semiconductors due to chemical and structural imperfections remains a scientific and technological challenge for the utilization of these materials for high frequency applications.

Progress:

We have improved our infrared wavelength modulation system which is capable of measuring a change in absorption at levels of 10^{-5} cm^{-1} out of a broad background in the spectral region 0.2-20 microns. Since it is not necessary to make electrical contacts to the samples there is not the possiblity of contamination by thermal processing necessary for DLTS techniques. An overview of the use of our wavelength modulation techniques for the spectroscopic characterization of semiconductor technology problems was presented at the SPIE 1985 Los Angeles Technical Symposium: Spectroscopy

Characterization Techniques for Semiconductor Technology II which was published in Conference Proceedings No. 524. A reprint of this publication is included in the Appendix. The abstract of this paper is as follows:

Deep Level Derivative Spectroscopy of Semiconductor
by Wavelength Modulation Techniques

R. Braunstein, S.M. Eetemadi, and R.K. Kim
Department of Physics, University of California,
Los Angeles, California 90024

An infrared wavelength modulated absorption spectrometer capable of measuring changes in the absorption coefficient of levels of 10^{-5} cm^{-1} in the spectral range 0.2-20 microns was employed to study bulk and surface absorption in semiconductors. The results of the study of deep levels in semi-insulating GaAs, surface layers on Si, GaAs, and HgCdTe, oxygen complexes in floating-zone silicon, and determination of strain in ion implanted layers are presented.

Since undoped semi-insulating GaAs substrates, grown by liquid encapsulated Czochralski are currently being used for the fabrication of high speed GaAs MESFET and integrated circuits, we initiated a detailed study of the deep levels in this material. The ingots for this study were obtained from a single source, the Hughes Research Laboratories, so as to test our techniques on materials that were characterized by ancillary measurements such as Hall and SIMS rather than random samples from diverse sources. Now that this work is complete it is our intention to examine material from other sources involved in the AFOSR GaAs material growth program. This work revealed a number of impurity and structural defects characteristic of this method of crystal growth. A significant multi-level structural complex at 0.40 eV was observed which could be annealed out by heat treatment. In addition, photo-quenching experiments allow us to detect residual impurities in the 0.6-1.4 eV region underlying the EL2 absorption

band. This work has been completed and is being submitted for publication to the Journal of Applied Physics. A copy of this manuscript is enclosed in the Appendix. The abstract of this work reads as follows:

Wavelength Modulation Absorption Spectroscopy of
Deep Levels in Semi-Insulating GaAs

S.M. Eetemadi and R. Braunstein

Department of Physics, University of California
Los Angeles, California 90024

Infrared wavelength modulation absorption spectroscopy was used in the specral region of 0.3-1.45 eV and the temperature range of 80-300K, to study deep level impurities and defects in undoped semi-insulating GaAs grown by the liquid encapsulated Czochralski technique (LEC). The measurements revealed two resonant type peaks with fine structure near 0.37 and 0.40 eV, as well as thresholds and plateaus at higher energies. The sensitivity of the measurements allows us to give credence to changes in the absorption coefficient at levels ~ 10^{-3} cm^{-1}. The absorption band at 0.37 eV is interpreted as being due to the intra-center transition between levels of accidental iron impurity, split by the crystal field. The absorption band near 0.40 eV, can be annealed out by heat treatment, and is considered to belong to a multilevel defect complex. Utilizing the photo-quenching behavior of the absorption in the spectral region of 0.6-1.4 eV, it was shown that conventional room temperature optical absorption may give erroneous results in measuring the concentration of the EL2 levels, because of appreciable absorption due to other residual deep levels in this spectral region, as revealed by the sensitivity of the wavelength modulation technique.

Since conventional optical absorption measurements lack the sensitivity to measure residual absorption overlapping the absorption due to EL2 in the spectral region 0.7-1.4 eV, they can lead to errors in estimating EL2 concentration. We have developed a method involving photo-quenching and wavelength modulation measurements to accurately measure such concentrations. This work has been completed and is being submitted to Applied Physics Letters. A copy of this manuscript is contained in the Appendix. The

abstract reads as follows:

Measurement of the EL2 and Chromium Concentration
in the Semi-Insulating GaAs

S.M. Eetemadi and R. Braunstein

Low temperature infrared wavelength modulation was performed on GaAs in conjunction with the photo-quenching of the absorption in the spectral region of 0.7-1.4 eV, due to the EL2 levels, to assess the accuracy of the conventional room temperature optical absorption spectroscopy in measuring EL2 and chromium concentrations; an accurate method for such measurements was suggested.

In our studies we measure low level absorption using direct wavelength modulation absorption/reflection. Recently wavelength modulation photoresponse spectroscopies have been used to infer absorption. A detailed experimental and theoretical analysis was completed showing that the latter technique as it is presently employed in the literature can contain spurious structures. This work has also been completed and is being submitted to the Journal of Applied Optics; a copy of this manuscript is enclosed in the Appendix, the abstract of which reads:

Re-examination of the Wavelength
Modulation Photoresponse Spectroscopies

S.M. Eetemadi and R. Braunstein

Department of Physics, University of California
Los Angeles, California 90024

Re-examination of the wavelength modulation photoresponse spectroscopies showed that the line shapes obtained by these methods are subject to distortions from several sources of spurious interference spectra. Limitations of these methods in studies of the deep levels and the interband transitions in semiconductors are discussed and a practical method for removal of the distortions due to the background spectra is suggested. Finally, a comparison is made between the wavelength modulation absorption/reflection and

the wavelength modulation photoresponse spectroscopies. It is concluded that the former are the most suitable modulation techniques for the above studies since they yield unambiguous line shapes.

B. Photo-Induced-Transient Spectroscopy of Semi-Insulating (LEC) GaAs

Problem:

Epitaxial growth of semiconductor layers for field-effect transistors (FET's) and electron transfer devices (CCD's) require well characterized semi-insulating substrates. On semi-insulating material it is not possible to use DLTS techniques to study deep levels due to the large depletion layer in such materials.

Progress:

We have employed our computer controlled photo-induced-transient spectrometer (P.I.T.S.) for the study of the electrical manifestation of deep levels in semi-insulating GaAs. A detailed study of the deep levels in LEC GaAs was completed in sections of the same samples that were used for our wavelength modulation measurements so as to obtain a possible correlation between optical absorption and P.I.T.S. measurements. Measurements were performed on samples which had a variety of heat treatments:

1. samples with ohmic contacts applied using an ultra-sonic iron;
2. ion-implanted samples that were given a high temperature anneal and slowly returned to room temperature;
3. rapidly quenched samples from 700K to room temperature.

There was a rich spectrum of deep levels in samples which were not subject to heat treatment. The difference between the as-grown samples and the same sample heat treatment is quite significant. Levels at 0.52, 0.42, and 0.36

eV in as-grown samples which readily anneal out seem to be correlated with the results observed in our wavelength modulation measurements which were identified as structural defects. However, an exact correlation between the levels observed by the wavelength modulation absorption and the levels detected by P.I.T.S. must take into account the fact that the latter essentially yield information on the thermal emission from the level to the band, whereas the former given information about intra-center transitions.

This work has been completed and is being prepared for publication. A draft copy is included in the Appendix. The abstract of this manuscript reads as follows:

Deep Levels in Semi-Insulating, Liquid Encapsulated-Czochralski-Grown GaAs

M.R. Burd and R. Braunstein

Department of Physics, University of California
Los Angeles, California 90024

Using photo-induced-transient spectroscopy in variously heat-treated samples of semi-insulating LEC grown GaAs, we detected seven deep levels. Six of these levels were matched with previously cataogued levels, four of them being hole-like and two being electron-like. The seventh level appears to be associated with a boron-related defect which has previously been seen only as a band in boron-implanted GaAs.

C. Raman Backscattering to Determine Surface Strain and Carrier Concentration

Problem:

Localized ion implantation into semi-insulating GaAs is one of the principal techniques for fashioning junctions and ohmic contacts in GaAs FET devices. In order to have precise control of threshold voltages in such

devices, precise control of the implantation profile is of prime importance. Studies of the redistribution profiles have usually been done by SIMS techniques. It would be desirable to have a nondestructive method of measuring the change in carrier concentration near a surface as well as stress and radiation damage.

Progress:

We have employed Raman backscattering to measure the shift in frequency of the unscreened and screened phonon plasma modes in the depletion layer and the bulk of GaAs as a function of various surface treatments. By observing the changes in the width and the position of the LO phonon in the depletion region, inhomogeneous strains associated with lattice defects can be deferred. In addition, the observation of the TO phonon transition in the scattering configuration employed where it should be forbidden gives a measure of surface structural damage. By studying the shift of the high frequency coupled L^+ mode in the bulk region beyond the depletion layer, it was possible to observe an increase or decrease of the charge carriers near the surface. Raman scattering is proving an excellent nondestructive technique for the study of surface treatment induced strain and changes in surface space charge layers. Measurements are being performed on GaAs, CdTe, and HgCdTe.

D. Determination of Hot-Carrier Drift Velocities by Photo-Mixing

Problem:

The advent of high resolution electons and x-ray lithographic techniques is leading towards an era in which ultra-small-electron devices will be

fabricated at the submicron level. In this spatial regime, size and related effects may be as important as the bulk properties of the host materials. Questions are arising whether classical device models may be extrapolated down to very small space and time scales usually encountered in sub-micron devices. At the smallest sizes ~ a few hundred Å, one does not know the extent to which conventional effective mass theories can be scaled down. In addition, the collisions acting on carriers cannot be assumed to occur instantaneously in space and time. In the sizes down to 0.1-0.5 μm the transport physics may still be based on the Boltzmann transport equation, but even for this type of device new physical phenomena became possible. These include overshoot velocity, ballistic transport, wider distribution of the carrier energy due to the existence of a transverse electric field in a depletion or inversion layer, and the effects of surface and interface scattering. In multi-valley semiconductors, optical excitation coupled with high electric fields can result in novel relaxation time shifts in the carrier distribution function.

Progress:

We have employed a technique of photo-mixing to measure drift velocities in the hot carrier small distance regimes. The method consists in frequency mixing two monochromatic optical frequencies in a semiconductor to generate a difference frequency whose power is determined by the mobility and lifetime of the material. We have previously studied photo-mixing in wide contact (of the order of mm's) bulk GaAs, Si, and Ge and showed that one can measure the saturation drift velocity and the temperature dependent mobility by this technique.

During the present period we have initiated measurements on GaAs with narrow gap contact. We ultimately expect to extend these measurements to sub-

micron structures, but for the present we have performed photo-mixing measurements in 6, 12, and 18 micron gaps as a function of electric field. Figures 1 and 2 show the mixing power, photo-current, and dark current as a function of electric field in 18 and 12 micron gaps. The smooth peaking of these quantities are indicative that we are reaching the saturation drift velocities. However, in Fig. 2 for the 12 micron gap structure begins to develop in the mixing signal, while the dark current and photo-current show no such structure. In Fig. 3 for a 6 micron gap more distinct structure develops in the mixing signal. Also in Fig. 3 we have plotted the derived quantities of effective mobility μ^* and effect velocity v^* calculated from the microwave power using the photo-mixing theory. The emergence of structure in μ^* and v^* as the dimensions are reduced indicates that we are beginning to see energy dependent scattering mechanisms. These measurements were performed at room temperature and will shortly be repeated as a function of temperature.

In the above measurements the magnitude of the mixing power is proportional to the square of the carrier mobility. Measurements were performed using the longitudinal modes of an Argon laser as well as a He-Ne laser and revealed that the mixing signal was dependent upon the penetration depth of the light. We plan to continue photo-mixing to the transport in small structures. At present we are performing measurements on 1, 2, 6, 12, 18 micron gap structures with $10^{17}/cm^3$ carrier concentration kindly supplied by Prof. Markoc of the University of Illinois. In view of the surprising emergence of structures in μ^* and v^* in such "gross" gaps we will continue measurements in this spatial region on undoped substrates to distinguis intrinsic and extrinsic scattering mechanism. In addition we plan to extend these measurements in the sub-micron regime.

III. PUBLICATIONS

The following are the published work or in preparation for publication:

1. "Deep Level Derivative Spectroscopy of Semiconductors by Wavelength Modulation Techniques," R. Braunstein, S.M. Eetemadi, and R.K. Kim, SPIE vol. 524 Spectroscopic Characterization Technique for Semiconductor Technology II (1985).

2. "Wavelength Modulation Absorption of Deep Levels in Semi-Insulating GaAs," S.M. Eetemadi and R. Braunstein (submitted to the Journal of Applied Physics).

3. "Re-Examination of the Wavelength Modulation Photo-response Spectroscopies," S.M. Eetemadi and R. Braunstein (submitted to the Journal of Applied Optics).

4. "Measurements of the EL2 and Chromium Concentration in Semi-Insulating GaAs," S.M. Eetemadi and R. Braunstein (submitted to Applied Physics Letters).

5. "Deep Levels in Semi-Insulating Liquid-Encapsulated-Czochralski GaAs," M.R. Burd and R. Braunstein (in preparation for submission to the Journal of Physics and Chemistry of Solids).

6. "Raman Scattering of the Sub-Surface of GaAs," R. Martin and R. Braunstein (in preparation for submission of the Journal of Vacuum Technology).

IV. PARTICIPATING SCIENTIFIC PERSONNEL

R. Braunstein	Principal Investigator
M. Burd	Ph.D. Candidate
B. Dorfman	Post Doctoral, participating with the group but supported by an NIH fellowship
M. Eetemadi	Ph.D. Candidate
R. Martin	Ph.D. Candidate
A. Melo	Post Doctoral

V. SCIENTIFIC INTERACTIONS

Communication was developed with materials synthesis groups at the Hughes Research Laboratory, Watkins and Johnson and the Avionics Laboratory at Wright-Paterson Airforce Base. These interactions included exchange of sample and technical discussion of the U.C.L.A. group's results. Photo-mixing measurements were performed on structures fabricated by Prof. Markoc's group at the University of Illinois. A seminar on Raman scattering from GaAs was given at the Watkins and Johnson Corp. at Palo Alto, California in June, 1984; discussions were had with Dr. Don Deal regarding plasma treatment of GaAs surfaces. An invited paper: "Deep Level Derivative Spectroscopy by Wavelength Modulation Techniques" was presented at the S.P.I.E. 1985 Los Angeles Technical Symposium: Spectroscopy Characterization Technique for Semiconductor Technology II.

Fig 1. Photo-mixing signal, photo-current, and dark current in a 18 micron gap on GaAs as a function of electric field at 251 MHZ using He-Ne longitudinal modes.

Fig. 2. Photo-mixing signal, photo-current, and dark current in a 12 micron gap on GaAs as a function of electric field at 251 MHZ using He-Ne longitudinal modes.

Fig3. Photo-mixing signal and derived effective mobility, μ^*, and effective velocity v^* in a 6 micron gap as a function of electric field at 251 MHZ using He-Ne longitudinal modes.

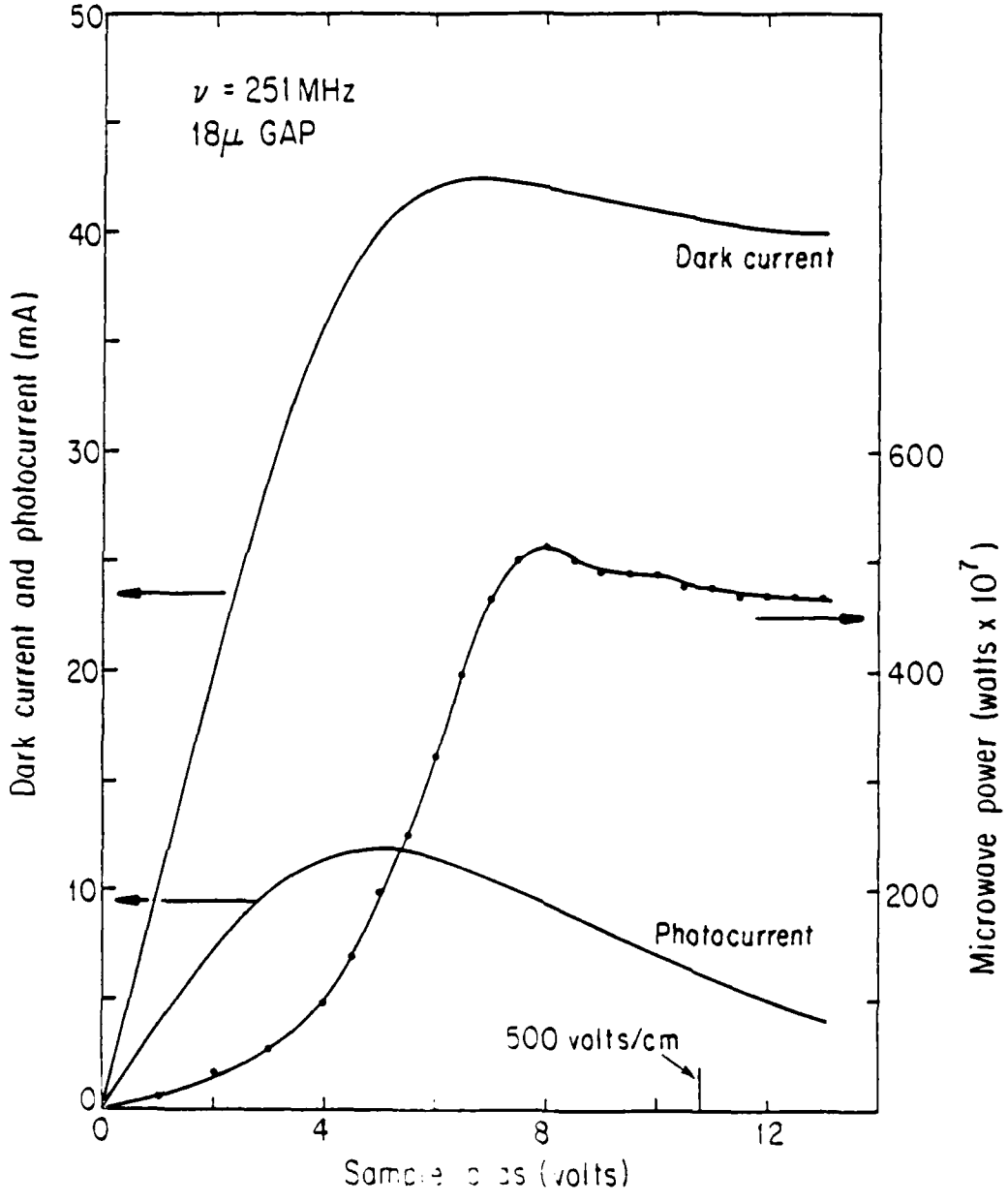
ν = 251 MHz
18μ GAP
Dark current
Photocurrent
500 volts/cm
Dark current and photocurrent (mA)
Microwave power (watts x 10^7)
Sample bias (volts)
0
10
20
30
40
50
200
400
600
0
4
8
12

Fig. 1

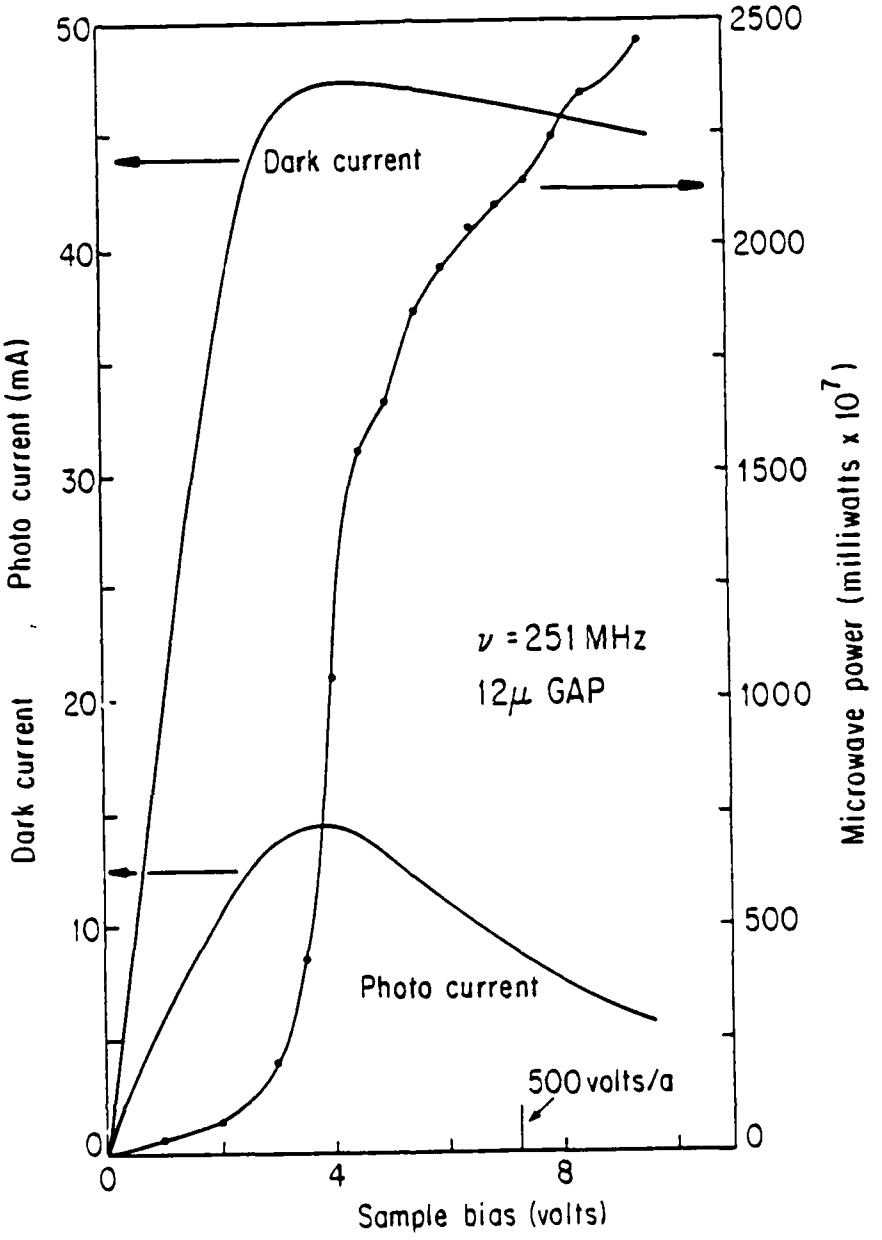
50
40
30
20
10
0
2500
2000
1500
1000
500
0
Dark current
Photo current (mA)
Microwave power (milliwatts x 10^{-7})
Dark current
ν = 251 MHz
12μ GAP
Photo current
500 volts/a
0
4
8
Sample bias (volts)

Fig. 2

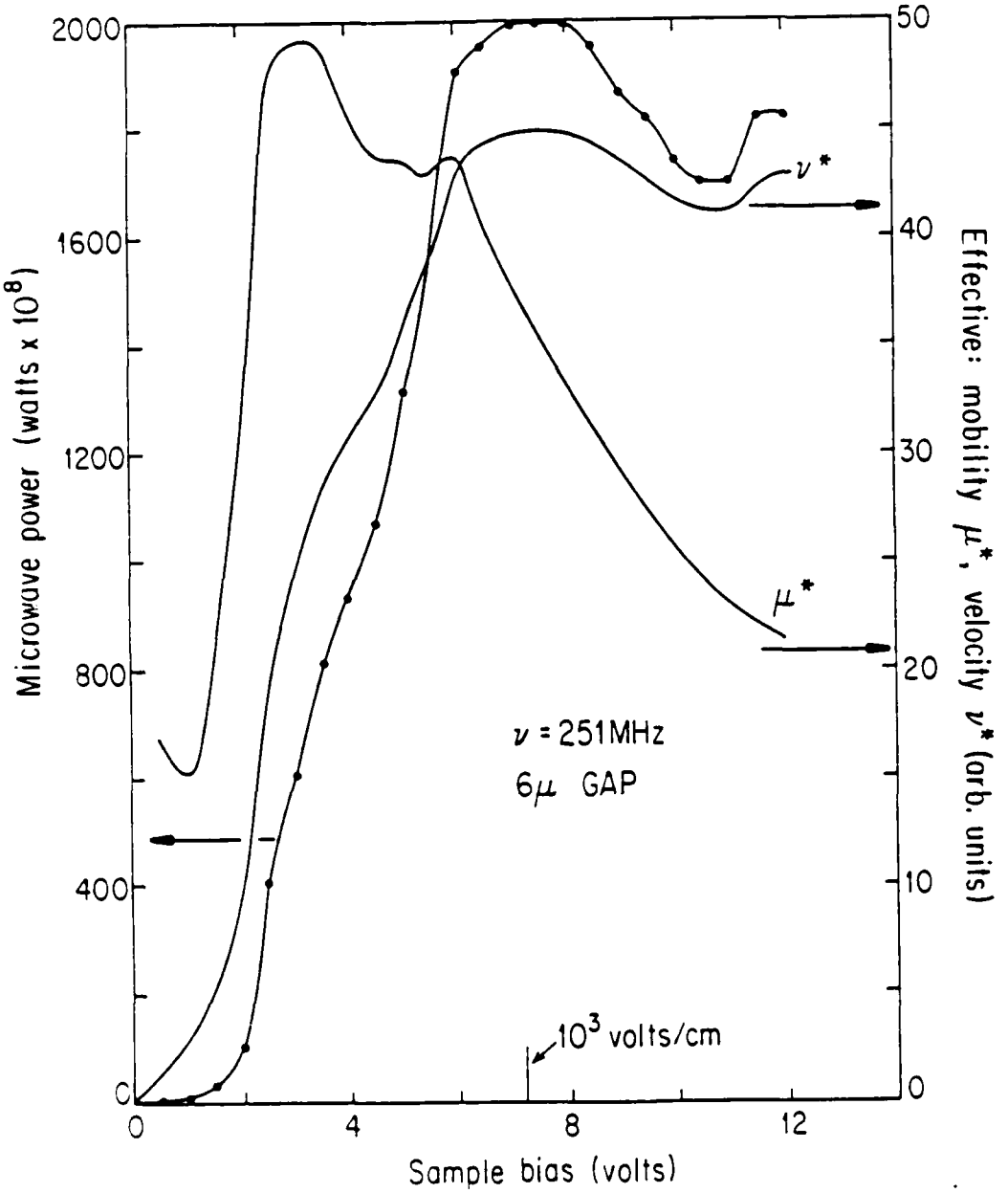
2000
1600
1200
800
400
0
Microwave power (watts x 10^8)
50
40
30
20
10
0
Effective mobility μ^*, velocity ν^* (arb. units)
ν^*
μ^*
ν = 251MHz
6μ GAP
10^3 volts/cm
0
4
8
12
Sample bias (volts)

Fig. 3

VI. APPENDIX

Reprinted from SPIE Vol 524—Spectroscopic Characterization Techniques for Semiconductor Technology II

Deep level derivative spectroscopy of semiconductors by wavelength modulation techniques

R. Braunstein, S. M. Eetemadi, and R. K. Kim

Department of Physics, University of California,
Los Angeles, California 90024

Abstract

An infrared wavelength modulated absorption spectrometer capable of measuring changes in the absorption coefficient of levels of 10^{-5} cm^{-1} in the spectral range 0.2-20 microns was employed to study bulk and surface absorption in semiconductors. The results of the study of deep levels in semi-insulating GaAs, surface layers on Si, GaAs, and HgCdTe, oxygen complexes in floating-zone silicon, and determination of strain in ion implanted layers are presented.

Introduction

The utilization of semiconductors in devices for the amplification, detection, generation, and signal processing of high frequency electromagnetic radiation in very high density configurations requires an intimate knowledge of the impurities and structure imperfections which affect device performance. It has been a scientific and technological challenge to develop nondestructive techniques to detect such imperfections and to develop a conceptual framework for understanding their microscopic electronic structure. In fashioning high density arrays of semiconductor devices, it is essential to start with well characterized, homogeneous substrates to obtain near-identical properties of individual circuit elements. Aside from knowing how to select the initial "winning" substrate, subsequent device processing can introduce unknown impurities or defects which can degrade device performance and consequently it would be desirable to have a technique which is capable of following the evaluation of a semiconductor's characteristics from its initial growth through the device processing phases.

A powerful array of enetron spectroscopies[1] exist for detecting chemical impurities but these require an ultra-high-vacuum environment and are not readily adaptable to analytical procedures which can ultimately be used on the production line. There exists an immense variety of junction techniques employing some form of deep level transient spectroscopy (DLTS) to study deep level defects whose variation depends on which junction parameter is finally measured.[2] However, apart from technical details, the end result one desires to extract from these measurements are the optical and thermal emission cross sections for electrons and holes, as well as the concentration of levels. In general excited state, thresholds for transitions between levels, and intra-center transitions between levels are not easily determined using the above techniques. The presence of high electric fields at the junctions adds complications to the interpretation of the data. In addition, thermal processing of the test structures can introduce further defects. Direct optical absorption measurements yield the quantities of interest, but at the level of sensitivity of DLTS techniques, on the order of 10^{12}-$10^{14}/cm^3$, it is not possible to employ conventional techniques. Consequently consideration has been given to optical modulation spectroscopies for detecting small structures out of a broad background.[3] A family of derivative spectroscopy techniques has been developed where the modulation parameter may be the electric field, stress temperature, or wavelength of the probing light beam. Recently, wavelength modulation photoresponse spectroscopies have evolved to measure photo-induced changes in voltage,[4] capacitance,[5] and current[6] from which the absorption coefficients are inferred. An examination of wavelength modulation photoresponse spectroscopies in contrast to direct wavelength modulation absorption/reflection indicates that the latter is the most suitable technique for studying deep levels since it yields unambiguous line shapes.[7]

We have developed an infrared wavelength modulated system capable of measuring changes in absorption coefficients at levels of 10^{-5} cm^{-1} out of a broad background in the spectral range 0.2-20 microns.[8] Since it is not necessary to make electrical contact to the sample one obviates possible contamination by thermal processing necessary for DLTS or photoresponse techniques. In addition, being an optical technique there are no restrictions on the resistivity of the sample. In this report we will discuss the use of this system in a number of studies concerned with characterization of semiconductors.

Infrared wavelength modulation system

The theory of operation of the infrared wavelength modulation system, its construction, and implementation has been previously reported.[8] For the purposes of the present discussion we shall indicate some general aspects of its operation. In one form of this system we have employed a Perkin-Elmer 301 spectrometer in a single beam sample-in and sample-out scheme shown in Fig. 1. The sample-in, sample-out and spectrometer wave-number positions are preset at intervals by stepping motors, these and the data collecting system are controlled by an on-line microprocessor (Motorola M6800) or a CAMAC based PDP 11/23 computer; a block diagram of the control system is shown in Fig. 2. The modulation of the wavelength is accomplished by the sinusoidal sweeping the output of the light beam across the exit slit of the monochromator by a vibrating mirror; this method of modulation is equally good for any wavelength and the amplitude can be continuously varied up to $\Delta\lambda/\lambda \sim 10^{-2}$. The system employes two lock-in amplifiers. As

shown in Figs. 1 and 2, lock-in amplifier I measures the intensity of the chopped radiation at frequency f_1 at a fixed wavelength with the sample-in and the sample-out while lock-in amplifer II, at frequency f_2, measures the derivative signal also with the sample-in and sample-out. Appropriate light sources, filters and detectors are employed for a given spectral region. At the end of a data taking cycle the energy derivative of the absorption as well as its integral are calculated by a PDP 11/23 computer and the results plotted. The constant of integration is supplied by the direct measurement of the absorption in a convenient spectral region.

Derivative absorption spectroscopy of GaAs:Cr

The above infrared wavelength modulated system was employed in a detailed study of the derivative absorption of GaAs:Cr.[9] Figures 3 and 4 show the integrated derivative data of semi-insulating GaAs:Cr at 300 K with various degrees of shallow donor-acceptor compensations. All the samples were semi-insulating and contained ~ $10^{16}/cm^3$ Cr. The samples in Fig. 3 were highly compensated while those in Fig. 4 were slightly more p- or n-type, respectively. The extensive fine structures with variation in absorption coefficient of $\Delta K \sim 10^{-1}$ to 10^{-2} cm^{-1} out of a relatively smooth background absorption of 1-2 cm^{-1} should be noted. Previously reported conventional optical absorption measurements revealed a few plateau-like structures, indicating that they had only observed the envelope of the absorption in this region.[10] The detailed extensive fine structure observed can be correlated with an energy level scheme of (Cr^{3+}-Cr^{2+}) ions in GaAs shown in Fig. 5 and interpreted in terms of transitions from Cr-ions to the valence and conduction bands and excited states. The complexity of the spectra is due to coupling of Cr to donor or acceptor complexes, and the subtle changes are due to the degree of compensation and consequent position of the Fermi level in these four semi-insulating samples. A complete analysis indicates that a comparable number of Cr atoms are at tetragonal and trigonal sites and can explain the rapid diffusion of Cr in GaAs.[9]

Semi-insulating LEC GaAs

An extensive study was made on semi-insulating GaAs grown by the liquid encapsulated Czochralski technique (LEC). These studies were performed in the spectral region 0.3-1.5 eV and the temperature range 80-300 K. In these samples, we observed a number of structures due to EL2, other defects, and impurities. Several fine structures were observed which can be interpreted in terms of intra-center transitions between levels of impurities split by the crystal field; the data were obtained with our derivative spectrometer and the integrated results are discussed below.

Figure 6 shows the absorption of semi-insulating LEC GaAs at 300 K. The threshold at 1.4 eV is the onset of the direct band-to-band transition, while the threshold at 1.0 eV is the onset of the EL2 defect. The small structure between 0.3 and 0.5 eV and threshold at 0.5 eV should be noted. The sensitivity of our measurement allows us to give credence to changes in absorption coefficient ~ 10^{-3} cm^{-1}. As the temperature is reduced to 160 K, we note the emergence of structure shown in Fig. 7 on a vastly expanded scale. When the sample temperature is reduced to 80 K, the structure with a threshold at 1.0 eV at room temperature abruptly quenches when the sample is illuminated with band gap light; see Fig. 8. When the sample temperature is increased and the measurement performed without band gap light present, the EL2 threshold returns. The metastability of this level and its possible identification as an anti-site defect of GaAs have been previously discussed.[11]

Figure 9 shows the structure observed in Fig. 8 on a vastly expanded scale possibly by the precision of our measurement. Note should be taken of the sharp structure at 0.36 - 0.38 eV, a broad peak at 0.4 eV, structure between 0.42 - 0.5 eV, and the threshold at 0.5 eV. Similar structures are observed in the same spectral region for other undoped LEC GaAs samples, but with changes in the relative intensities of the various structures. The structures at 0.36 - 0.38 eV and the threshold at 0.5 eV seem to be correlated, indicating they are due to the same level. The structures at 0.36 - 0.38 eV are very similar to that which is observed for deliberately Fe doped in a number of semiconductors,[12] and so can be identified as an intra-center transition of Fe^{2+} in GaAs. (Estimating the oscillator strength for Fe, our samples contain ~ 10^{16} Fe/cm^3.) The threshold at 0.5 eV whose intensity scales with this intra-center transition corresponds to the transition from the valence band to the Fe levels. This is further substantiated by the fact that the position of this threshold moves with a temperature coefficient similar to the GaAs band gap; a similar observation has been made from Hall measurements.[13] The resonant-like band around 0.4 eV with its possible fine structure seems to be an intra-center transition. Photo-induced-transient spectroscopy (P.I.T.S.) electrical measurements made on the same samples as the optical measurements reveal levels at 0.4 and 0.8 eV, the latter being due to EL2. A level at 0.4 eV has been reported in semi-insulating GaAs by a number of measurements[14] which was originally ascribed to oxygen in O-doped GaAs. Recently a combination of temperature-dependent Hall-effect measurements, spark-source mass spectroscopy, and secondary ion mass spectroscopy measurements have indicated that neither oxygen nor any other impurity can account for the 0.4 eV level and consequently it is probably due to a pure defect.

Thermal annealing and quenching experiments on a range of LEC GaAs samples revealed that some of these levels are probably due to structure imperfections.[15] The subtle charges in these levels could readily be followed by our wavelength modulatin technique.

Surface absorption

The sensitivity of our system enables us to study surface absorption. Although the primary aim of this report is to demonstrate the power of infrared wavelength modulation spectroscopy as a characterization technique for bulk semiconductors, we shall show some examples of measurements on alkali halides[8] since recently a great deal of material preparation studies have taken place to improve these maerials for light guiding applications. First we shall discuss an example of measurements on KBr which reveal both surface and bulk absorption. These clean alkali halides are potentially useful insulators in MIS structures. Subsequently we describe some examples of surface absorption on semiconductor.

The absorption spectra of a typical KBr crystal obtained with a conventional double-beam spectrometer are shown in Fig. 10. This crystal was grown from material which was selectively ion filtered and reactive gas treated for purification prior to crystal growth. As can be seen, virtually no absorption structure can be seen above the noise level of the instrument, confirming the relative purity of the sample.

Figure 11a shows the integrated derivative spectra of the above KBr sample taken with the sample in the laboratory atmosphere. The richness of the observed spectra should be noted in contrast to the featureless spectral shown in Fig. 10 for the same sample. The right-hand ordinate in Fig. 11 indicates the absorption coefficient at 3.8 μm as inferred from a laser calorimeter measurement with a DF laser; the left-hand ordinate indicates the relative change of absorption obtained by integrating the wavelength modulation derivative data. The depth of the modulation of the monochromator frequency used to obtain these data was 10 cm^{-1}. The zero of the ΔK cm^{-1} wavelength modulation result is registered with the absorption calibration point of 0.4×10^{-4} cm^{-1} obtained by laser calorimetry. Therefore, to obtain the actual absorption coefficient at a particular wavelength, one merely adds or subtracts the appropriate ΔK value at a given frequency to the 0.4×10^{-4} cm^{-1} value. This type of representation of the data allows us to display the fine structure excursions in absorption above and below the calorimetric point. Successive runs on this sample reveal that the structure shown in Fig. 11 is reproducible within a mean deviation of $\Delta K \sim 10^{-6}$ cm^{-1}. Consequently, the noise level is at the level of the width of the drafting lines. The data points were taken at 5 cm^{-1} frequency intervals. The sample thickness was 4 cm.

When this sample is placed in a dry N_2 atmosphere, a continuous change in the spectral distribution of the absorption is observed until the spectra stabilize after the sample has been in this gaseous ambient for an hour. The dominant features of the spectra of this sample when in the laboratory atmosphere displayed in Fig. 11a are: a band near 2.5 μm with the fine structure, multiple structure between 3 to 4 μm with fine structure, a sharp strong band at 4.2 μm, a band at 5 μm, and mutliple structures between 6 to 12 μm. The data shown in Fig. 11b are for this same sample in a dry N_2 atmosphere. Although there is a distinct change in the spectra in Fig. 11b compared to Fig. 11a, some of the original prominent features can still be recognized. The sharp peak at 4.2 μm is greatly reduced, and the band at 5 μm is gone, while some of the original structure between 5.8 and 12.0 μm is still present; however, a valley develops around 9 μm. Analysis of the observed spectra has allowed us for the first time to identify volume and surface impurities in highly pure KBr and other alkali halides.[8]

Using our infrared wavelength modulation system, we have been able to study the growth of nature oxides on freshly etched silicon surfaces. We can easily detect the 9 micron SiO absorption band in a 10 Å layer of silicon with a signal-to-noise ratio of 100/1, indicating that we have the capabilities of studying the growth of a fraction of a monolayer of adsorbed species. An example of this band is shown in Fig. 12 immediately after the silicon surface was etched with HF. Studies of oxides on GaAs and HgCdTe have enabled us to study the formation of OH^- in oxides on GaAs as well as the presence of TeO_2 on HgCdTe due to various surface treatments.

Determination of strain in layered semiconductors

In the growth of semiconductor layers by various epitaxial techniques such as M.B.E., L.P.E., and C.V.D., and the doping of layers by ion implantation and other techniques, an important technological problem is the assessment of the homogeneity of doping, alloy composition, and strain in the layers. We have used our wavelength techniques to determine shifts in various critical points as a function of doping and strain in several semiconductors.

One of the major fabrication processes used in the fabricate of n-type channel FET's on semiconducting GaAs is the utilization of ion implantation. The assessment of defects subsequent to implantation and annealing is of prime importance, especially so for shallow implanted layers ~ 1000 Å. We have observed the effects of ion implantation by the nondestructive methods of wavelength modulation. Local strain was observed by measuring the shift of the imaginary part of the dielectric function of GaAs in the neighborhood of the E_1 and $E_1+\Delta$ critical point. Implants of Be, Sb, S, In, and double implanted Sb and Be were studied. the implanting fluxes were of the order of $10^{13}/cm^2$, compared to ion unimplanted GaAs, positive and negative shifts of the energy of the critical point were observed, indicating that we are able to distinguish contraction or expansion of the lattice.

In addition, we found that the intensity of ϵ_2 the imaginary part of the dielectric function at the $E_1+\Delta$ critical point decreased as a function of n-type doping. These results can be interpreted in terms of screening of the hyperbolic exciton associated with this critical point.

Difference wavelength modulation spectroscopy of oxygen in floating-zone silicon

The use of infrared spectroscopy to identify relative amounts of oxygen in silicon is routine.[16] Usually the concentration of dissolved oxygen is deduced from the infrared absorption at about 9 μm (1100 cm^{-1}). The relationship between the intensity of this band and the dissolved oxygen has been demonstrated reliably in experiments by comparing the absorption in samples containing the oxygen isotopes O^{16} and O^{18}.[17,18]

It has been shown that this band is associated with interstitial oxygen and is due to an infrared-active antisymmetric type of vibration of the Si_2O "molecule."[19] This model has been questioned and it has been suggested[20] that the oxygen in silicon is not in a bound state, forming fine second-phase SiO_2 particles and the absorption at 9 μm is due to this oxygen. Attempts have been made to explain the changes of optical and electrical properties of silicon after various heat treatments by the phase transitions of these second-phase particles of SiO_2.[20] Other workers showed that absorption spectra of silicon samples around 9 μm with relatively low oxygen concentration have a complex structure. They observed a peak at 1128 cm^{-1}, and another peak at 1135 cm^{-1}, and they attributed these peaks to dissolved oxygen in the lattice and in the second-phase SiO_2 particles, respectively. They suggested that other electrically inactive states of oxygen in silicon might exist, and there might be a threshold oxygen concentration which is necessary for any significant formation of SiO_4^+ complexes to occur.

Nearly all previous optical studies of oxygen in silicon were performed on silicon samples grown by the Czochralski method, which presumably have oxygen contents in the range of 10^{17}–10^{18} atoms/cm^3. Practically no information is available on the state of oxygen in float-zone grown silicon. The reason for this, we believe, is that float-zone grown silicon has low oxygen content (≤ 10^{16} atoms/cm^3), and the detection limit of conventional differential absorption methods is ~ 1×10^{16} atoms/cm^3. Oxygen concentration in the range of ~ 10^{16} atoms/cm^3 contributes ~ 0.5 cm^{-1} to the absorption coefficient at about 9 μm. In addition, the intrinsic lattice band of silicon contributes ~ 0.8 cm^{-1} to the absorption coefficient at about 9 μm. This fact clearly indicates the difficulty of the study of the samples with low oxygen content.

But we believe that the mechanism of oxygen complex formation and thermal donors can be understood better if we can understand how the oxygen complex formation is initiated for low oxygen content. In this spirit, we initiated the study of oxygen in silicon with low oxygen content (≤ 10^{15} atoms/cm^3) using an infrared difference wavelength modulation technique. Several float-zone grown silicon samples were studied, all with oxygen content below the detection limit of conventional methods ~ 1×10^{16} atoms/cm^3. Measurements were made on different sections of the same ingot, that is, the seed-end and the tail-end of the dimensions ~ 2 cm in diameter and 1 cm in thickness.

Our infrared wavelength modulation technique[22] was employed to study the 9 μm absorption band of these samples at room temperature. To eliminate the absorption due to the intrinsic lattice vibration of silicon and surface effects, we used a sample-in and sample-out procedure, which enables a comparison of the derivative of the absorption of a sample with a reference sample. With this procedure, the derivative spectrum of the difference of the absorption between a sample and the reference crystal is obtained. A conventional spectrophotometer run of the reference crystal, which is a seed-end of another float-zone silicon, showed just a trace of oxygen at 9 μm; that is, at 9 μm the oxygen contributes approximately 0.15 cm^{-1} to the absorption coefficient. From this we can approximate the oxygen content of reference crystal to be ~ 10^{15} atoms/cm^3. The detector used in this study was PbSnTe at liquid nitrogen temperature.

The integrated results of these derivative spectra of the difference for a series of samples are shown in Figs. 13, 14, 15, and 16. The figures show the relative variations of absorption of samples with respect to the reference crystal. Therefore, the positive side of the absorption of the sample in the figures means more absorption and negative side of the absorption means less absorption than the reference crystal at the appropriate wavenumbers. In all the figures, the upper drawing is the experimental result of the seed-end and the lower one is the result of the tail-end of the same ingot with respect to the reference crystal with ~ 10^{15} oxygen atoms/cm^3.

In this study, it should be noted that since we are taking the derivative of the difference of absorption at appropriate frequencies between sample and the reference crystal, the shift or the different width of the bands of the crystals represent changes relative to the reference crystal. Consequently, it is interesting to note that because of the sensitivity of the difference derivative technique ($\Delta k \sim 10^{-5}$ cm^{-1}), the subtle spectra changes introduced by various heat treatments can be studied by comparing it with the reference even though the change of spectral distribution caused by heat treatment on the sample by itself is difficult to determine!

In Fig. 13, we note that a band emerges at 1123 cm^{-1} (8.9 μm) in the tail-end (lower figure). It is not clear exactly what complex is responsible for this band. We can clearly see a shoulder at 1108 cm^{-1} (9 μm) in the tail-end (lower figure) which appears to be Si_2O. The results on two different ingots are shown in Figs. 14 and 15 and we can see about the same level of absorption due to Si_2O at 1108 cm^{-1} in both parts of the same ingot. However, we can immediately note that the spectral distribution changes even within the same ingot depending on which part of the ingot the sample is taken from. This is not unreasonable if we consider the fact that the crystals are float-zone samples and the sensitivity of our system.

As shown in all of the figures, at low oxygen content the infrared absorption mechanism in the 9 μm region is complicated. This indicates the existence of oxygen in different energy states. This is understandable if we keep in mind the fact that, although oxygen is interstitial in the sense that it does not occupy a lattice site, it can occupy slightly different positions of varying energy.[23] During growth, oxygen atoms are randomly trapped in the silicon lattice, and at room temperature thermal agitation permits the oxygen atom to occupy a number of slightly different configurations of varying energy.

In Fig. 16 the absorption is stronger than the previous samples; it appears that if the oxygen content exceeds a certain value ~ 10^{16} atoms/cm^3, the absorption mechanism at 1108 cm^{-1} dominates. This band at 1108 cm^{-1} we attribute to the form of freely dissolved Si_2O "quasimolecule." In the above figure we can also note a band at 1048 cm^{-1} (9.5 μm) in both seed and tail-ends; this band might be related to still another complex which can be formed if the oxygen content reaches a certain value (~ 10^{16} atoms/cm^3).

In concluding, we summarize our results:

1) Even though the use of float-zone silicon as an oxygen free reference is a common practice, our results show the float-zone silicon also contains oxygen.

2) The state of oxygen in silicon is in the form of complexes.

3) If the oxygen concentration exceeds a certain value, the oxygen in Si_2O "quasimolecule" starts dominating the infrared absorption mechanism at about 9 μm.

4) Different parts of the same ingot of float-zone grown silicon have different oxygen content which is responsible for infrared absorption around 9 μm.

5) Our wavelength modulation system can detect the variation in the absorption coefficient of ~ 10^{-6} cm^{-1}. If we approximate the scattering cross section of oxygen responsible for absorption at 9 μm to be ~ 10^{-18} cm^2, we have the capability of detecting oxygen at levels of ~ 10^{12} atoms/cm^3!

Summary

In this paper we have shown that infrared wavelength modulation is a sensitive and versatile spectroscopic characterization technique for a variety of semiconductor technology problems. In particular the results of a study of deep levels in semi-insulating GaAs, surface layers in Si, GaAs, and HgCdTe, oxygen complexes in floating-zone Si, as well as the determination of strain in ion implanted layers were presented.

Acknowledgments

The support of this work by the Air Force Office of Scientific Research under AFOSR-83-0169B, the Army Research Office-Durham under DAAG29-81-K-0164, and the State of California - MICRO program is gratefully acknowledged.

References

1. Czanderna, A. W., editor, Methods of Surface Analysis, Vol. 1, Elsevier Scientific Publishing Co., Amsterdam-Oxford-New York, 1975.
2. Lang, D. V., in Thermally Stimulated Relaxation in Solids, edited by P. Bräunlick, Springer-Verlag, Berlin-Heidelberg,New York, 1979.
3. Willardson, R. K., and Beer, A. C., editors, Semiconductors and Semimetals, Vol. 9, Academic Press, New York, 1977.
4. Lagowski, J., Walukiewicz, W., Slusarczuk, M. M. G., and Gatos, H. C., J. Appl. Phys. 50, 5059 (1979).
5. Kamieniecki, E., Lagowski, J., and Gatos, H. C., J. Appl. Phys. 51, 1863 (1980).
6. T. Nishino and Y. Hamakawa, Phys. Stat. Sol. (b) 50, 345 (1972).
7. Eetemadi, S. M., and Braunstein, R., to be published.
8. Kim, R. K., and Braunstein, R., Appl. Opt. 23, 1166 (1984).
9. Braunstein, R., Kim, R. K., Matthews, D., and Braunstein, M., Physica 117B and 118B (1983).
10. Clerjaud, B., Hennel, A. M., and Martinez, G., Solid State Comm. 33, 983 (1980).
11. Martin, G., Appl. Phys. Lett. 39, 747 (1981).
12. Barnowski, J. M., Allen, J. W., and Pearson, G. L., Phys. Rev. 160, 627 (1967).
13. R. W. Haisty, Appl. Phys. Lett. 7, 208 (1965).
14. Look, D. C., Chaudhuri, S., and Sizelove, J. R., Appl. Phys. Lett. 42, (a) (1983).
15. Eetemadi, S. M., and Braunstein, R., to be published.
16. Patel, J. R., in Semiconductor Silicon, edited by H. R. Huff, R. J. Kriegler, and Y. Takeishi, Electrochemical Society, Princeton, 1981, p. 189.
17. Kaiser, W., Phys. Rev. 105, 1751 (1957).
18. Kaiser, W., Frisch, H. L., and Reiss, H., Phys. Rev. 112, 1546 (1958).
19. Kaiser, W., Keck, P. H., and Lange, C. F., Phys. Rev. 101, 1264 (1956).
20. Malyshev, V. A., Sov. Phys. Semicond. 8, 92 (1974).

21. Ryzhkova, E. M., Trapeznikova, I. I., Chelnokov, V. E., and Yakovenko, A. A., Sov. Phys. Semicond. 11, 628 (1977).
22. Braunstein, R., Kim, R. K., and Braunstein, M., Laser Induced Damage in Optical Materials: 1979, Boulder, CO, USA. 30-31 Oct. 1979 (Washington D. C., U.S.A.: NBS 1980), pp. 99-117.
23. Hrostowski, H. J., and Kaiser, R. K., Phys. Rev. 107, 966 (1957).

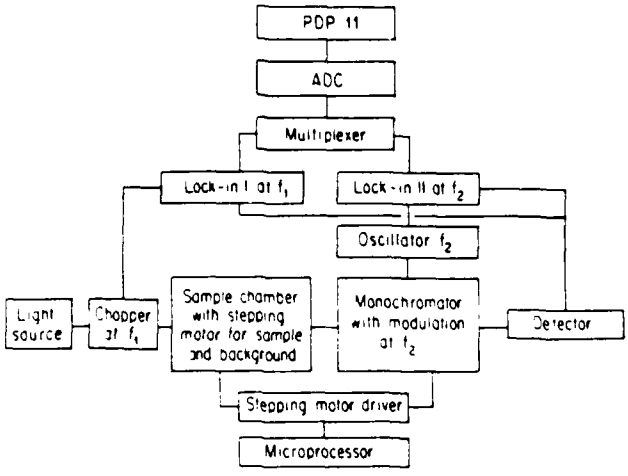

Figure 1. Block diagram of the infrared wavelength modulated system.

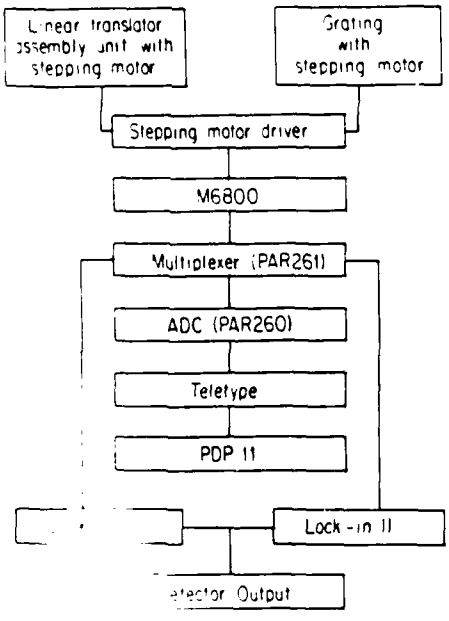

Figure 2. Block diagram of control system for data-taking cycle.

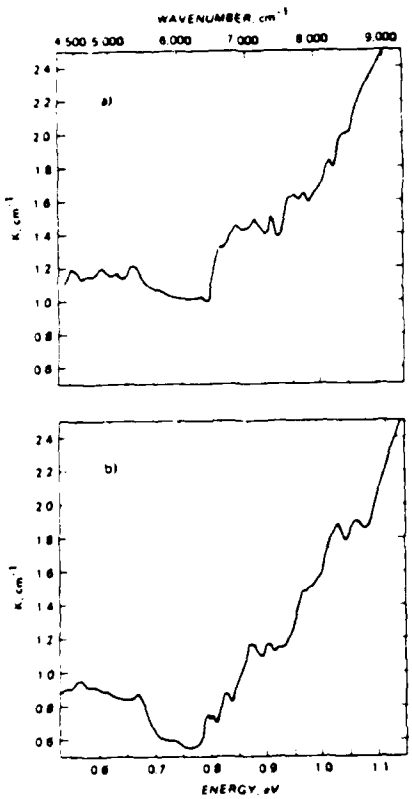

Figure 3. a) and b) Semi-insulating GaAs:Cr.

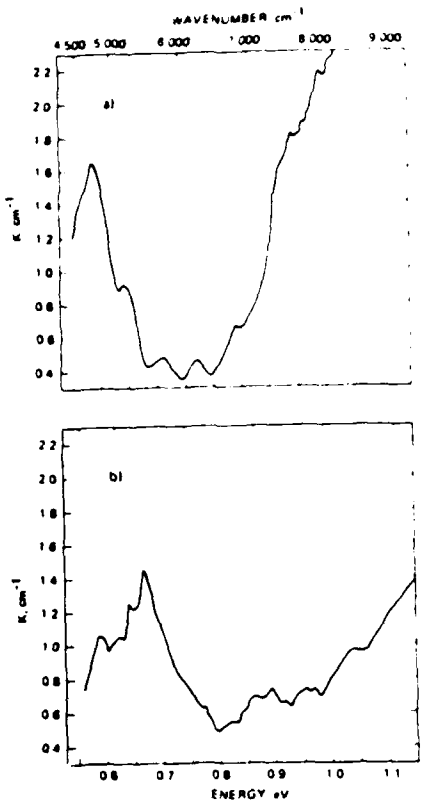

Figure 4. a) p-type, b) n-type GaAs:Cr.

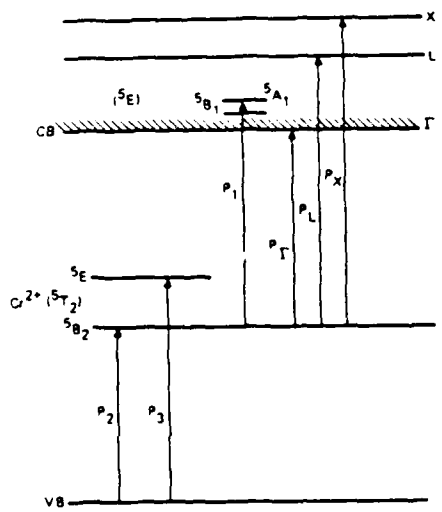

Figure 5. Energy levels of (Cr^{3+}-Cr^{2+}) ions in GaAs:Cr.

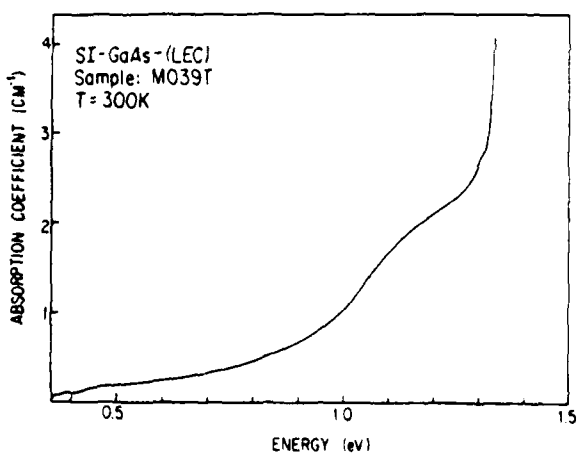

Figure 6. Wavelength modulation absorption spectra of LEC-GaAs at 300 K.

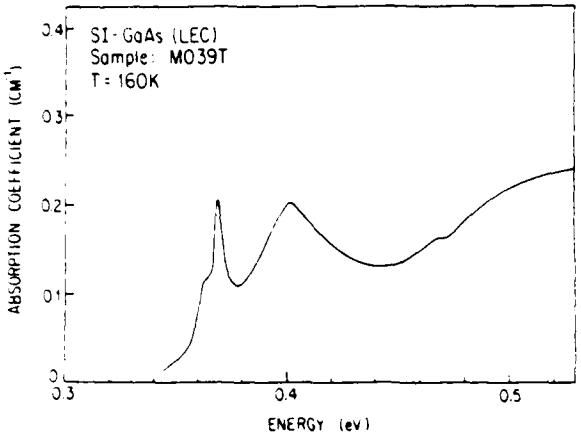

Figure 7. Wavelength modulation absorption spectra of LEC-GaAs at 160 K.

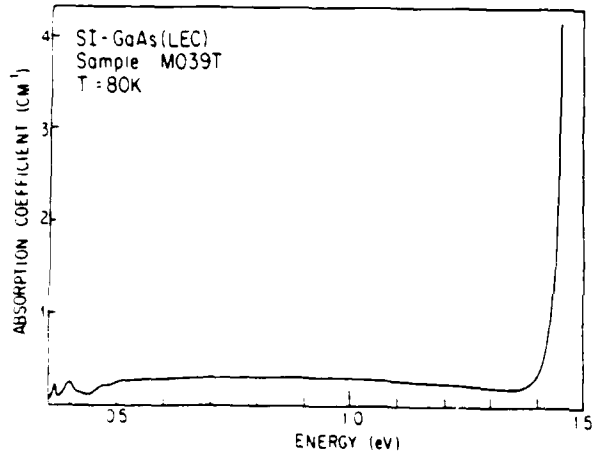

Figure 8. Wavelength modulation absorption spectra of LEC-GaAs at 80 K with EL2 photo-quenched.

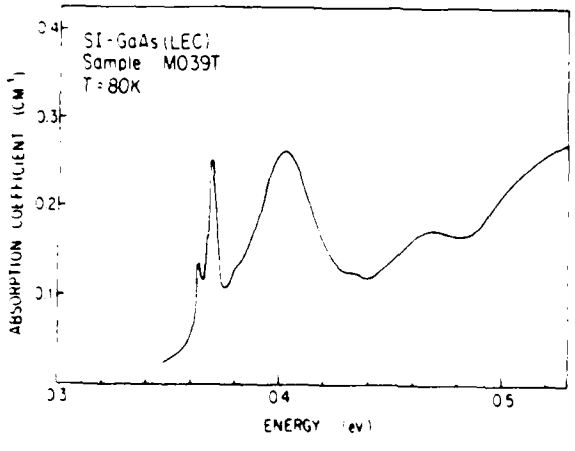

Figure 9. Wavelength modulation absorption spectra of LEC-GaAs at 80 K on a vastly expanded scale compared to Fig. 8.

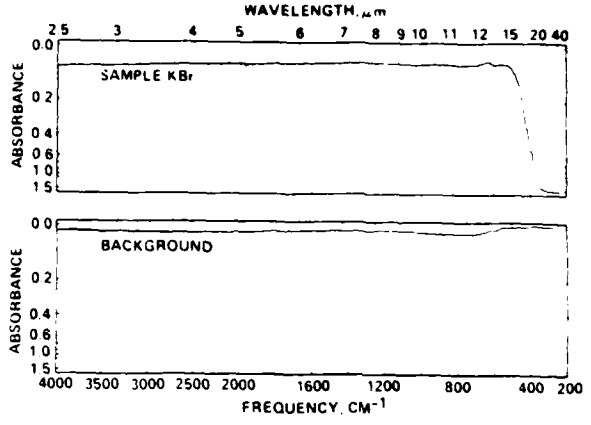

Figure 10. Absorption spectrum of a typical KBr sample obtained by a conventional double-beam instrument.

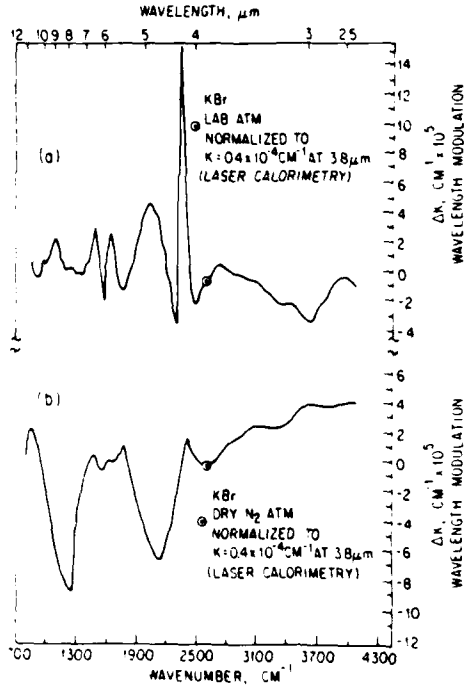

Figure 11. Wavelength modulation absorption spectra of KBr; ΔK is the change in the absorption coefficient in cm^{-1}; (a) in the laboratory atmosphere; (b) in a dry N_2 atmosphere.

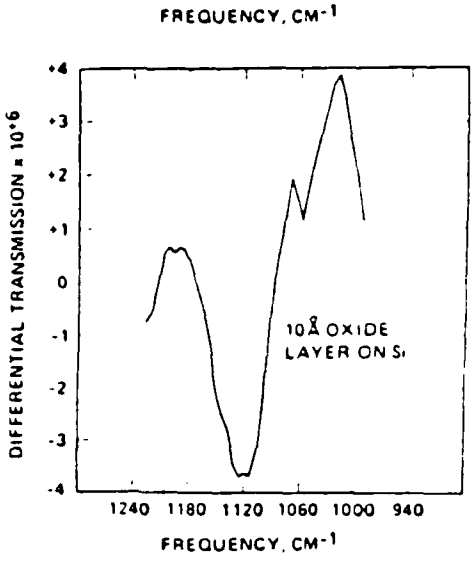

Figure 12. Wavelength modulation absorption spectra of a 10 A oxide layer of Si.

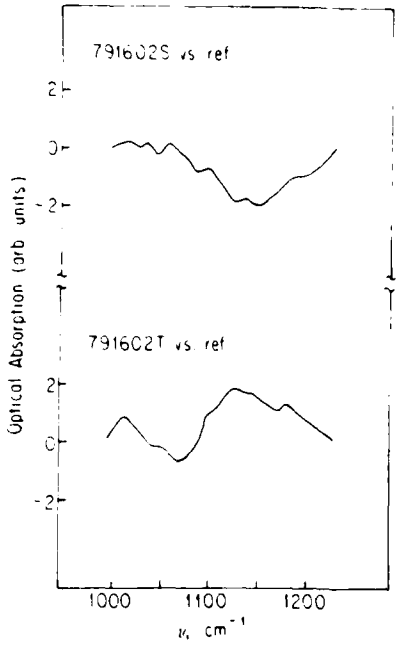

Figure 13.

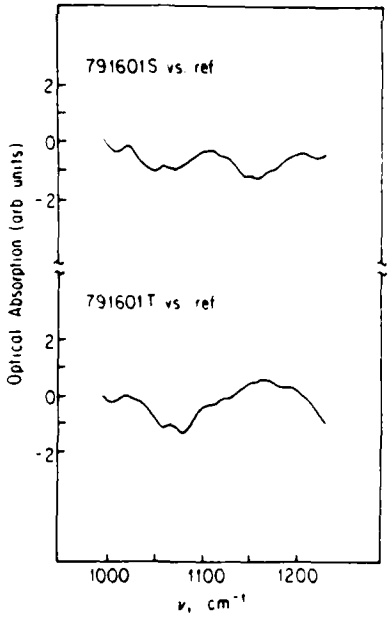

Figure 14.

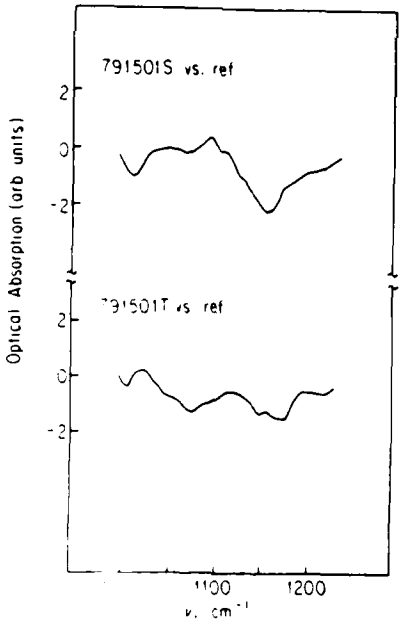

Figure 15.

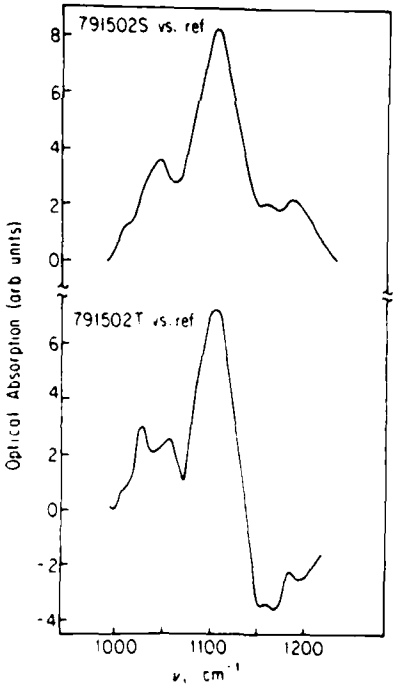

Figure 16.

Figures 13, 14, 15, 16. The relative optical absorption of the seed (top curve) and tail-end (bottom curve) of 791602, 791601, 791501, and 791502, respectively, float-zone Si ingots with respect to a Si reference containing ~ 10^{15} oxygen atoms/cm^3.

Wavelength Modulation Absorption Spectroscopy of Deep Levels in Semi-Insulating GaAs

S. M. Eetemadi and R. Braunstein

Department of Physics, University of California,
Los Angeles, California 90024

Infrared wavelength modulation absorption spectroscopy was used in the specral region of 0.3-1.45 eV and the temperature range of 80-300K, to study deep level impurities and defects in undoped semi-insulating GaAs grown by the liquid encapsulated Czochralski technique (LEC). The measurements revealed two resonant type peaks with fine structure near 0.37 and 0.40 eV, as well as thresholds and plateaus at higher energies. The sensitivity of the measurements allows us to give credence to changes in the absorption coefficient at levels $\sim 10^{-3}$ cm^{-1}. The absorption band at 0.37 eV is interpreted as being due to the intra-center transition between levels of accidental iron impurity, split by the crystal field. The absorption band near 0.40 eV, can be annealed out by heat treatment, and is considered to belong to a multilevel defect complex. Utilizing the photo-quenching behavior of the absorption in the spectral region of 0.6-1.4 eV, it was shown that conventional room temperature optical absorption may give erroneous results in measuring the concentration of the EL2 levels, because of appreciable absorption due to other residual deep levels in this spectral region, as revealed by the sensitivity of the wavelength modulation technique.

I. INTRODUCTION

Deep levels in semiconductors continue to be the subject of considerable theoretical[1-6] and experimental[7-15] research as our understanding of these levels is far from complete. The presence of deep levels in semiconductors at concentrations of $10^{15}/cm^3$ or even less, can significantly affect the carrier lifetime, mobility, and the rate of radiative transitions, and thus performance of microelectronics and opto-electronics devices made from these materials.[9] The fascinating features of the physics of deep levels, coupled with great technological interest in this field has intensified searches for sensitive experimental techniques for their detection and characterization at these low levels of concentrations.

The various space charge spectroscopy techniques (such as TSC, DLTS and DLOS)[8-11] developed in recent years are commonly employed electrical measurements to detect deep levels. With very good sensitivities, they can provide thermal activation energy, carrier capture cross section and concentration of deep levels (and optical cross section in some cases). The main drawback of these techniques, however, is that measurements are carried out in space charge regions, i.e., in the presence of high electric fields ($\sim 10^4$ - 10^5 V/cm), the effect of which on the emission rate is not thoroughly understood.[4,15-17] Furthermore, since these measurements require fabrication of p-n junctions or Schottky barriers or ohmic contacts which could result in the introduction of process related impurities and or defects into the sample. In addition, the above techniques employing essentially thermal processes usually do not yield excited states of levels. Photoluminescence type experiments, although very sensitive for shallow levels,[18-22] have limited sensitivity in the case of deep levels due to appreciable phonon coupling resulting in competition

between different possible radiative and nonradiatve mechanisms.

Extrinisic optical absorption spectroscopy has been amongst the most favored techniques of studying impurity and defect levels at high level of concentrations.[23-25] These measurements are done on bulk materials and therefore are free from high electric fields and process related impurity or defects. The absorption coefficient along with its spectral and temperature dependence can give information about the photoionization energy, excited states, temperature dependence of the level, electron-phonon coupling, and the symmetry of the localized wavefunction as well as their concentration.[4] However conventional optical absorption techniques usually suffer from poor sensitivity at low levels of concentration of the order of 10^{12} - 10^{16} cm^3 usually encountered for deep levels. Consequently considerations have been given to optical derivative spectroscopies which can measure absorption coefficients at levels of 10^{-3} to 10^{-5} cm^{-1}.[26]

Several modulation schemes have been developed in optical derivative spectroscopy. Electro-modulation, peizo-modulation, thermo-modulation and wavelength modulation are examples of this technique depending on whether the modulating parameter is the applied electric field, strain, temperature or the wavelength of the probing light beam.[27,28] However, these techniques have primarily been used to study the intrinsic optical properties of materials.

The techniques of extrinsic electro-absorption has been used in some cases to study deep levels in semiconductors.[29] They have not, however, been extensively employed, since they require high resisitivity material in order that sufficiently high electric fields can be applied to obtain adequate modulation. In addition, the present knoweldge of the effect of electric fields on the properties of deep levels is not sufficient for a complete interpretation of the experimental results.

Wavelength modulation absorption sepctroscopy, in contrast allows one to obtain the derivative spectrum by modulating the wavelength of the probing light beam, and thus has a straightforward relationship to the conventional absorption measurements with improved sensitivity.[30] The difficulty in this case is the presence of spurious structures in the spectrum due to background derivative spectra, which poses a serious problem expecially in the infrared region of spectra. This problem has been overcome by using a sample in-sample out technique and an on-line computer for collecting data and numerically decorrelating the spectra from the background.[31]

Undoped semi-insultaing (SI) GaAs substrates, grown by liquid encapsulated Czochralski (LEC) are currently being used for the fabrication of high speed GaAs MESFET and integrated circuits (IC's).[32] Deep levels play a crucial role in controlling the carrier concentration and hence the resistivity of the substrates. Therefore much attention has been focussed on detection and characterization of the deep levels in this technologically important material.

A detailed study of the derivative absorption of GaAs: Cr[33] has been reported. In the present study, we have employed a modified wavelength modulation absorption spectrometer to study the deep levels in the semi-insulating GaAs (LEC). The spectrometer was used in the spectral region of 0.3-1.45 eV and the temperature range of 80-300K, to study deep level impurities and defects in undoped semi-insulating GaAs (LEC). The measurements revealed two resonant type peaks with fine structures near 0.37 and 0.40 eV, as well as thresholds and plateaus at higher energies. The sensitivity of our measurements allows us to give credence to changes in the absorption coefficient at levels $\sim 10^{-3}$ cm^{-1}. The absorption band at 0.37 eV is interpreted as being due to the intra-center transition between levels of accidental iron impurity, split by the crystal field. The absorption band near 0.40 eV, annealed out as a result of

heat treatment, and therefore is considered to belong to a multilevel defect complex.

The spectrum between 0.6 and 1.45 eV was identified as being due to a native defect commonly referred to as EL2.[34] Utilizing the unusual photo-quenching behavior[35] of this level we were able to re-examine the accuracy of the conventional room temperature optical absorption, commonly used in measuring the EL2 concentration, and showed that these methods typically can have up to 20% error.

II. EXPERIMENTAL TECHNIQUES

Our previously reported wavelength modulated spectrometer[31] has been modified (for the low temperature operation) by adding to it a low temperature optical dewar essential to this work. We have also improved the stability, reproducibility and control of the modulating system, as well as the signal processing. The schematic diagram of the system is shown in Fig. 1.

A liquid transfer refrigerator, with an optical window shroud and a sample holder suitable for the sample-in-sample out technique, and a digital temperature indicator/controller, were used for the low temperture operation. A tungsten/halogen light source, and quartz windows were used for the spectral range of 0.55 - 1.50 eV. For the 0.3 - 0.55 eV region, a Globar light source and Potassium Chloride windows were used. The detector throughout the spectral region was a Golay cell.

The modulation of the wavelength was accomplished by sinusoidal oscillation of a diagonal mirror located near the exit slit of the monochromator, and mounted on the shaft of an optical scanner. The internal oscillator of a lock-in amplifier was used to drive the scanner through a current amplifier driver

circuit. The new modulation system has several advantages over the one previously employed. It is frequency tunable (1-100 Hz), has high amplitude and frequency stability, and allow large wavelength excursions. With the new system the amplitude of modulation can be controlled from 0.2 to 150 A precision. There was no wabbling, and no crosstalk with other mechanically vibrating components. These features were desirable for reducing noise and drift, as well as optimizing the modulation frequency compatible with the detector response, and consistent with the chopper frequency to avoid harmonic or sub-harmonic pick-up. It can also be used to conveniently and very precisely calibrate the spectral slit width, the depth of modulation, and to select these quantities for optimum resolution, signal-to-noise ratio, and minimum distortion in the derivative signal, for a given spectral region. A DC offset feature of this scanner also allows one to set the monochromator calibration electrically rather than mechanically. Data was taken at discrete energies with a resolution set by the slit width and depth of modulation which for this work was 0.00075 - 0.0015 eV.

An on-line computer steps the sample, in and out of the light beam, as well as steps the wavelength, and collects data from the output of lock-in amplifiers at controllable rates for additional signal averaging. These operations are conveniently done using a LSI-11/23 computer and its peripherals in the form of a CAMAC system. The data taking cycle is shown in Fig. 2. The method of data analaysis is similar to that previously employed.[31] The wavelength modulation technique yields essentially the energy derivative of the absorption coefficient. To obtain the value of the absorption coefficient, one numerically integrates the observed derivative spectra, and normalizes it to the absorption coefficient obtained by a direct measurement in the same apparatus at fixed wavelengths where the absorption coefficient can be measured with good

precision.

The undoped semi-insulating GaAs samples used in this work were cut from five different ingots, all grown in pyrolitic boron nitride (PEN) crucibles, by the liquid encapsulated Czochralski technique (LEC), with B_2O_3 as the encapsulant. They had resistivities greater than $10^7 \Omega$-cm, and Hall mobilities of 4570-6319 cm^2/V sec. They were typically 3 mm thick and the surface were polished with Br-methanol. The samples were grown by the Hughes Research Laboratory, Malibu.

III. RESULTS

Figure 3 shows the absorption spectra of an undoped SI GaAs (LEC) at 300 K. The threshold near 1.4 eV is the onset of the interband transition, while the spectra between 0.7 and 1.4 eV is the characteristic absorption of a deep level due to a presumably native defect complex, commonly referred to as the EL2 level.[35] The small structures between 0.3 and 0.5 eV, and the threshold at 0.5 eV should be noted. In conventional absorption spectroscopy these small variations would be buried in the systems noise, whereas with our technique variations as small as 10^{-3} cm^{-1} have significance. As the temperature is reduced to 160 K, we note the sharpening of the thresholds, and emergence of distinct resonance type structures, shown in Fig. 4. The structures below 0.52 eV are shown in Fig. 5 on a vastly expanded scale possible by the precision of our measurement. Upon lowering the temperature to 80 K the structures sharpen further, and some finer ones appear as seen in Fig. 6. Note should be taken of the sharp structure at 0.36 - 0.38 eV, a broad peak at 0.4 eV with side lobes, and the threshold near 0.5 eV. Figures 7-10 show the observed structures in the same spectral region and temperature for other undoped LEC GaAs samples.

It should be noted that the general shape of the resonant structure at 0.36-0.38 remains unchanged as its intensity varies from Figs. 6-9. In contrast the broad peak at 0.4 eV changes its intensity as well as the details of its shape. No distinct pattern was observed in the structures at 0.43-0.47 eV. Fig. 11 shows the spectra of the sample M039 after the sample had been annealed in a N_2 atmosphere at 450^{o}C for four hours. The difference between this and Fig. 6 should be noted. The peak at 0.4 eV has been annealed out as a result of heat treatment.

When the temperature was lowered to below 140 K, and the sample was illuminated with a 50 W tungsten halogen lamp, the structures between 0.7 and 1.3 eV quenched (see Fig. 12) and remained in the quenched state for several hours even after the background illumination had been turned off. The magnitude and the details of the shape of the post-quenched spectra varied from sample to sample. Its magnitude at 1.2 eV was 10-20% of the total room temperature absorption coefficient at the same energy.

IV. DISCUSSION

The above results are discussed in the following subsections. In section A the resonant spectra at 0.37 is discussed and attributed to accidental iron impurities. Section B is devoted to the comparison of the spectra at 0.4 eV among the various samples, as well as its behavior under heat treatment, and is considered to be the signature of a multi-level defect complex. The results of our observation in the spectral range of 0.7-1.4 eV are discussed in Sec. C.

A. Iron in Undoped GaAs

In the spectra below 0.55 eV, the sharp peak at 0.37 eV can be attributed

to the presence of iron in these materials; a similar absorption peak has been reported in GaAs substrates intentionally doped with iron.[25] Sharp zero-phonon photoluminescence lines near 0.37 eV has also been seen in iron doped GaAs materials.[36] Similar sturctures in absorption and photoluminescence have also been observed for iron in other III-V compounds as well.[25,36] Paramagnetic resonance experiments have shown that iron is incorporated substitutionally in the Ga sublattice, and acts as a deep acceptor.[37] At the Ga site, Fe loses three electrons to the bonds, becoming Fe^{3+} in a $3d^5$ configuration, and when an electron is trapped, a Fe^{2+} in a $3d^6$ configuration is created.

The energy levels of Fe^{2+} in $3d^6$ configuration derived on the basis of the crystal field theory and up to second order term in the spin-orbit correction have been reported in the literature.[38] At a site of tetrahedral symmetry (T_d), the lowest free ion term, ^5D, of $Fe^{2+}(3d^6)$, is split by the crystal field into a ground state doublet ^5E and $^5T_2$ excited state. Allowance for the spin-orbit coupling lifts the degeneracy of the $^5T_2$ level and in the second order approximation it lifts also the degeneracy of the ^5E levels, as shown in Fig. 13. The absorption and luminescence peaks mentioned above are due to the internal transitions between ^5E and $^5T_2$ multiplets.

The central peak at 0.37 eV in Figs. 5-9 can be attributed to the zero phonon transition from the lowest ^5E multiplet to the lowest level of $^5T_2$ multiplet. The structure appearing as a weak shoulder on the low energy side of the line and about less than 2 meV away from the main peak can also be attributed to a zero-phonon transition from the second lowest level of ^5E to lowest level of $^5T_2$. This transition has been reported as well resolved into a separate peak when the measurement is done at about liquid Helium temperature.[25] From the position of the main two zero-phonon lines, and Fig. 13, we obtain a value of $\Delta \sim 3000\ cm^{-1}$ for the crystal field energy. In

agreement with the reported values of Δ in the III-V compounds.[4] The other side structures are harder to interpret partly because it is difficult to distinguish between vibronic and electronic levels. As for the Jahn-Teller distorion, its effect on the ^5E states is not pronounced but it alters the splitting of $^5T_2$ levels.[39] Such changes would be observable in transitions involving higher energy levels of $^5T_2$. Unfortunately, these transitions cannot be seen in our data, because they have much smaller oscillator strengths[25,39] and therefore are buried under the structures due to other residual impurities or defects.

A detailed analysis of iron levels is not the main concern of this work. For that, one would have to study these levels in substrates doped with iron at concentrations much above that of the residual impurities and defects. Our aim in this work was rather to make a broad survey of deep levels in the undoped SI GaAs substrates. To our knowledge this is the first observation of the distinct iron signature in the bulk of-as-grown undoped SI GaAs by optical absorption or emission techniques. Estimating the value of the oscillator strength, the lowest detected concentration of Fe^{2+} was 5×10^{15} cm^{-3} in our work. Although Fe^{2+} in GaAs does have a distinct photoluminescence signature at 0.37 eV, to our knowledge no such emission band has been reported in the undoped-as-grown materials. Emission lines, however, do appear after the substrates are heated to about 700°C because of accumulation of iron in the near surface region at concentrations of 10^{17} to 10^{18} cm^{-3}.[40] Therefore it is significant that we have been able to detect Fe at levels of 10^{15} cm^{-3}. It should also be noted that in the absence of absorption bands due to other residual deep levels - interfering with the iron absorption spectra - the sensitivity of our present measurement would allow detection of iron at an order of magnitude below the above concentration level.

The threshold near 0.5 eV whose intensity scales with the intra-center transition at 0.37 eV can be identified with a transition from the valence band to the lower multiplet of Fe^{2+}. This is further substantiated by the fact that the position of this threshold moves with a temperature coefficient of $-(5.0\pm0.5)\times10^{-4}$ eV/K, which is similar to the temperature coefficient of the GaAs band gap; a similar observation has been made from Hall measurements.[41] A deep acceptor level at aobut 0.5 eV from the valence band, due to iron impurity has also been reported by several investigators.[42,43]

One might also expect to observe thresholds at higher energies due to the photoionization of electrons from Fe^{2+} levels to the conduction band. Figs. 3 and 4 show absorption thresholds in the range of 0.7 to 1.4 eV. However, in Sec. C it will be shown that these thresholds bear no relation to the presence of iron. They are rather attributed to another level commonly referred to as EL2,[35] which is believed to originate from a native defect sample. The absorption spectra due to EL2 can be quenched out at 80 K if the sample is illuminated by band gap light (see Sec. C). The remaining spectra shown in Fig. 12 does not contain any strong photoionization threshold. We therefore conclude that the magnitude of the photoionization cross section for electronic transition from the Fe^{2+} levels to the conduction band is very small. It can be argued that since the site symmetry of iron is tetrahedral, transitions from d-orbitals to conduction band s-like orbitals may be strongly prohibited by the selection rules.

B. Multilevel Defect Complex

Another dominant absorption band common to all the substrates we studied is the resonant spectra whose peak is near 0.4 eV, with a peak absorption coefficient typically below [illegible] cm^{-1}, a half width of about 30 meV, and usually

with two sides lobes. Being a peak rather than a threshold it can be interpreted as being due to an electronic transition between levels associated with the same center. The peak magnitude, and the detail shape of this structure as well as its sidebands varied from sample to sample as seen from Fig. 5 to 10, indicating that it is not associated with a simple multilevel impurity. It is more likely that this structure is due to a complex defect formed during the crystal growth or in the cooling period following the growth; whose exact structure is sensitively dependent upon the thermal history of the sample. To explore the possible origin of this level, sample M039 was cleaned, etched and annealed in a nitrogen atmosphere for four hours, at a temperature of 450 C. In contrast to the spectra of M039 shown in Fig. 6, the post-annealed spectra, shown in Fig. 11, indicated that the spectra at 0.4 eV has been annealed out. We thus conclude that i) the structure is a defect or defect complex; ii) this defect introduces two main levels into the gap separated by 0.4 eV; iii) these levels may split into more levels depending on the exact nature of the defect's immediate surrounding or additional complexing. These additional complexes could vary from sample to sample if they do not have identical thermal history. This would account for variations of the fine structures of the spectra among the samples. To our knowledge this is the first observation of this multilevel defect in SI LEC GaAs by optical techniques. A possibly related level has been observed by the photo-induced-transient spectroscopy (P.I.T.S.) in these samples.[44] However, an exact correlation between the levels observed by the wavelength modulation absorption and the level detected by P.I.T.S. must take into account the fact that the latter essentially yields information on the thermal emission from the level to the band, where as the former gives information about the intra-center transitions.

C. The EL2 in SI GaAs

The absorption spectra in the 0.6-1.4 eV shown in Figs. 3 and 4, are due to a deep level known as the EL2 which is associated with a native defect.[34] This defect is responsible for producing undoped semi-insulating GaAs by compensating the shallow impurities.[45,46] The exact origin and microscopic structure of this defect is still subject to considerable debate. Many of the investigations on this defect have involved studies of the correlation between the distribution pattern across the wafer, of the EL2 concentration, dislocation density, resistivity, as well as their relation to the stoichiometry of the melt, and conditions of the crystal growth.[47-50] Central to many of these studies is the precise measurement of the EL2 concentration and its distribution. Optical absorption spectroscopy, at room temperature, has commonly been used for this purpose, since it provides a convenient and nondestructive way of measuring the local concentration of the EL2 with good spatial resolution.[35] In this method the value of the absorption coefficient at about 1.2 eV is taken to be a measure of the EL2 concentration. However, we have shown that the presence of other residual deep levels, even at low concentrations, may give rise to appreciable absorption spectra in the neighborhood of the EL2 spectra.[51] Hence the apparent near-infrared absorption spectra cannot be a priori attributed to the EL2 levels alone.

The EL2 level has been shown to exhibit unusual properties, among them, the quenching of photoluminescence,[52] photocapacitance,[53] and optical absorption,[35] at low temperature ($T \lesssim 140$ K). In particular, the near-infrared absorption spectra due to EL2 quenches out at low temperature after the sample is illuminated with light of $0.9 \lesssim h\nu \lesssim 1.35$ eV and remains in the quenched state for many hours, even after the background illumination has been

turned off. The sensitivity of the wavelength modulation absorption spectroscopy together with the photo-quenching behavior of the EL2 allowed us to separate the EL2 spectra in the total absorption spectra and to observe the absorption spectra due to all other residual deep levels. Figure 12 shows the absorption due to all the deep levels other than the EL2 in the spectral region of 0.3 - 1.5 eV. The spectra of another SI GaAs sample in the spectral region of 0.5 - 1.5 eV is also shown in Fig. 14, in which the solid curve is the room temperature spectra and the dotted curve is the post-quenching spectra (at 80 K) due to residual absorption. As is seen from these figures, the post-quenching spectra do not exhibit any strong threshold associated with the photoionization of electrons from the iron impurity levels. In surveying several samples of undoped SI GaAs (LEC) we found that in a typical sample up to 20% of the room temperature optical absorption coefficient may be due to residual deep levels other than the EL2.[51]

Therefore in cases where the EL2 concentration and distribution must be measured with better than 10% accuracy,[49] room temperature optical absorption is not adequate. In such cases, the use of infrared wavelength modulation absorption in conjunction with the photo-quenching[51] represent a more accurate method of measuring the EL2 concentration.

V. CONCLUSIONS

In summary, wavelength modulation absorption was used to investigate the deep levels in the undoped SI GaAs (LEC) which is currently of high technological interest. Extensive low temperature measurements permitted observation of structures with fine details in the spectra of the SI GaAs at 0.37 eV and 0.4 eV. The structures near 0.37 eV were identified as intra-center transitions between the levels of accidental iron impurities incorporated in the Ga sublattice. To our knowledge this was the first observation of the iron absorption spectra in the SI GaAs at such low levels of concentration. The structure at 0.4 eV was considered as being due to an intra-center transition associated with a growth related multi-level defect complex. The fine details of this structure were found to be sensitive to the thermal history of the sample, and the whole structure was annealed out at about 450 C. Such a level and its characeristics have not been previously reported.

Measurements at liquid nitrogen temperature also allowed us to utilize the photo-quenching behavior of the absorption bands in the spectral region of 0.7 - 1.45 eV to assess the accuracy of the conventional room temperature optical absorption spectroscopies in measuring the deep level concentrations. It was demonstrated that the non-selectivity of such measurements may give erroneous results in measuring the concentration of specific deep levels, because of appreciable absorption due to the collective contribution of other residual deep levels. This result holds special significance in the current investigations on the origin of the non-uniform distribution of the main electron trap, the EL2 level, in the undoped SI GaAs (LEC).

ACKNOWLEDGMENTS

The support of this work by the Air Force Office of Scientific Research under AFOSR-83-0169B, the Army Research Office-Durham under DAAG29-81-K-0164, and the State of California-MICRO program is gratefully acknowledged.

REFERENCES

1. A. G. Milnes, Deep Impurities in Semiconductors (Wiley, New York, 1973).
2. S. T. Pantelides, Rev. Mod. Phys. 50, 797 (1978).
3. M. Scheffler, in Festkorperprobleme XXII, ed. by A. P. Grosse (Vieweg, Braunschweig, 1984), p. 115.
4. M. Jaros, Deep Levels in Semiconductors (Adam Hilger Ltd., Bristol, U.K., 1982).
5. V. F. Masterov, Sov. Phys. Semicond. 18, 1 (1984).
6. P. Vogl, Adv. Electron. Electron Phys. 62, 101 (1984).
7. R. K. Watt, Point Defects in Crystals (Wiley, New York, 1977).
8. C. T. Sah, Solid State Electron. 19, 975 (1976).
9. H. G. Grimmeiss, Ann. Rev. Mater. Sci. 7, 341 (1977).
10. G. L. Miller, D. V. Lang, and L. C. Kimerling, Ann. Rev. Mater. Sci. 7, 377 (1977).
11. A. Chantre, G. Vincent, and D. Bois, Phys. Rev. B 23, 5335 (1981)
12. A. Mircea and D. Bois, Inst. Phys. Conf. Ser. 46, 82 (1979).
13. G. M. Martin, in Semi-Insulating III-V Materials, Nottingham 1980, ed. by G. J. Rees (Shiva Publ., Orpington, U.K.), p. 13.
14. U. Kaufmann and J. Schneider, Adv. Electron. Electron Phys. 60, 81 (1982).
15. G. Vincent, A. Chantre, and D. Bois, J. Appl. Phys. 50, 5484 (1979).
16. A. Mircea and R. Mitonneau, J. Phys. Lett. (Orsay, Fr.) 40, L-31 (1979).
17. D. Pons and S. Makram-Ebeid, J. Phys. (Orsay, Fr.) 40, 1161 (1979).
18. J. J. Hopfield, G. D. Thomas, and M. Gershenzon, Phys. Rev. Lett. 10, 162 (1963).
19. P. J. Dean, J. D. Cuthbert, G. D. Thomas, and R. T. Lynch, Phys. Rev. Lett. 18, 122 (1967).

20. R. A. Street and W. Senske, Phys. Rev. Lett. 37, 1292 (1976).

21. E. Cohen and M. D. Sturge, Phys. Rev. B 15, 4020 (1977).

22. A. C. Carter, P. J. Dean, M. S. Skolnick, and R. A. Stradling, J. Phys. C 10, 5111 (1977).

23. E. Burstein, G. S. Picus, B. Henvis, and R. Wallis, J. Phys. Chem. Solids 1, 65 (1956).

24. W. H. Kleiner and W. E. Kragg, Phys. Rev. Lett. 25, 1490 (1970).

25. J. M. Baranowski, J. W. Allen, and G. L. Pearson, Phys. Rev. 160, 627 (1967).

26. R. Braunstein, R. K. Kim, and M. Braunstein, in Proceedings of the Symposium on "Laser Induced Damage in Optical Materials" (NBS-SP-620), Boulder, CO, USA, 1980 (Washington D.C., USA: NBS 1981), pp. 29-43.

27. M. Cardona, Modulation Spectroscopy (Academic Press, New York, 1969).

28. R. K. Willardson and A. C. Beer, editors, Semiconductors and Semimetals, Vol. 9, Modulation Techniques (Academic Press, New York, 1977).

29. A. D. Jonath, E. Voronkov, and R. H. Bube, J. Appl. Phys. 46, 1754 (1975).

30. M. Welkowsky and R. Braunstein, Rev. Sci. Instrum 43, 399 (1972).

31. R. K. Kim and R. Braunstein, Appl. Opt. 23, 1166 (1984).

32. R. Zucca, B. M. Wehch, P. M. Asbeck, R. C. Eden, and S. I. Long, in Proceedings of the Semi-Insulating II-V Materials Conference, Nottingham 1980, edited by G. J. Rees (Shiva, Orpington, U.K., 1980), p. 335.

33. R. Braunstein, R. K. Kim, D. Matthews, and M. Braunstein, Physica 117B and 118B (1983).

34. G. M. Martin, A. Mitonneau, and A. Mircea, Electron. Lett. 13, 191 (1977).

35. G. M. Martin, Appl. Phys. Lett. 39, 747 (1981).

36. W. H. Koschel, S. G. Bishop, and B. D. McCombe, in Proceedings of the 13th Internat'l Conference on Physics of Semiconductors, Rome, 1976, p. 1065.

37. E. M. Ganapol'skii, Sov. Phys. Solid State 15, 269 (1973).

38. W. Low and M. Weger, Phys. Rev. 118, 1119 (1960).

39. G. A. Slack, F. S. Ham, and R. M. Chrenko, Phys. Rev. 152, 376 (1966).

40. P. E. R. Nordquist, P. B. Klein, S. G. Bishop, and P. G. Siebermann, Inst. Phys. Conf. Ser. 56, 569 (1981).

41. R. W. Haisty, Appl. Phys. Lett. 7, 208 (1965).

42. V. I. Fistul, L. Ya. Pervova, E. M. Omelyanovskii, and E. P. Rashevskaya, Sov. Phys. Semicond. 8, 311 (1974).

43. D. V. Lang and R. A. Logan, J. Electron. Mater. 4, 1053 (1975).

44. M. R. Burd, Private Communication.

45. D. E. Holmes, R. T. Chen, K. R. Elliott, and C. G. Kirkpatrick, Appl. Phys. Lett. 40, 46 (1982).

46. H. Winston, Solid State Technol. 26, 145 (1983).

47. G. M. Martin, G. Jacob, G. Poilbaldu, A. Goltzone, and C. Schwab, Inst. Phys. Conf. Ser. 59, 281 (1981).

48. M. R. Brozel, I. Grant, R. M. Ware, and D. J. Stirland, Appl. Phys. Lett. 42, 610 (1983).

49. D. E. Holmes, R. T. Chen, K. R. Elliott, and C. G. Kirkpatrick, Appl. Phys. Lett. 43, 305 (1983).

50. S. Miyazawa, Y. Ishii, S. Ishida, and Y. Nanishi, Appl. Phys. Lett. 41, 853 (1983).

51. S. M. Eetemadi and R. Braunstein, to be published.

52. P. W. Yu, Appl. Phys. Lett. 44, 330 (1984).

53. G. Vincent and D. Bois, Solid State Commun. 27, 431 (1978).

FIGURE CAPTIONS

Fig. 1. Block diagram of the wavelength modulation absorption system.

Fig. 2. Block diagram of the data taking cycle.

Fig. 3. Absorption spectra of the MO39T SI GaAs (LEC) sample; T = 300 K, spectral range: 0.3 - 1.5 eV.

Fig. 4. Absorption spectra of the MO39T SI GaAs (LEC) sample; T = 160 K, spectral range: 0.3 - 1.5 eV.

Fig. 5. Absorption spectra of the MO39T SI GaAs (LEC) sample; T = 160 K, spectral range: 0.3 - 0.52 eV.

Fig. 6. Absorption spectra of the MO39T SI GaAs (LEC) sample; T = 80 K, spectral range: 0.3 - 0.52 eV.

Fig. 7. Absorption spectra of the MO43T SI GaAs (LEC) sample; T = 80 K, spectral range: 0.3 - 0.52 eV.

Fig. 8. Absorption spectra of the MO32T SI GaAs (LEC) sample; T = 80 K, spectral range: 0.3 - 0.52 eV.

Fig. 9. Absorption spectra of the MO40T SI GaAs (LEC) sample; T = 80 K, spectral range: 0.3 - 0.52 eV.

Fig. 10. Absorption spectra of the MO47T SI GaAs (LEC) sample; T = 80 K, spectral range: 0.3 - 0.52 eV.

Fig. 11. The post-annealed absorption spectra of the MO39T SI GaAs (LEC) sample: T = 80 K, spectral range: 0.3 - 0.52 eV.

Fig. 12. The post-illumination absorption spectra of the MO39T SI GaAs (LEC) samples; T = 80 K, spectral range: 0.3 - 0.52 eV.

Fig. 13. Energy level scheme of the ^5D level of Fe^{2+} ($3d^6$) in GaAs.

Fig. 14. The total absorption spectra at 300 K (solid curve) and the residual absorption spectra after photo-quenching at 80 K (dotted curve) of the MO43T SI GaAs (LEC) sample.

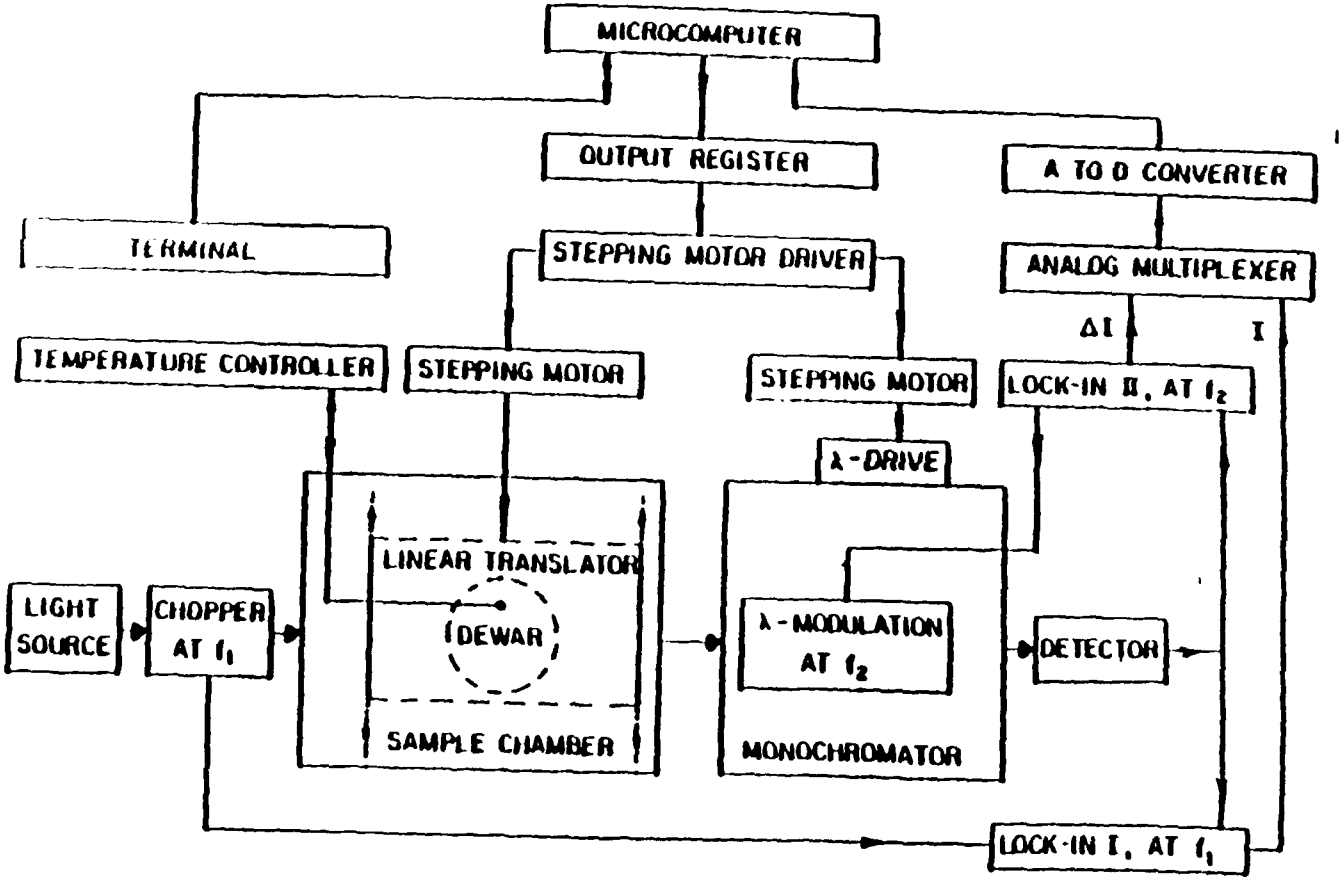
MICROCOMPUTER
OUTPUT REGISTER
A TO D CONVERTER
TERMINAL
STEPPING MOTOR DRIVER
ANALOG MULTIPLEXER
ΔI
I
TEMPERATURE CONTROLLER
STEPPING MOTOR
STEPPING MOTOR
LOCK-IN II, AT f2
λ-DRIVE
LINEAR TRANSLATOR
LIGHT SOURCE
CHOPPER AT f1
DEWAR
λ-MODULATION AT f2
DETECTOR
SAMPLE CHAMBER
MONOCHROMATOR
LOCK-IN I, AT f1

FIG. 1

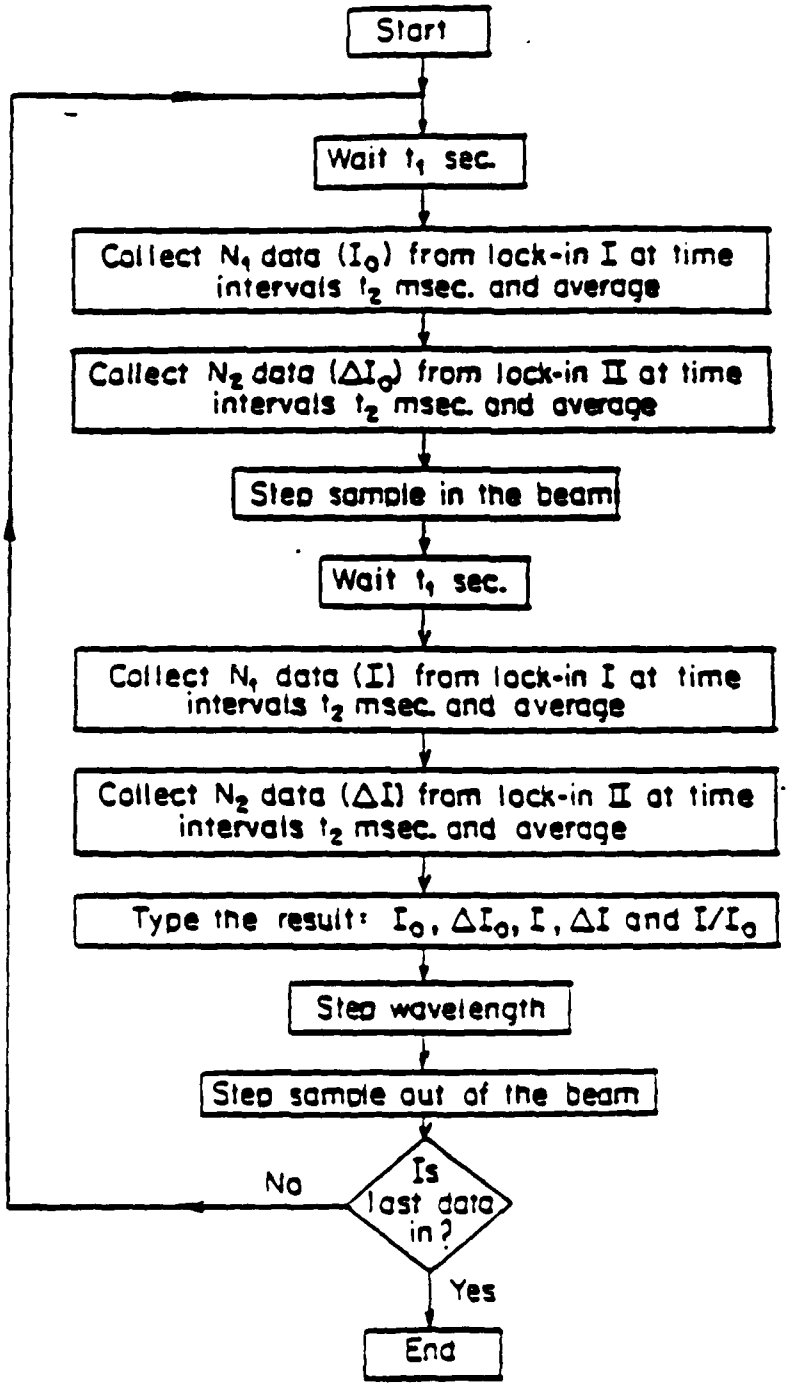
Start
Wait t_1 sec.
Collect N_1 data (I_0) from lock-in I at time intervals t_2 msec. and average
Collect N_2 data (ΔI_0) from lock-in II at time intervals t_2 msec. and average
Step sample in the beam
Wait t_1 sec.
Collect N_1 data (I) from lock-in I at time intervals t_2 msec. and average
Collect N_2 data (ΔI) from lock-in II at time intervals t_2 msec. and average
Type the result: I_0, ΔI_0, I, ΔI and I/I_0
Step wavelength
Step sample out of the beam
Is last data in?
No
Yes
End

Fig. 2

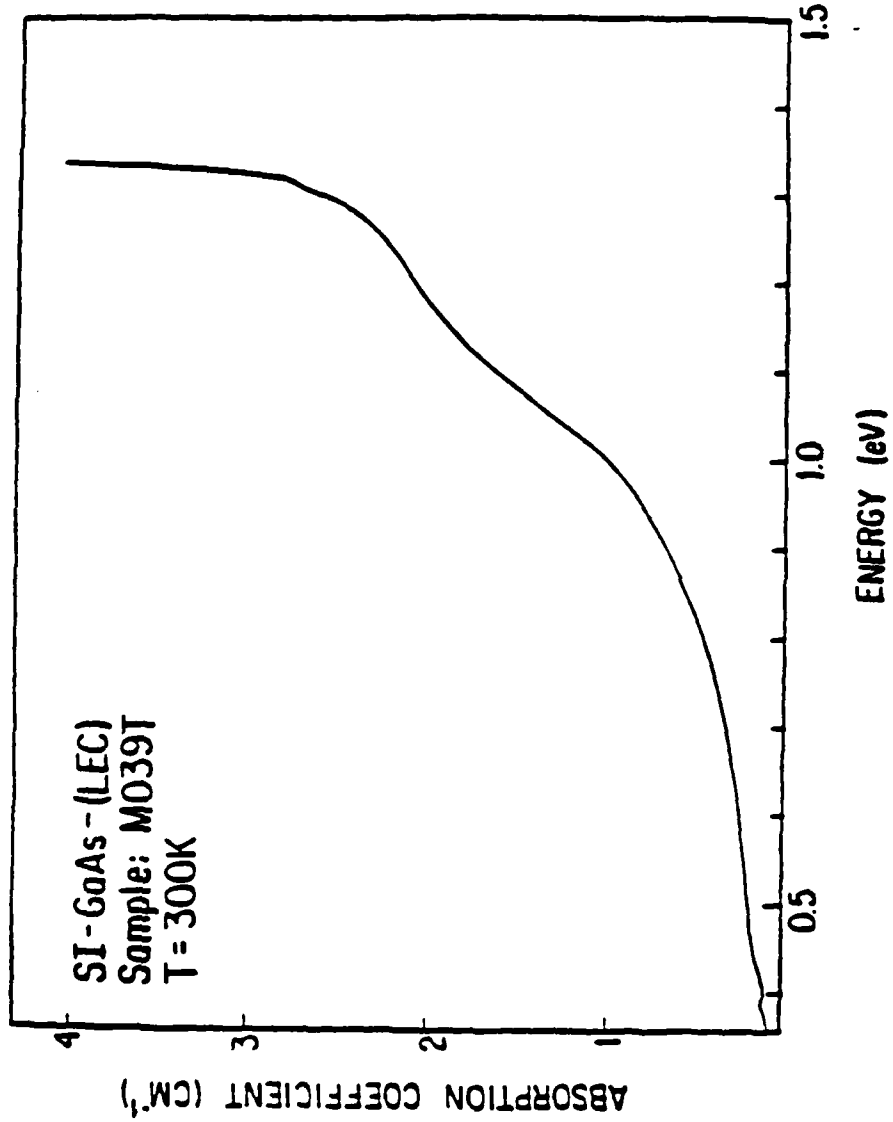
SI-GaAs-(LEC)
Sample: M039T
T=300K
ABSORPTION COEFFICIENT (CM⁻¹)
ENERGY (eV)
0.5
1.0
1.5
1
2
3
4

Fig. 3

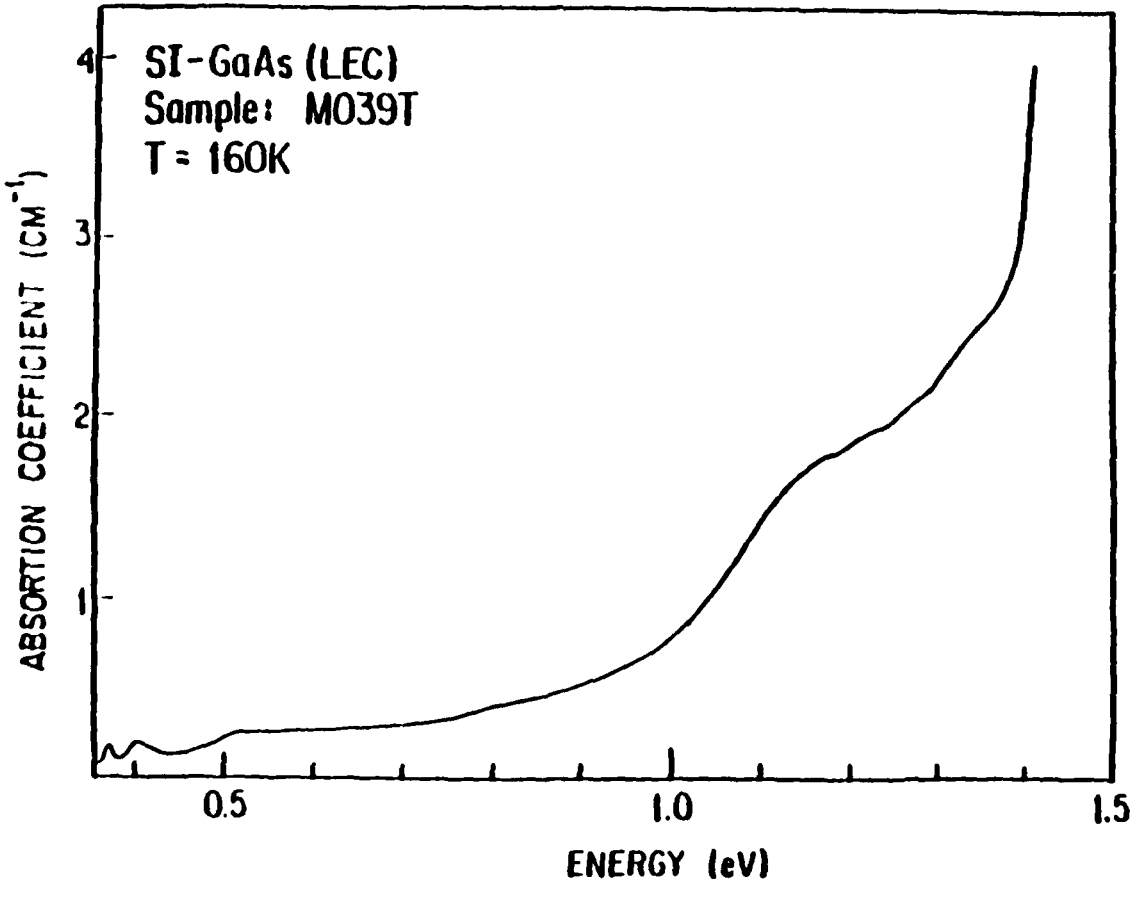
SI-GaAs (LEC)
Sample: M039T
T = 160K
ABSORTION COEFFICIENT (CM^{-1})
4
3
2
1
0.5
1.0
1.5
ENERGY (eV)

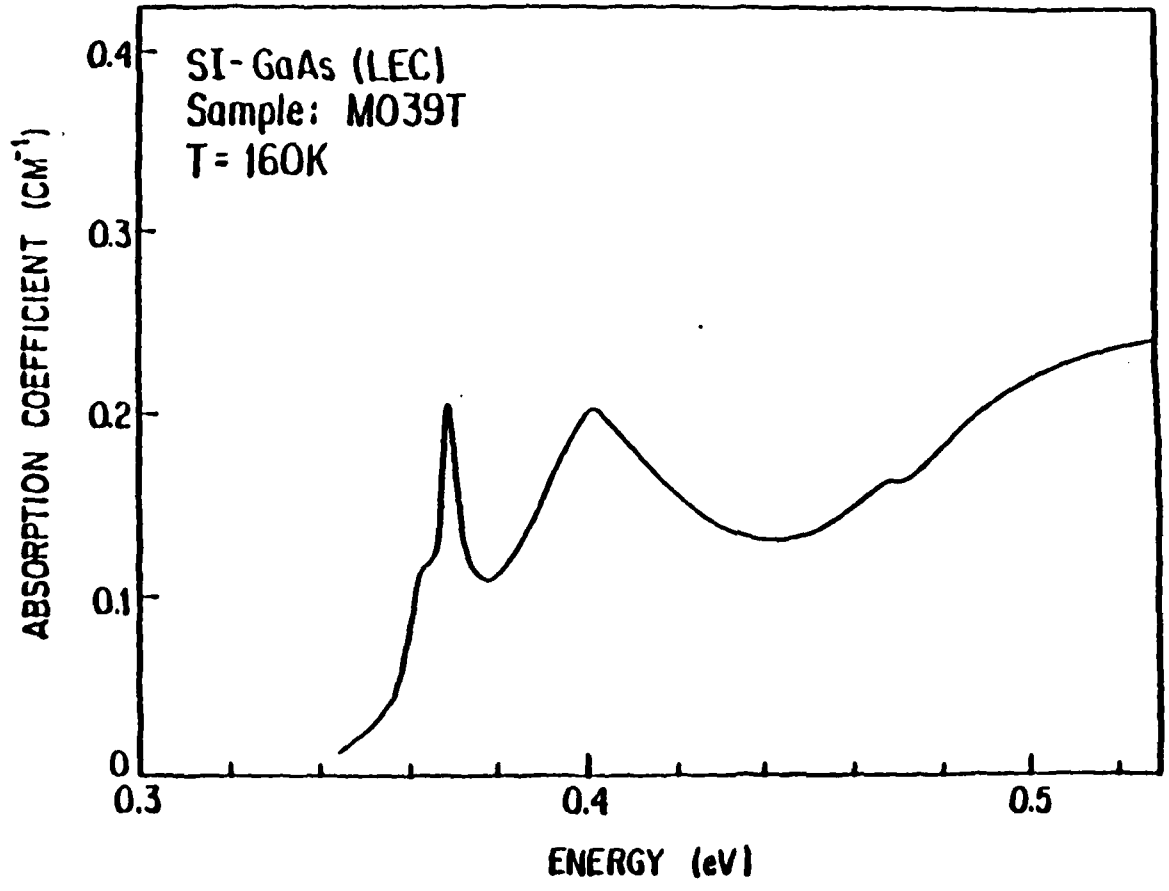
SI-GaAs (LEC)
Sample: M039T
T = 160K
ABSORPTION COEFFICIENT (CM⁻¹)
0.4
0.3
0.2
0.1
0
0.3
0.4
0.5
ENERGY (eV)

FIG. 5

FIG. 6

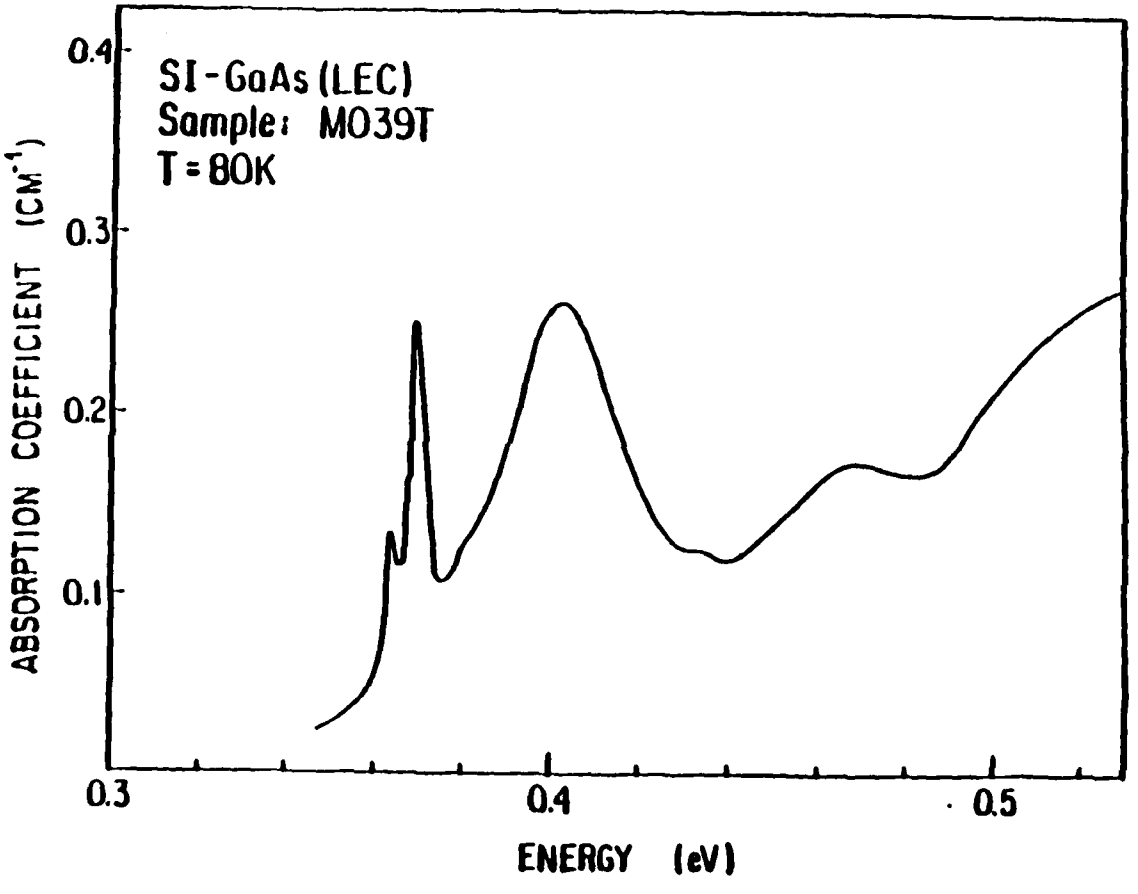
SI-GaAs (LEC)
Sample: M039T
T = 80K
ABSORPTION COEFFICIENT (CM^{-1})
0.4
0.3
0.2
0.1
0.3
0.4
0.5
ENERGY (eV)

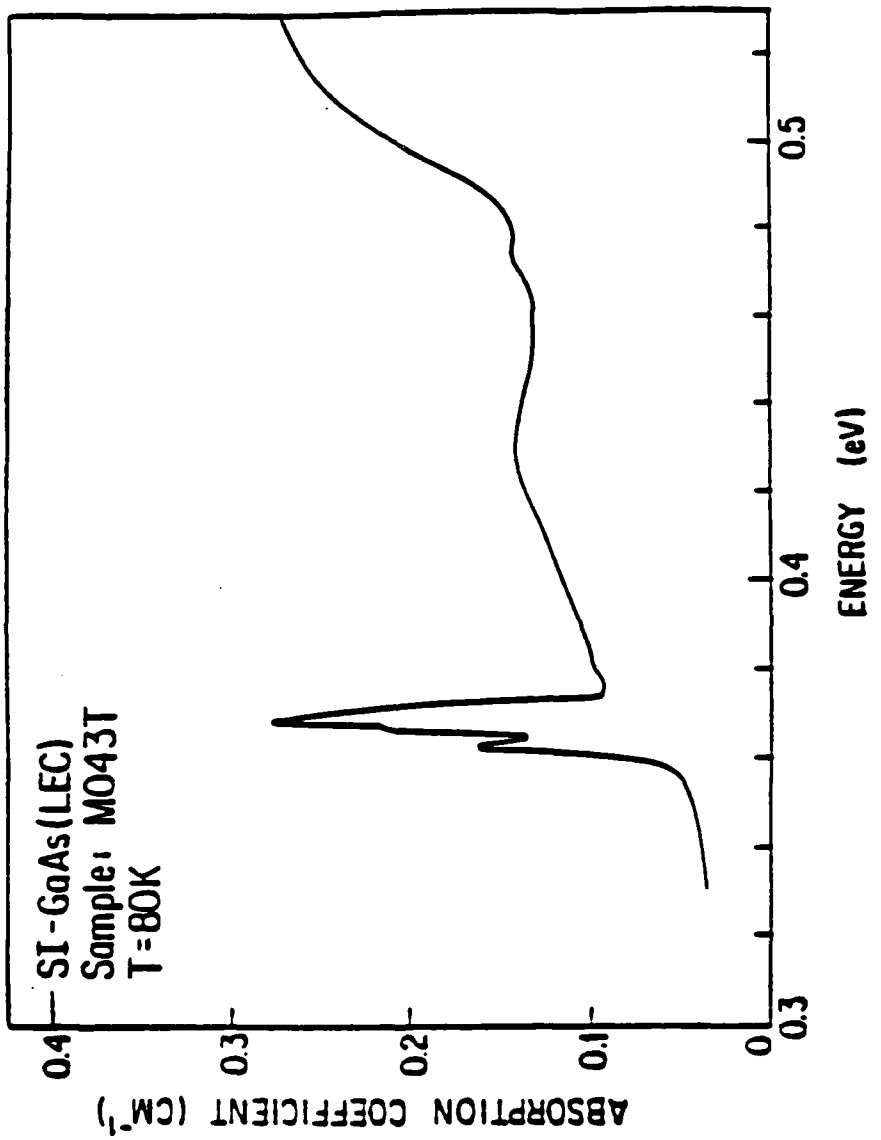
SI-GaAs(LEC)
Sample: MO43T
T=80K
ABSORPTION COEFFICIENT (CM⁻¹)
0
0.1
0.2
0.3
0.4
0.3
0.4
0.5
ENERGY (eV)

Fig. 7

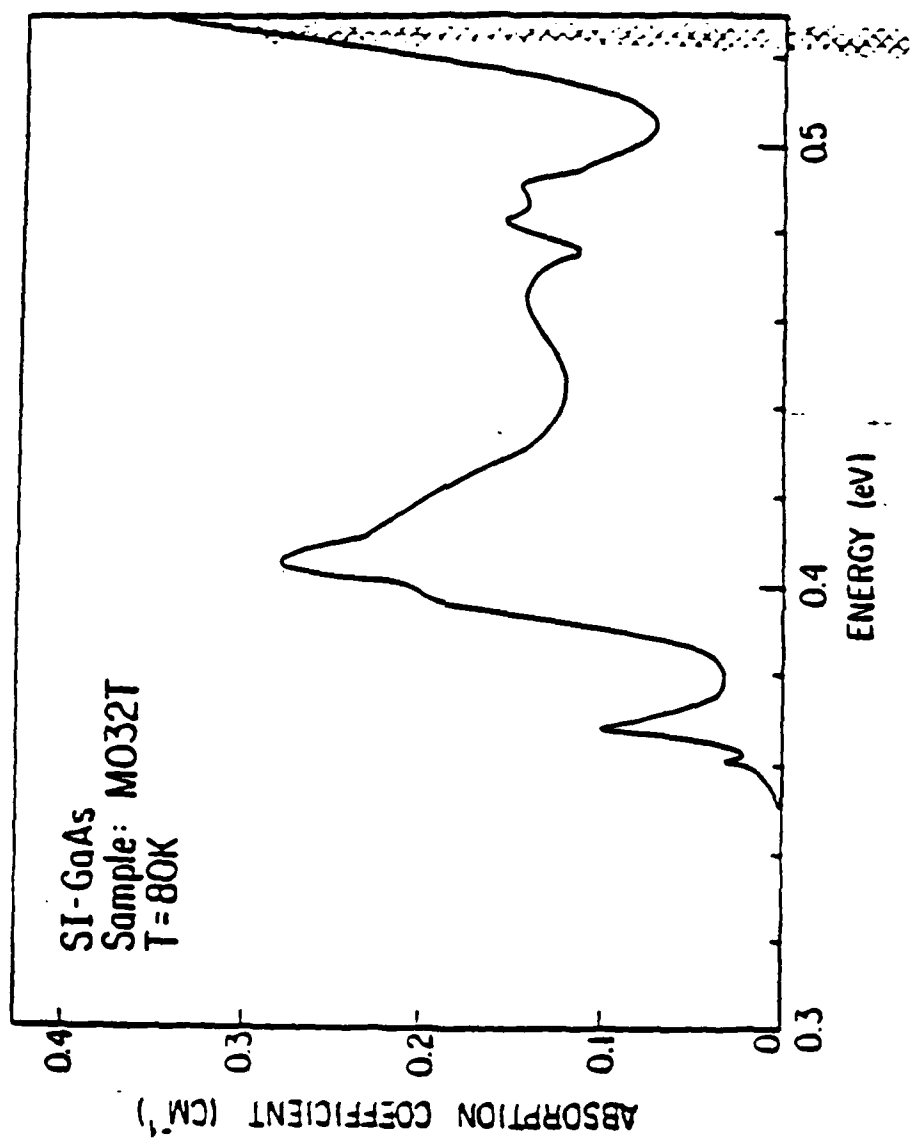
SI-GaAs
Sample: M032T
T=80K
0.4
0.3
0.2
0.1
0
0.3
0.4
0.5
ENERGY (eV)
ABSORPTION COEFFICIENT (CM⁻¹)

Fig. 8

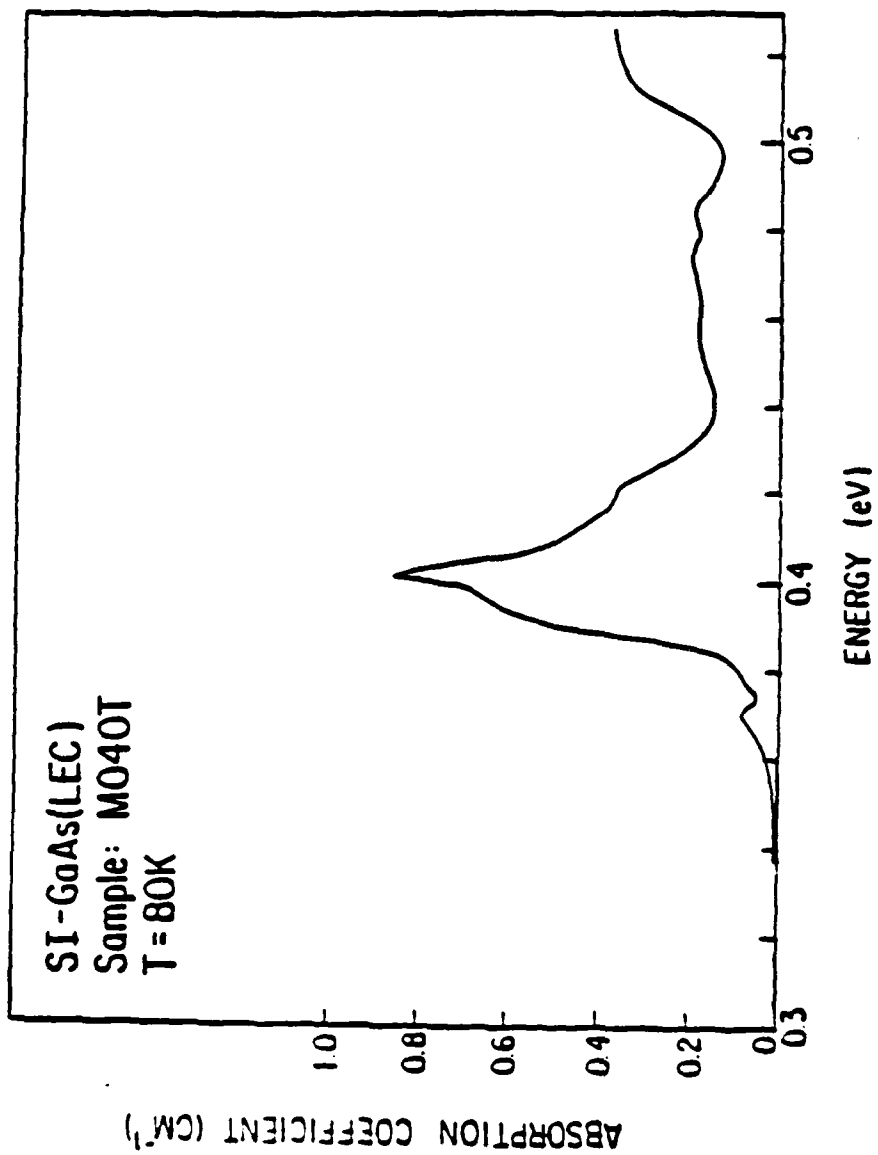
SI-GaAs(LEC)
Sample: M040T
T=80K
ABSORPTION COEFFICIENT (CM⁻¹)
1.0
0.8
0.6
0.4
0.2
0
0.3
0.4
0.5
ENERGY (eV)

Fig. 9

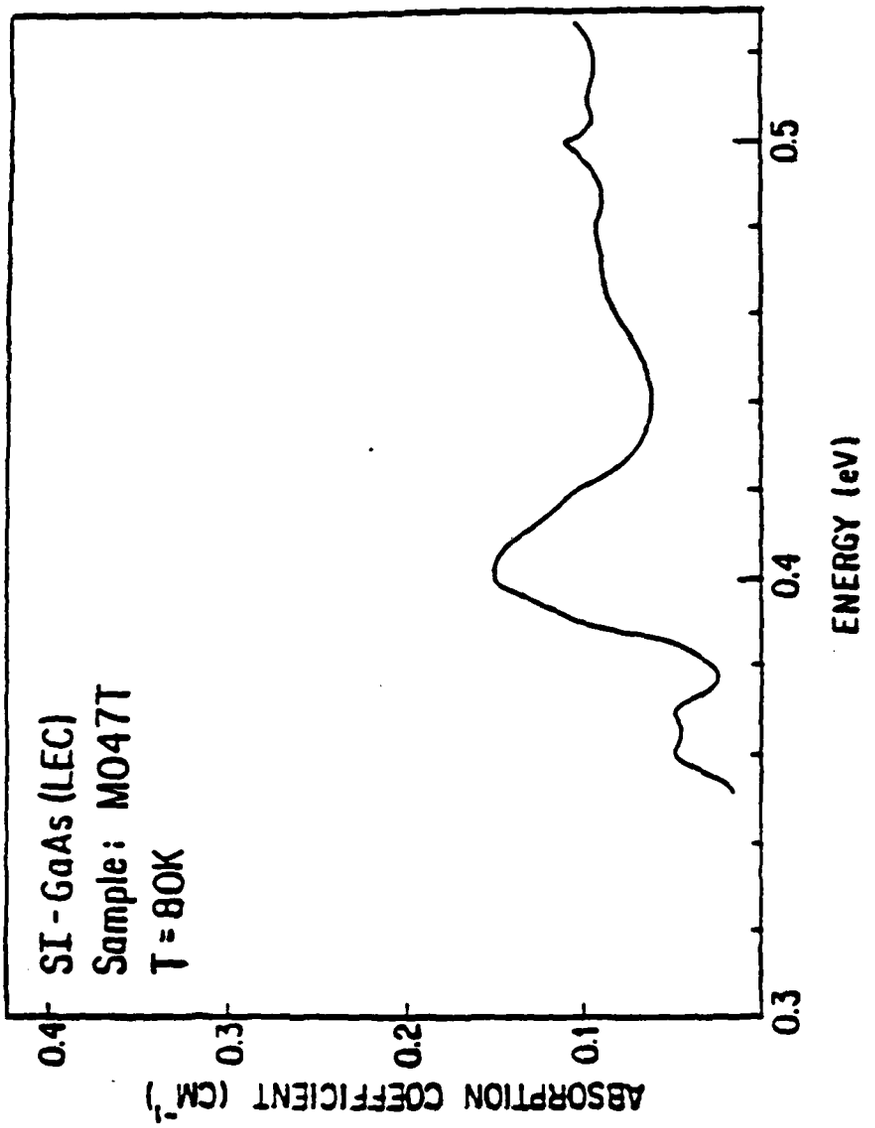
SI-GaAs (LEC)
Sample: M047T
T=80K
ABSORPTION COEFFICIENT (CM⁻¹)
0.4
0.3
0.2
0.1
0.3
0.4
0.5
ENERGY (eV)

Fig. 10

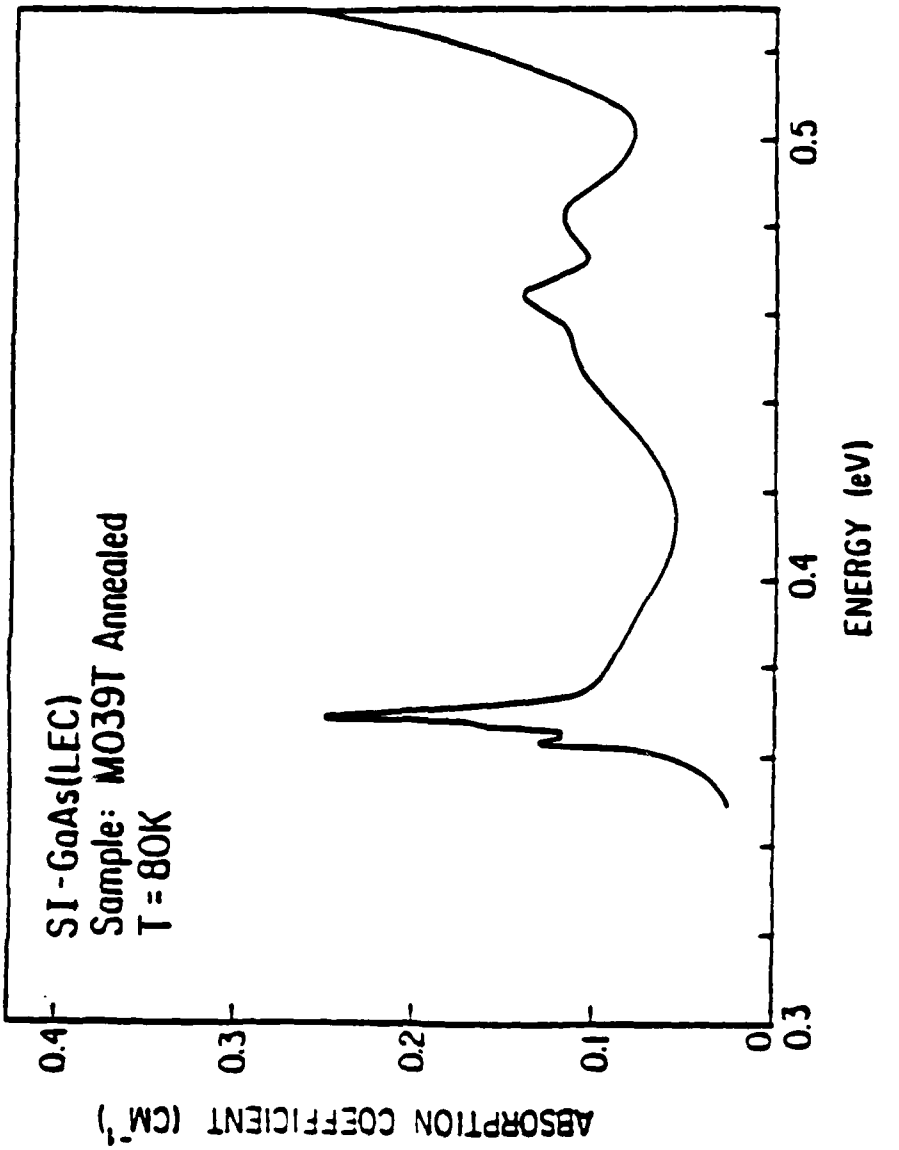
SI-GaAs(LEC)
Sample: M039T Annealed
T = 80K
ABSORPTION COEFFICIENT (CM⁻¹)
0.4
0.3
0.2
0.1
0
0.3
0.4
0.5
ENERGY (eV)

Fig. 11

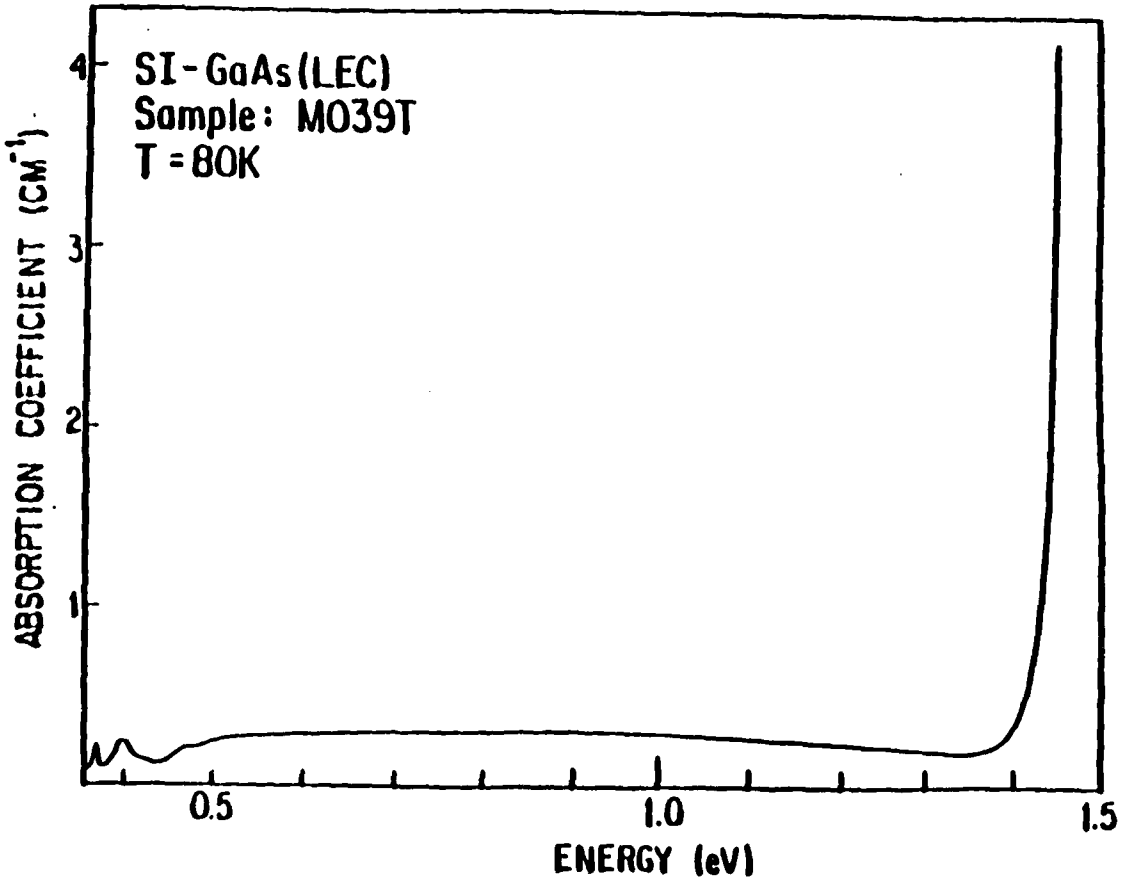
SI-GaAs(LEC)
Sample: M039T
T = 80K
ABSORPTION COEFFICIENT (CM⁻¹)
4
3
2
1
0.5
1.0
1.5
ENERGY (eV)

Fig. 12

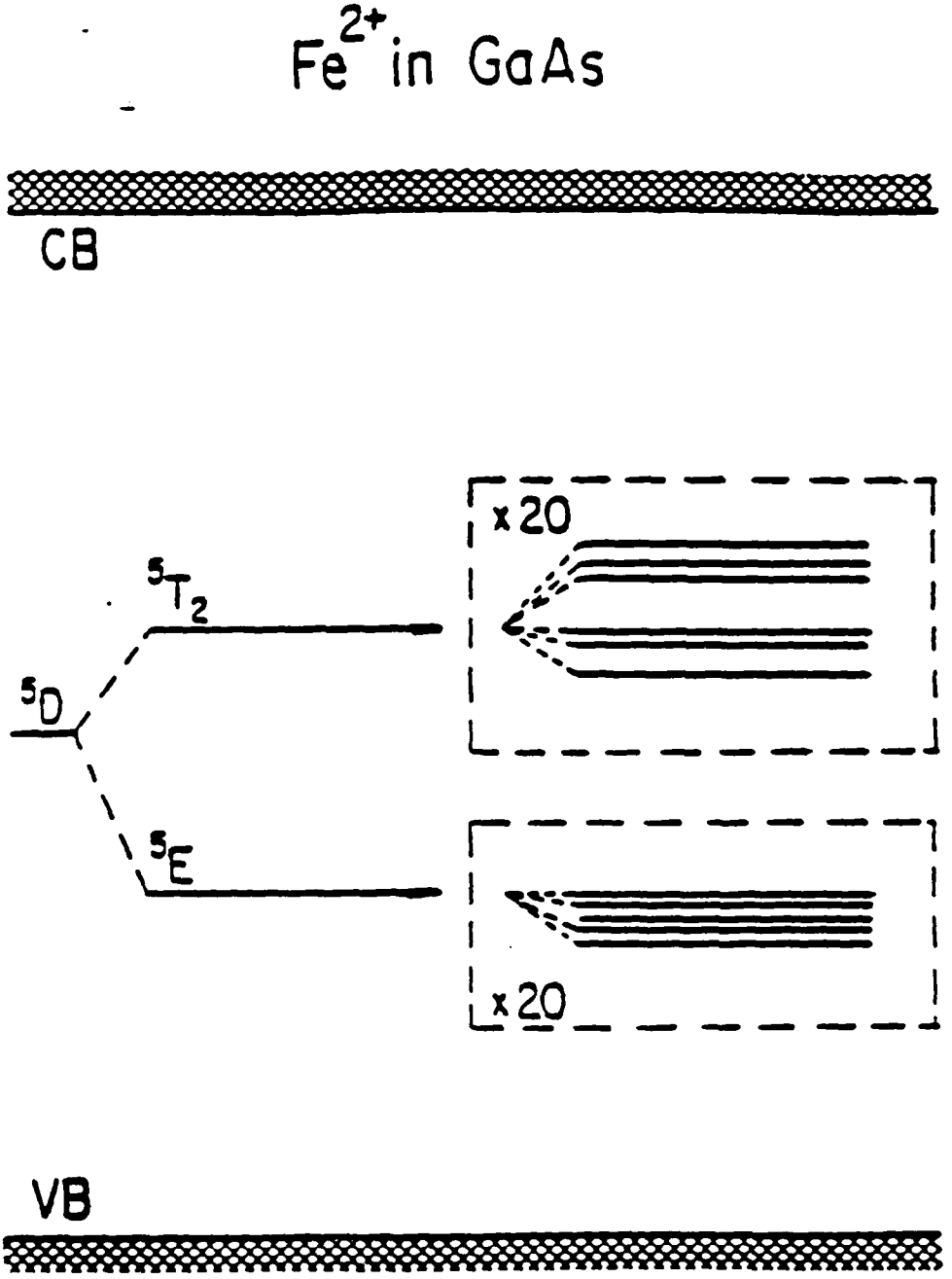

Fig. 13

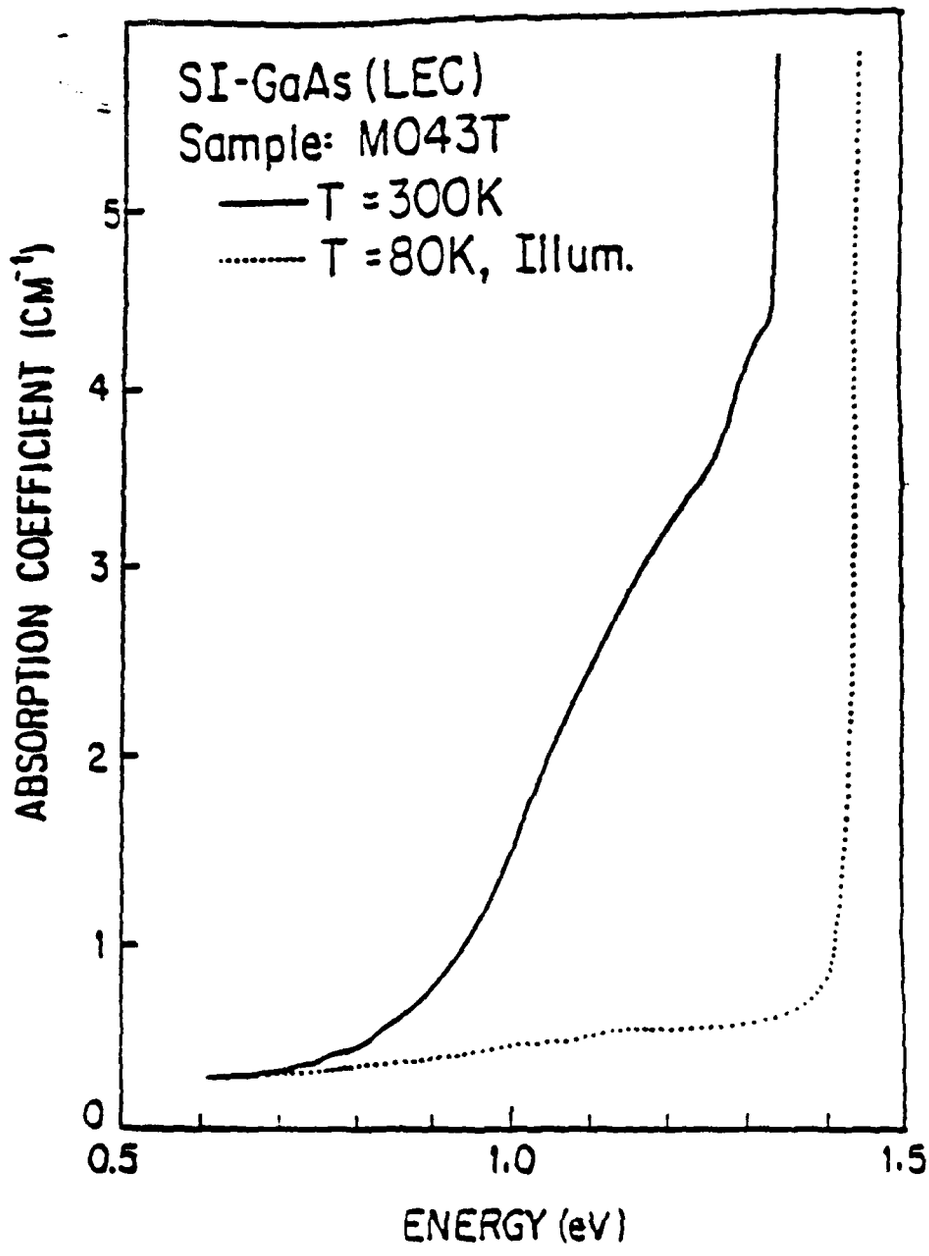
SI-GaAs (LEC)
Sample: M043T
T = 300K
T = 80K, Illum.
ABSORPTION COEFFICIENT (CM⁻¹)
0
1
2
3
4
5
0.5
1.0
1.5
ENERGY (eV)

Fig. 14

Measurement of the EL2 and Chromium Concentration in the Semi-Insulating GaAs

S. M. Eetemadi and R. Braunstein

Department of Physics, University of California,
Los Angeles, California 90024

Low temperature infrared wavelength modulation was performed on GaAs in conjunction with the photo-quenching of the absorption in the spectral region of 0.7-1.4 eV, due to the EL2 levels, to assess the accuracy of the conventional room temperature optical absorption spectroscopy in measuring EL2 and chromium concentrations; an accurate method for such measurements was suggested.

The deep chromium acceptor level at E_v + 0.73 eV, and the deep donor level, commonly referred to as EL2, at E_c - 0.74 eV are responsible for controlling the compensation mechanism of semi-insulating (SI) GaAs, grown by the liquid encapsulated Czochralski (LEC) technique.[1-6] Non-uniformities in the concentration of deep levels could adversely affect the yield, reliability, and performance of the devices made from these substrates. The correlation between the distribution pattern across the wafer, of the concentration of the deep levels, resistivity, dislocation density, as well as their relation to the stoichiometry of the melt and conditions of the crystal growth, are essential in understanding the origin and nature of these nonuniformities.[6-9] Central to many of these studies is the measurement of the concentration and the distribution of the deep levels, especially EL2 and chromium. However, many of the standard methods of measuring deep level concentration are either not suitable or not easily applicable to the semi-insulating materials. Optical absorption spectroscopy at room temperature in the near infrared spectral region is considered a convenient, rapid, and nondestructive way of measuring the local concentration of deep levels with good spatial resolution,[2] and is used in the above reference studies, for EL2 and chromium concentration profiles in SI GaAs. However, for low concentration of impurities or defects, conventional optical absorption lacks sensitivity, and the improved sensitivity of infrared wavelength modulation must be employed.[10] The purpose of the present work was to make an assessment of the accuracy of the room temperature optical absorption method in measuring the EL2 and chromium concentrations.

In undoped SI GaAs, EL2 seems to be the dominant deep level. The total absorption coefficient of this defect and other residual impurities can be

written as

$$\alpha(E) = N_{EL2}\,\sigma^{e}(E) f_{EL2} + N_{EL2}\,\sigma^{h}(1 - f_{EL2}) + \sum_{j} N_j[\sigma_j^{e} f_j + \sigma_j^{h}(1-f_j)] \quad (1)$$

where N_{EL2} is the EL2 concentration, σ^{e} and σ^{h} are the photo-ionization cross section for electrons and holes respectively, f_{EL2} is the occupancy of the EL2 level which depends on the relative position of the Fermi energy and the EL2 level. The last term represents the absorption coefficient due to all other residual impurity and defect levels present in the material. It is commonly assumed that the EL2 levels are almost completely filled (f_{EL2} close to unity) if the Hall measurements indicate strongly n-type character for the SI GaAs. Thus the second term in Eq. (1) can be omitted and the first term becomes $N_{EL2}\sigma^{e}$. Furthermore, if independent measurements such as secondary ion mass spectroscopy (SIMS) indicate very low concentration of other deep levels compared to the EL2, the magnitude of the last term in Eq. (1) is assumed to be negligible. The above two assumptions simplify Eq. (1) to $\alpha(E) = N_{EL2}\sigma^{e}$. This is the form commonly used in conjunction with the reported values of the photo-ionization cross section to obtain the concentration of EL2 levels in the SI GaAs.

The validity of the first assumption regarding the occupancy of the EL2 level has been discussed.[11] It is shown that in the typical SI GaAs, the occupancy of the EL2 level changes most noticeably in the region where the Hall mobility is still high, and the sign of the Hall constant indicates a dominant contribution from electrons. Therefore, changes in the optical absorption coefficient cannot be a priori attributed to the changes in the EL2

concentration. However, the validity of the second assumption regarding the smallness of the collective contribution of all the other residual deep levels (hereafter referred to as residual absorption coefficient), to the total absorption coefficient, has not been studied, and no estimate of its magnitude is available.

The following arguments suggest that, even if the concentration of residual deep levels is individually small compared to the EL2, the magnitude of the residual absorption coefficient may still be appreciable, and therefore cannot be a priori ignored. Firstly, the photoionization spectra of deep levels are broad and often featureless, extending beyond $2E_j$, where E_j is the threshold energy of the j-th deep level.[12] Thus the photoionization cross section of all other deep levels present in the material may have appreciable values in the 1.1 - 1.2 eV region, in the neighborhood of the EL2 spectra. Secondly, even though the concentration of the individual residual deep levels are small compared to the EL2, the number of different types of such levels in SI GaAs is usually large. And lastly, the values of the photoionization cross section of deep levels span several orders of magnitude, and some of the less dominant levels, in concentration, may have a much larger photoionization cross section, making $N_j\sigma_j$ appreciable.

The object of the present work was to make an estimate of the magnitude of the residual absorption coefficient, and thus, of the error that results in ignoring its contribution when the room temperature optical absorption coefficient is used to measure the EL2 concentration in the undoped SI GaAs.

Low temperature wavelength modulation absorption, with and without background illumination, made it possible to separate the absorption coefficient of EL2 from other residual deep levels. The experiment showed that, in the typical undoped SI GaAs, with EL2 as the dominant deep level,

about 10-20% of the absorption coefficient was due to residual deep levels. The significance of this error is discussed, and an appropriate method which completely eliminates this error is suggested. Special problems which arise in the case of the chromium doped SI GaAs (LEC) are also discussed.

The EL2 level has been shown to exhibit unusual properties--among them, the quenching of photoluminescence,[13] photocapacitance,[14] and optical absorption,[2] at low temperature ($T \lesssim 140$ K). In particular, the near-infrared absorption spectra due to EL2 quench out at low temperature after the sample is illuminated with light of $0.9 \lesssim h\upsilon \lesssim 1.35$ eV and remains in the quenched state for many hours, even after the background illumination has been turned off. These properties have been explained by postulating the existence of a metastable state of the EL2, accessible at low temperature with background illumination,[15] or by a charge-state-controlled structural relaxation model.[16] Taking advantage of the quenching of the absorption coefficient, we studied the near infrared absorption spectra of undoped SI GaAs samples of different ingots, all grown in pyrolitic boron nitride (PBN) crucibles, by the liquid encapsulated Czochralski (LEC), and B_2O_3 as the encapsulant. They had resistivity greater than 10^7 Ω-cm, Hall effect mobilities of 4570-6319 cm^2/V sec, electron concentrations in the range $(1.3 - 2.4) \times 10^7$ cm^{-3}, and EL2 levels virtually 100% occupied. The samples were typically 3 mm thick with the surfaces polished with Br-methanol.

These studies were performed using a wavelength-modulated spectrometer described elsewhere,[10] with sensitivity of 10^{-4} cm^{-1} in the near infrared spectral region. The spectra were first taken at room temperature from 0.6 eV to 1.45 eV; a typical result is shown in Fig. 1 (solid curve). The samples were then cooled down, while in the dark, to 80 K. The values of the absorption coefficients at 1.2 eV were recorded, and while monitoring its

value at this energy, the samples were illuminated with a 50 W tungsten/halogen lamp, until complete quenching of the absorption was reached in 10-20 minutes, and no further change in the absorption coefficients was observed. The illumination was then turned off, and the samples were left in darkness for another 20 minutes. This last step was done to avoid a possible non-equilibrium population of other deep levels present, as will be explained in connection with the dependence of the chromium level population on illumination. The post-illumination and relaxation spectra thus obtained are also shown in Fig. 1 (dotted curve). The resulting spectra, except for finer details revealed in our experiments due to better sensitivity, were in general agreement with other reported spectra.[2] As the samples were warmed up, the absorption coefficient monitored at 1.2 eV recovered in the manner shown in Fig. 2.

The shape of the residual absorption spectra at 80 K, from 0.6 eV to 1.45 eV, varied in detail from sample to sample but was generally a small and rather flat plateau. Its magnitude also varied from sample to sample, and at 1.2 eV the variation was typically 10-20% of the total absorption coefficient for a given temperature prior to the quenching by illumination.

The above result indicates that in typical LEC SI GaAs, only 80-90% of the absorption coefficient measured as 80 K may be attributed to the EL2, and the rest is due to the presence of other deep levels. The following argument shows that this result is also true for measurements performed at room temperature. At 1.2 eV the value of the absorption coefficient at 300 K was nearly equal to that measured at 80 K. Furthermore, since near 1.2 eV the residual absorption spectra are quite flat and featureless (dotted curve in Fig. 1), the magnitude of the residual absorption coefficient at room temperature is not expected to be appreciably different from its value at 80 K. Hence, the ratio of the residual and total absorption coefficient at room

temperature and 80 K should be nearly the same. Therefore in typical undoped SI GaAs (LEC), up to 20% of the apparent room temperature spectra of the EL2 might be due to the spectra of other residual deep levels.

The significance of the above result can be appreciated in the context of the following reported observations:

Fabrication of high-performance GaAs IC's makes stringent demands on the uniformity of the substrate materials. Very marked non-uniformities in the electrical properties across the wafers of SI GaAs (LEC) has been reported.[9,17] Since the semi-insulating properties of this material are achieved by the compensation of residual shallow impurities by deep levels,[3,18] much attention has been focused on the distribution of deep levels in the starting substrate material. The deep donor EL2, which is thought to be an "antisite defect," is the dominant deep level in the melt grown GaAs. Optical absorption and photoluminescence experiments have shown that the distribution of the EL2 levels follows a characteristic "W" or "U" shaped pattern along the diameter of the SI GaAs wafers.[7,19-21] The variations in the concentration of the EL2, as measured by room temperature optical absorption, have been reported to be up to ± 10% of the average EL2 concentration.[8] Similar patterns have also been observed in the distribution of dislocation densities.[7,20,22] However, some uncertainty remains about the quantitative correlation between the profiles of the dislocation density and the EL2 concentration,[8,22] and hence the association of "antisite defects" to the dislocation climb processes.[23] It must also be added that there have been reports of precipitation of some impurities around the dislocation centers, and hence the impurity concentration might be high in regions of high dislocation density.[24,25]

As mentioned, the EL2 concentration profile has been obtained primarily by room temperature optical measurements. In the light of our results regarding

the percent contribution of residual deep levels to the apparent measured spectra of EL2, it is quite conceivable that an increase in the absorption coefficient in regions of high dislocation density is due to the increase in the concentration of precipiate impurities rather than the EL2. Therefore studies of the quantitative correlation between the distribution of EL2 and dislocation density require techniques which can selectively measure the EL2 concentration with accuracies much better than 10%. The low temperature method suggested below completely separates the EL2 contribution from other deep levels and thus provides an accurate measure of the EL2 concentration.

The method is to first measure the pre-illumination spectra at a temperature below ~ 120 K by a very low intensity and quasi-chromatic light to avoid any partial quenching of the absorption coefficient. The absorption spectra due to EL2 are subsequently quenched out by illuminating the sample with intense light of $h\nu > 1.1$ eV and the remaining spectra are recorded after a period of relaxation in the dark for about 20 minutes. The difference between the pre-illumination and the post-relaxation spectra, thus obtained, would belong to EL2 levels, and their concentration can be obtained from the value of the photoionization cross section[2] and the occupancy of the level.[11] This is in contrast to the commonly used method, in which the room temperature absorption coefficient at ~ 1.2 eV is attributed to the EL2 level alone, and is used as a measure of the EL2 concentration. As we showed above, in LEC SI GaAs substrates, even if the precise occupancy of the EL2 is known, the room temperature measurement of the EL2 concentration could still be in error by up to 20%, because of the collective contribution of other deep levels present in the material. It should also be mentioned that the reported values of the photoionization cross section, which have been obtained by calibrating the room temperature absorption coefficient with independently measured

concentration, are subject to the same error. However, the newly suggested low temperature method can be used in the same manner to obtain a more accurate value of the EL2's photoionization cross section.

The low temperature pre- and post-quenching absorption (LTPPQA) method suggested above can also be used to obtain concentration of chromium or other level impurities and defects. In GaAs:Cr materials it has been established that Cr centers can be in any of the various stable charged states, Cr^{2+}, Cr^{3+}, and Cr^{4+} (Cr^{4+} is seen primarily in p-type materials) depending on the position of the Fermi level.[26-30] Furthermore, it is believed that it is the $(Cr^{3+})/(Cr^{2+})$ ratio, which plays the dominant role in the compensation mechanism.[6,31] However, direct measurement of $(Cr^{3+})/(Cr^{2+})$ by optical absorption of room temperature is difficult because of the presence of the EL2 levels in appreciable amounts in the melt grown materials and hence the total absorption coefficient is due to the Cr as well as the EL2 spectra. An indirect method of obtaining the $(Cr^{3+})/(Cr^{2+})$ ratio has been to estimate the EL2 contribution by taking it to be equal to the spectra of an undoped SI GaAs multiplied by a constant factor.[6] The EL2 spectra thus found are subtracted from the total absorption spectra, to obtain the spectra due to Cr levels alone, from which the $(Cr^{3+})/(Cr^{2+})$ ratio is estimated.

The present LTPPQA method has the distinct advantage that it directly eliminates the EL2 contribution, revealing the remaining spectra. Figure 3 shows the spectra of another undoped SI GaAs (LEC) sample before and after quenching of the EL2. The residual absorption coefficient is about 70% of the total absorption coefficient at 1.2 eV, and consists of several thresholds. Although the post-quenching spectra still have some of the structures reminiscent of the unquenched EL2 spectra (at 10 K),[2] additional illumination and recycling of the quenching procedure did not change the spectra, thus

ruling out contribution to the remaining spectra of a possible partially quenched state of EL2 level. The various thresholds of the residual absorption coefficient in Fig. 3 (dashed curve) resembled the photoionization thresholds of the various reported charged states of Cr,[6] indicating that chromium is perhaps the dominant accidental deep level impurity in this sample.

As it was pointed out earlier, in using the LTPPQA method, especially in obtaining Cr spectra and after the EL2 has been quenched out, it is necessary to keep the sample in darkness for several minutes before the remaining spectra are recorded. This step is required for the following reason. It has been demonstrated in experiments such as low temperature EPR,[28,32,33] ESR,[27] and photoconductivity,[34] that in GaAs:Cr, the occupancy of the various change states of Cr can be changed by illuminating the sample with light. Illumination of the Cr^{3+} centers with light of $h\nu > 0.75$ eV increases the concentration of Cr^{2+} and Cr^{4+} while decreasing the number of Cr^{3+} states.[35] The system, however, has been observed to return to the equilibrium population in minutes after the light is turned off.[33] This relaxation time is characteristically much less than the time (several hours) that the EL2 remains in its "metastable stabe," if the measurement is done at temperature well below the quenching temperature (< 40 K). Therefore, following the quenching out of the EL2 spectra, if the background illumination is turned off, the Cr charged states would reach their equilibrium population (in minutes), while the metastable of the EL2 remains effectively unaltered. The remaining spectra thus obtained are primarily due to the appropriate equilibrium concentration of Cr charged states. Although the dependence of charged states population on the background illumination has been most extensively studied for Cr in GaAs, other multilevel impurity and defects are prone to the same phenomena and thus are subject to the above consideration. It must also be pointed out that a portion

of the remaining spectra can still be due to residual impurities or defects other than EL2 and Cr, which in contrast to EL2 in SI GaAs can no longer be directly measured and remains as the error of the measurement. This error would, however, be small if the material under study has relatively high Cr concentration. The LTPPQA method can be similarly used for other impurities or defects besides Cr in GaAs materials.

In summary, we have shown that, using the magnitude of the near infrared absorption coefficient as a measure of the EL2 concentration requires, in addition to the position of the Fermi energy, knowledge of the magnitude of the residual absorption due to the photoionization of all other deep levels, even if they are individually present in small concentration. The use of infrared wavelength modulation absorption and photoquenching represents a practical method for measuring the magnitude of this residual absorption.

Acknowledgments

The support of this work by the Air Force Office of Scientific Research under AFOSR-83-0169B, the Army Research Office-Durham under DAAG29-81-K-0164, and the State of California-MICRO program is gratefully acknowledged.

References

1. G. M. Martin, in Semi-Insulating III-V Materials, Nottingham 1980, ed. by G. J. Res (Shiva Publ., Orpington, U.K.), p. 13.
2. G. M. Martin, Appl. Phys. Lett. 39, 747 (1981).
3. D. E. Holmes, R. T. Chen, K. R. Elliott, and C. G. Kirkpatrick, Appl. Phys. Lett. 40, 46 (1982).
4. G. M. Martin, J. P. Farges, G. Jacob, and J. P. Hallais, J. Appl. Phys. 51, 2840 (1980).
5. G. M. Martin, A. Mitonneau, D. Pons, A. Mircea, and D. W. Woodard, J. Phys. C 13 (1980).
6. G. M. Martin, G. Jacob, G. Poilblaud, A. Goltzone, and C. Schwab, Inst. Phys. Conf. Ser. 59, 281 (1981).
7. M. R. Brozel, I. Grant, R. M. Ware, and D. J. Stirland, Appl. Phys. Lett. 42, 610 (1983).
8. D. E. Holmes, R. T. Chen, K. R. Elliott, and C. G. Kirkpatrick, Appl. Phys. Lett. 43, 305 (1983).
9. S. Miyazawa, Y. Ishii, S. Ishida, and Y. Nanishi, Appl. Phys. Lett. 43, 853 (1983).
10. R. K. Kim and R. Braunstein, Appl. Opt. 23, 1166 (1984).
11. W. Walukiewicz, J. Lagowski, and H.C. Gatos, Appl. Phys. Lett. 43, 192 (1983).
12. M. Jaros, Deep Levels in Semiconductors (Adam Hilger Ltd., Bristol, U.K., 1982).
13. P. W. Yu, Appl. Phys. Lett. 44, 330 (1984).
14. G. Vincent and D. Bois, Solid State Commun. 27, 431 (1978).
15. D. Bois and G. Vincent, J. Phys. (Paris) 38, L351 (1977).
16. M. Levinston, Phys. Rev. B 28, 3660 (1983).

17. Y. Nanishi, H. Yamazaki, T. Mizutani, and S. Miyazawa, Inst. Phys. Conf. Ser. 63, 7 (1982).

18. H. Winston, Solid State Technol. 26, 145 (1983).

19. M. Tajima, Japan J. Appl. Phys. 21, L227 (1982).

20. D. E. Holmes, R. T. Chen, and J. Yang, Appl. Phys. Lett. 42, 420 (1983).

21. Y. Mita, S. Sugata, and N. Tsukada, Appl. Phys. Lett. 43, 842 (1983).

22. F. Haegawa, N. Iwata, N. Yamamoto, and Y. Nannichi, Japan J. Appl. Phys. 22, L502 (1983).

23. E. R. Weber, H. Ennen, U. Kaufmann, J. Windschief, and J. Schneider, J. Appl. Phys. 53, 6140 (1982).

24. A. V. Markov, S. S. Shirifin, and L. M. rgvlis, Sov. Phys. Crystallogr. 27, 620 (1982).

25. D. V. Klyachko and V. G. Krigel, Sov. Phys. Solid State 25, 676 (1983).

26. A. M. White, in Proceedings of the Semi-Insulating Materials Conference, Nottingham 1980, edited by G. J. Rees (Shiva, Orpington, U.K., 1980), p. 3.

27. U. Kaufmann and J. Schneider, Appl. Phys. Lett. 36, 747 (1980).

28. G. H. Strauss, J. J. Kerbs, S. H. Lee, and E. M. Swiggard, Phys. Rev. B 22, 3141 (1980).

29. A. M. Hennel, W. Szuszkiewicz, M. Blanski, and G. Martinez, Phys. Rev. B 23, 3933 (1981).

30. D. C. Look, S. Chaudhuri, and L. Eaves, Phys. Rev. Lett. 49, 1729 (1982).

31. A. Goltzene, C. Schwab, G. M. Martin, G. Jacob, and J. Poiblaud, Inst. Phys. Conf. Ser. 56, 557 (1981).

32. G. H. Strauss and J. J. Krebs, Inst. Phys. Conf. Ser. 33a, 84 (1977).

33. A. M. White, J. J. Krebs, and G. H. Strauss, J. Appl. Phys. 51, 419 (1980).

34. A. L. Lin and R. H. Bube, J. Appl. Phys. 47, 1859 (1976).

35. O. V. Vakulenko, G. D. Melnikov, and V. A. Skryshevskii, Sov. Phys. Semicond. 16, 1239 (1982).

Figure Captions

Fig. 1. The total absorption spectra at 300 K (solid curve), and the residual absorption spectra at 80 K (dotted curve) of the MO43T SI GaAs (LEC) sample.

Fig. 2. Typical thermal regeneration of the absorption coefficient (measured at 1.2 eV).

Fig. 3. The total absorption spectra at 300 K (solid curve), and the residual absorption spectra at 80 K (dotted curve) of the MO47T SI GaAs (LEC) sample.

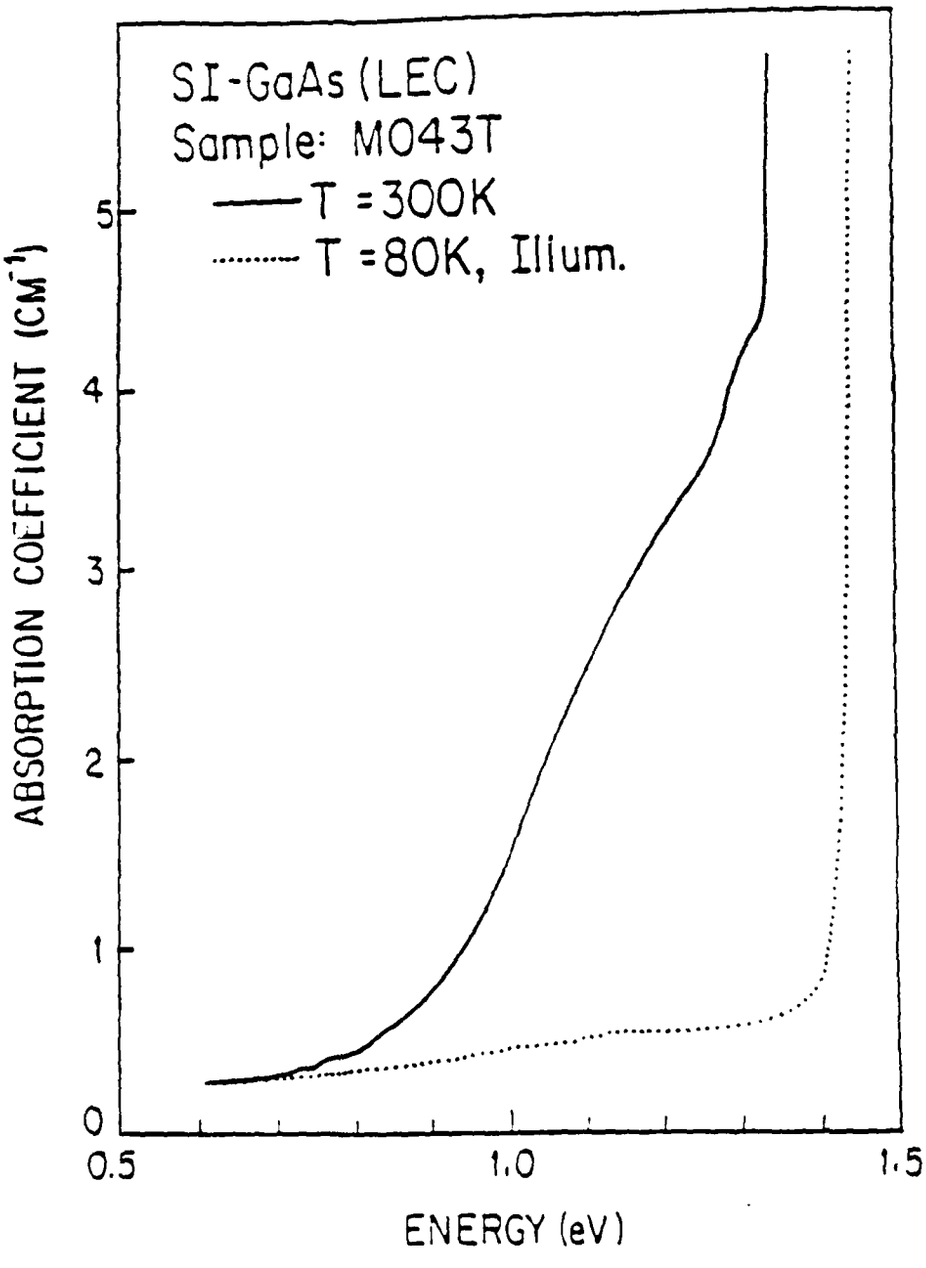
SI-GaAs (LEC)
Sample: M043T
T = 300K
T = 80K, Illum.
ABSORPTION COEFFICIENT (CM⁻¹)
0
1
2
3
4
5
0.5
1.0
1.5
ENERGY (eV)

Fig. 1

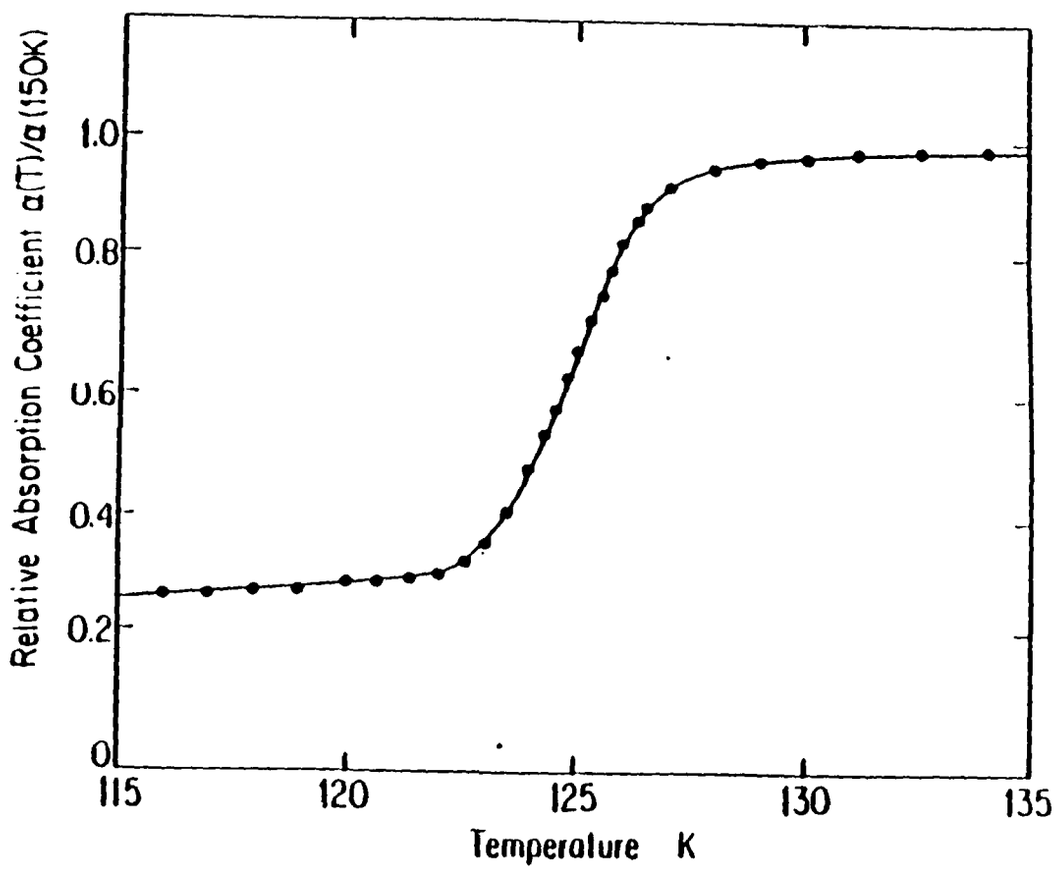
Relative Absorption Coefficient α(T)/α(150K)
1.0
0.8
0.6
0.4
0.2
0
115
120
125
130
135
Temperature K

Fig. 2

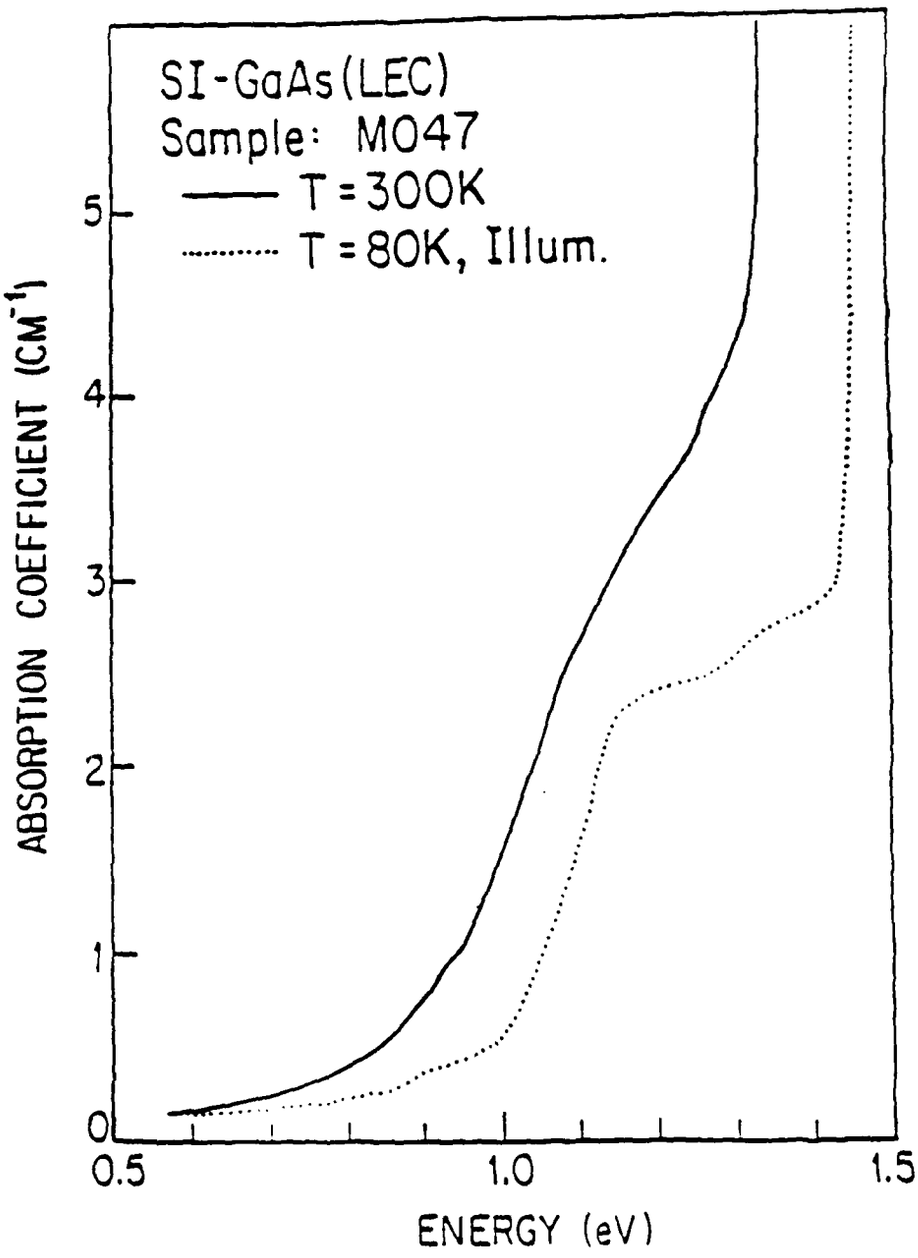
SI-GaAs(LEC)
Sample: M047
T = 300K
T = 80K, Illum.
ABSORPTION COEFFICIENT (CM^{-1})
0
1
2
3
4
5
0.5
1.0
1.5
ENERGY (eV)

Fig. 3

Re-examination of the Wavelength Modulation Photoresponse Spectroscopies

S. M. Eetemadi and R. Braunstein

Department of Physics, University of California,

Los Angeles, California 90024

Re-examination of the wavelength modulation photoresponse spectroscopies showed that the line shapes obtained by these methods are subject to distortions from several sources of spurious interference spectra. Limitations of these methods in studies of the deep levels and the interband transitions in semiconductors are discussed and a practical method for removal of the distortions due to the background spectra is suggested. Finally, a comparison is made between the wavelength modulation absorption/reflection and the wavelength modulation photoresponse spectroscopies. It is concluded that the former are the most suitable modulation techniques for the above studies since they yield unambiguous line shapes.

I. INTRODUCTION

To measure low level absorption, wavelength modulation techniques are employed. In one form, direct wavelength modulation absorption is utilized,[1] while in other implementations the wavelength modulation photoresponse of the sample is used to infer the absorption.[2-4] In this report we present a re-examination of the wavelength modulation photoresponse spectroscopies in general, and their application to the studies of the deep levels and interband transitions in semiconductors. Some of the limitations of these techniques, as well as the necessary precautions in interpreting the experimental results, are also discussed. A comparison was made between wavelength modulation absorption/refraction and wavelength modulation photoresponse spectroscopies.

Optical modulation spectroscopy has been extensively used in the past to study the optical absorption and reflection of materials.[5] Being a derivative technique in nature, it is far more sensitive than conventional spectroscopic methods for detecting small structures out of a broad background.[6] Various modulation parameters such as applied electric field, stress, temperature, and wavelength of the probing light beam have been combined with absorption and refelction spectroscopy to form a whole family of derivative spectroscopy techniques.[7] More recently, other derivative techniques combining the wavelength modulation and the photoresponse (photo-induced changes in voltage, capacitance, and current) spectroscopies have been introduced as a new approach to the study of absorption in semiconductors. Wavelength modulation photoconductivity,[2] photovoltage,[3] and photocapacitance,[4] are some examples. Such techniques have been used to study the interband transitions as well as transition involving the photoionization of the deep levels in some semiconducting materials.

In these methods, samples are prepared in the form of a p-n junction,[2] a

metal-insulator-semiconductor (MIS),[3] or a Schottky barrier[4] with semi-transparent electrodes. The changes in the photoresponse induced in the space-charge region, by wavelength modulation of the incident light beam, are measured using a phase-locked amplifier synchronous with the wavelength modulator. The derivative photoresponse spectrum thus obtained is interpreted as being proportional to the derivative of the absorption coefficient, and thus to the derivative of the photoionization cross section.[3] In particular, for the transitions involving photoionization of the deep levels, the derivative surface photovoltage (DSPV) is given by[4]:

$$\frac{dV_s}{d\lambda} = - V_s \, I_o \, A \, \frac{n_t}{N_D - N_A} \, \frac{d\sigma}{d\lambda} \quad , \tag{1}$$

where V_s is the surface photovoltage, I_o is the incident photon flux, n_t is the concentration of the occupied traps being probed, and $N_D - N_A$ is the net doping concentration. The constant, A, depends on the thermal generation and recombination of the traps, and σ is the photoionization cross section.

Wavelength modulation reflection and transmission spectroscopies have a serious experimental difficulty because the spectra contain substantial spurious structures originating from the derivative of the background spectra which must be properly removed in order to obtain the true spectra of the sample itself.[8] The structures in the background spectrum are due to the spectral dependence of the light source intensity, various optical components of the experimental system, and the atmospheric absorption, especially in the infrared region of the spectra. These structures have been successfully removed by various ingenious methods of background derivative subtractions,[5] including double beam-single detector[9] and single beam sample-in sample-out techniques.[1] However, the question of the effect of the background spectra on

the derivative photoresponse results has not yet been addressed in the previous theoretical and experimental works on this subject.

To investigate the possible effects of the background spectra, a preliminary derivative surface photovoltage (DSPV) experiment was conducted on a silicon sample prepared in the form of a semi-transparent MOS structure, and the result was compared with the derivative of the incident photon flux spectrum. Similarities between changes in the structures observed in both spectra were taken as an indication of possible superposition of the derivative of the background spectra on the DSPV spectra, and prompted us to re-examine the theory of the wavelength modulation surface photovoltage spectroscopy.

The result of our investigation showed that the proportionality relationship, eq. (1), between the DSPV and the derivative of the absorption coefficient is not valid in general. the DSPV spectra are rather a superposition of several terms, one of which includes the derivative of the background spectra; these additional terms are the various sources of distortions depend on the spectral region under investigation. Important implications of this result in the DSPV studies of the deep levels and the interband transitions are further explored below and modifications of the experimental technique for the removal of the major portions of the background spectra are suggested. The following discussion is focused primarily on the wavelength modulation surface photovoltage. The analysis, however, applies equally to other modulation photoresponse spectroscopies as well.

II. EXPERIMENTAL RESULTS

The derivative surface photovoltage measurements were performed on n-type silicon substrates (100) utilizing MOS structures. The experimental system used is described elsewhere.[10] The MOS structures were made by evaporating a 400 A semi-transparent gold electrode on an oxide layer (1000 A thick) grown on silicon by a standard dry oxidation technique.[11]

Typical sub-band-gap derivative surface photovoltage spectra (dV_s/dE) obtained at 83 K are shown in Figs. 1(a) and 2(a). To obtain a good signal-to-noise ratio it was necessary to keep the modulation amplitude and the spectral slit width of the monochromator fairly large: $\Delta\lambda/\lambda \sim 10^{-2}$. The derivatives of the incident photon flux spectra for the same instrument and spectral region with comparable amplitude of modulation were obtained using a PbS detector. These are shown for comparison in Figs. 1(b) and 2(b). With the sensitivity of the PbS detector a much better resolution, $\Delta\lambda/\lambda \sim 2\times10^{-3}$ is also possible, as shown in Fig. 3.

The dominant structure in Fig. 1(a) is due to the interband transition near the indirect band gap of silicon with emission and absorption of phonons. It is similar to other reported DSPV results.[12] The smaller structures below 1.15 eV may in principle be associated with the multi-phonon absorption. However, they can also be considered to be a manifestation of similar structures in the derivative of the background spectra dI_o/dE, shown in Fig. 1(b). Comparison of Fig. 2(a) and 2(b) also suggests a strong correlation between the structures in the DSPV and the derivative of the background spectra near 0.65 and 0.9 eV. In fact, signatures of the derivative of the background spectra are quite commonly observed in the wavelength modulated spectra of the reflected and transmitted light beam as predicted by the theory of the corresponding wavelength modulation spectroscopy.[8] These can be

corrected for by subtraction of the experimentally determined background.[8,9] In contrast, the theory of the DSPV, as formulated in Eq. (1), is not consistent with the above observation. In the next section we present our analysis of the theory of the DSPV spectroscopy, which clearly shows that the DSPV spectra can contain signatures of the derivative of the background spectra as well as other possible sources of distortions in the various regions of spectra.

III. DERIVATIVE OF SURFACE PHOTOVOLTAGE (DSPV)

The theory of surface photovoltage has been treated by a number of authors.[13] For the purpose of this study, the changes in the surface potential of a semiconductor, V_s, induced by the light of intensity I_o and wavelength λ may be written, for small signals (surface photovoltage << surface potential), in the form[13]:

$$V_s(\lambda) = I(\lambda)\ \alpha(\lambda)\ F(\lambda) \quad , \tag{2}$$

where

$$F = F(L_o, \alpha, T, E_f;\ \tau_b, n_b, p_b;\ E_t, n_t, \sigma_{ph}^{n}, \sigma_{ph}^{p}, e_n e_p, S) \quad .$$

F is a complicated function of diffusion length L_o, absorption coefficient α, temperature T, Fermi energy E_f, bulk carrier lifetime for electrons and holes and concentrations τ_b, n_b, p_b, respectively, deep levels energy E_t, concentration n_t, photoionization cross sections σ_{ph}^{n}, σ_{ph}^{p} for electrons and holes, respectively, and their thermal emission rates e_n and e_p, in the semiconductor as well as the effective surface recombination velocity S. The exact functional dependence of F on these parameters is not needed for our

discussion; however, it is rather important to note its implicit wavelength dependence through $\alpha(\lambda)$, $\sigma_{ph}^{n}(\lambda)$, and $\sigma_{ph}^{p}(\lambda)$. $I(\lambda)$ is the actual photon flux entering the space charge region of the semiconductor. Quite often in the past, $I_o(\lambda)$, which is the incident photon flux illuminating the MOS structure has been used instead of $I(\lambda)$, thus ignoring the spectral dependence of the transmittance through the metal and the insulating layers $I(\lambda)$ and $I_o(\lambda)$ are related by[14]:

$$I(\lambda) = I_o(\lambda)\, T(\lambda) \tag{3}$$

with

$$T(\lambda) = n_3 \left| \frac{(1+r_1)(1+r_2)(1+r_3)\, \exp(\delta_1+\delta_2)}{1 + r_1 r_2 \exp^2\delta_1 + r_1 r_3 \exp^2(\delta_1+\delta_2) + r_2 r_3 \exp^2\delta_2} \right|^2 \tag{4}$$

where r_i are the Fresnel reflection coefficients at the interfaces and are defined in terms of the complex refractive indices ($N = n+ik$) of the media involved as follows:

$$r_1 = \frac{1-N_1}{1+N_1}, \qquad r_2 = \frac{N_1-N_2}{N_1+N_2}, \qquad r_3 = \frac{N_2-N_3}{N_2+N_3}. \tag{5}$$

The phase factors for normal incidence are written

$$\delta_1 = -i\left(\frac{2\pi}{\lambda}\right) N_1 d_1, \qquad \delta_2 = -i\left(\frac{2\pi}{\lambda}\right) N_2 d_2. \tag{6}$$

For the MOS structure considered here, N_1 and d_1 are respectively the complex refractive index and thickness of the semi-transparent gold electrode, N_2 and d_2 apply to the SiO_2 film, and N_3 to the silicon substrate. In essence the wavelength dependence of $T(\lambda)$ is due to the spectral dependence of: the absorption coefficient of the light in the metal and insulator layers, the reflection coefficients at the interfaces, and the interference pattern due to

the internal multiple reflections from the interfaces; to simplify the discussion we write:

$$T(\lambda) = T[N_1(\lambda),\ N_2(\lambda),\ N_3(\lambda),\ g(\lambda)] \quad , \tag{7}$$

where $g(\lambda)$ symbolizes the interference phenomena. Combining Eqs. (2) and (3), we have:

$$V_s = I_o(\lambda)\ T(\lambda)\ \alpha(\lambda)\ F(\lambda) \quad , \tag{8}$$

which together with Eq. (7) form the basis of our analysis of the wavelength modulation surface photovoltage.

If the wavelength of the incident light beam is modulated as:

$$\lambda = \lambda_o + \Delta\lambda \cos \omega t \quad , \tag{9}$$

where $\Delta\lambda$ and ω are the amplitude and the frequency of modulation, respectively, then the surface photovoltage, $V_s(\lambda)$, becomes a periodic function of time, $V_s(\lambda_o + \Delta\lambda \cos \omega t)$. For small $\Delta\lambda$, the modulated surface photovoltage can be expanded in powers of $\Delta\lambda$, or:

$$V_s(\lambda_o + \Delta\lambda \cos \omega t) = V_s(\lambda_o) + \Delta\lambda \frac{dV_s}{d\lambda_o} \cos \omega t + O(\Delta\lambda)^2 + \cdots \quad . \tag{10}$$

The modulated surface photovoltage is detected by a standard lock-in amplifier tuned to the reference frequency ω. Hence, the output voltage of the lock-in amplifer is proportional to the amplitude of the first harmonic, i.e., $\Delta\lambda(dV_s/d\lambda)$. Similarly, the right-hand side of Eq. (8) can be expanded in powers of $(\Delta\lambda)$. By comparing the first harmonic terms on both sides, we

obtain:

$$\frac{dV_s}{d\lambda} = I_o(\lambda)\, T(\lambda)\, F(\lambda)\, \frac{d\alpha(\lambda)}{d\lambda} + T(\lambda)\, F(\lambda)\, \alpha(\lambda)\, \frac{dI_o}{d\lambda}$$

$$+ I_o(\lambda)\, F(\lambda)\, \alpha(\lambda)\, \frac{dT(\lambda)}{d\lambda} + I_o(\lambda)\, T(\lambda)\, F(\lambda)\, \frac{dF(\lambda)}{d\lambda} \quad . \qquad (11)$$

It must be added that, in order to incorporate the response of the system to a time varying incident light intensity, the above equation must be multiplied by a frequency response function $G(\omega)$.[15] However, since this factor is to first order independence of the wavelength, it is treated here as a constant of proportionality. Its effect on the temperature dependence of the DSPV spectra is discussed in a later section.

In contrast to Eq. (1), Eq. (11) shows that the DSPV signal is not in general proportional to $d\alpha/d\lambda$ and therefore its various terms introduce different degrees of distortion which depend on the relative size of their spectral changes in the spectral region of interest. The most notorious source of the distortion is the spectral changes of $I_o(\lambda)$, the background. The distortion introduced by I_o is present in all four terms of Eq. (11), but its effect is most dramatic in the second term which contains $dI_o/d\lambda$. This term affects the DSPV spectra in the near infrared region of spectra which corresponds to the sub-band-gap transitions in some semiconductors (e.g., Si, GaAs), as well as in the ultraviolet region of the spectra where the interband transitions occur. The spectral dependence of $dt(\lambda)/d\lambda$, however, is more pronounced in the region of the interband transition. Hence, in what follows, the sub-band-gap transitions which involve the impurity and defect levels are discussed separately from the inter-band transitions.

IV. DISCUSSION

1. Sub-Band-Gap Transitions.

Sub-band-gap electronic transitions associated with the deep levels are categorized as: i) the intra-center transitions between different levels of the same impurity or defect, and ii) photoionization of the electrons or holes into the conduction or valence bands.

i) Intra-Center Transitions: The intra-center transitions often produce sharp zero-phonon lines in the optical absorption and photoluminescence spectra at low temperature. For example, transition metal impurities at high and moderate concentrations in the III-V compounds have been extensively studied using these methods, yielding a great deal of information regarding the impurity's site symmetry, concentrations, and crystal field strength.[16] At lower concentrations these transitions were observed by wavelength modulation absorption spectroscopy.[17] Generally the positions of the sharp zero-phonon lines are the best signatures of the centers involved. However, intra-center transitions between the deep levels generally do not delocalize the carriers and so no spatial charge separation occurs. Consequently such transitions cannot be detected by the wavelength modulation surface photovolage spectroscopy. This is one of the disadvantages of the DSPV as compared to the wavelength modulation absorption spectroscopy.

If, however, one of the levels involved is a shallow level, then a photo-thermal ionization may occur, in which the carrier is first optically excited into the shallow level and subsequently ionized to the conduction or valence band by thermal excitation, producing a change in the surface potential. Whether this produces a wavelength modulation surface photovoltage depends on the temperature as well as the incident frequency, since the thermal emission

rate depends exponentially on E_i/kT, where E_i is the photoionization energy of the shallow level.[12] Hence, temperature and frequency scans of the DSPV spectra may be useful in detection and identification of such transitions.

ii) Deep Level to Band Transitions: In contrast to intra-center transitions, the deep level to band transitions have characteristically broad and often featureless absorption spectra, resulting in broad peaks and shoulders in the derivative of the absorption coefficient, $d\alpha/d\lambda$. Furthermore to obtain accurate information on the parameters which characterize the deep levels such as photoionization energy, concentrations, site symmetry, local potential and electron-lattice relaxation, one often needs to analyze the line shape of the absorption spectra as well as its temperature dependence.[16] Hence any spurious line shape due to the various possible sources of distortions would lead to inaccurate information about the parameters of interest and, consequently, the cross correlations between the experimental results and the theoretical predictions. The effects of the last three terms of Eq. 11 in the DSPV spectra are therefore especially significant in the [illegible] a priori ignored. In particular, the [illegible] contains numerous structures, as seen [illegible] DSPV spectra. Although some [illegible] from the background, $I_0(\lambda)$,[2,3] [illegible] their removal. Hence the [illegible] limited usefulness in studies [illegible] section we will suggest a [illegible] background contributions from

2. Temperature Dependence of the DSPV Spectra.

The temperature dependence of the absorption spectra, $\alpha(\lambda, T)$, is very valuable in studies of the deep centers and their electron-lattice relaxation. It is also an important parameter for comparing the theoretical results to those of experiments.[16] Unfortunately, the relationship between the temperature dependence of the DSPV and that of $\alpha(\lambda, T)$ is not a simple one, which makes it rather difficult to interpret the results.

The temperature dependence of the DSPV comes from that of $G(\omega,T)$, $\alpha(\lambda,T)$, $F(\lambda,T)$, as well as $dF/d\lambda$ and $d\alpha/d\lambda$ [see Eq. (11) and the paragraph following it]. The temperature dependence of the frequency response function, $G(\omega,T)$, is similar to that of the ac photoconductivity,[15] and since $G(\omega,T)$ stands as a proportionality factor, it can be treated in a similar way. But $F(\lambda,T)$ is in general a complicated function of temperature through its arguments, and appears in a nontrivial way in the expression for $dV_s/d\lambda$, Eq. (11). In some rather simple cases,[13] $F(\lambda,T)$ can be written:

$$F(\lambda,T) \propto \frac{L(T)\tau_b(T)S(T)}{[\alpha(\lambda,T)L(T) + 1]\,[L(T) + S(T)\tau_b(T)]} \quad , \tag{12}$$

where S is the effective surface recombination velocity. Therefore

$$\frac{dF}{d\lambda} \propto \frac{L^2(T)\tau_b(T)S(T)}{[\alpha(\lambda,T)L(T) + 1]^2\,[L(T) + S(T)\tau_b(T)]} \times \frac{d\alpha(\lambda,T)}{d\lambda} \quad . \tag{13}$$

It is clear from Eqs. (11), (12), and (13) that even when $F(\lambda,T)$ has a fairly simple form, it is by no means trivial to extract the temperature dependence [illegible] to arrive at an accurate interpretation of the temperature dependence of the DSPV spectra in relation to the parameters characterizing the deep levels involved. Such difficulties are not usually encountered in the wavelength modulation absorption spectroscopy, which directly measures $d\alpha(\lambda,T)/d\lambda$.

AD-A172 692 CHARACTERIZATION OF INFRARED PROPERTIES OF LAYER SEMICONDUCTORS(U) CALIFORNIA UNIV LOS ANGELES DEPT OF PHYSICS R BRAUNSTEIN 08 AUG 86 AFOSR-TR-86-0861 2/2

UNCLASSIFIED AFOSR-83-0169 F/G 7/4 NL

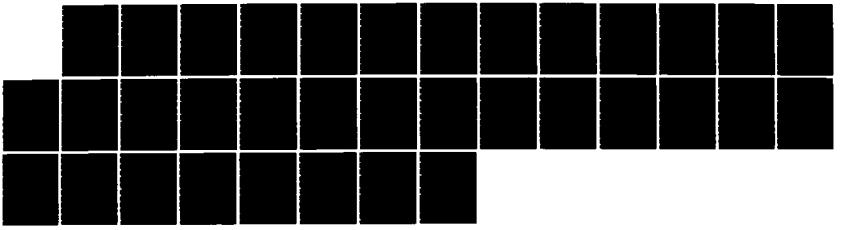

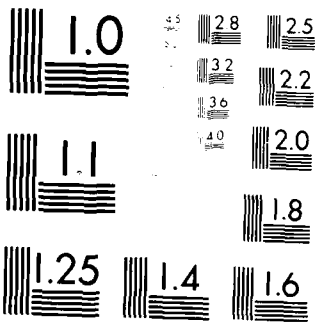

3. Interband Transitions.

Optical modulation spectroscopy has been a powerful tool in studies of the interband transitions in solids.[5] These techniques have allowed small structures immersed in a large but relatively smooth background spectrum to be observed and correlated with the critical points in the band structures.[18] In order to identify the types of critical points involved in the optical transitions and correlate them with the existing band structure calculations, experimentally unambiguous line shapes are necessary. Amongst the various modulation spectroscopies, the wavelength modulation reflectance has the unique advantage of having a straightforward relationship to the normal reflectance and other optical constants.[18] This allows one to obtain experimentally unambiguous line shapes which is the basis of the semi-empirical energy band calculations.

Wavelength modulation surface photovoltage spectroscopy is the youngest member of the family of modulation techniques which have been used to study the interband transitions of semiconducting materials. However, the main advantage of the wavelength modulation technique is lost in the DSPV spectroscopy, since it no longer has a direct or simple relationship with the optical constants. It is seen from Eq. (11) that the DSPV line shapes are distorted by the interference of the various spurious spectra. We discuss below the effects of the various terms of Eq. (11) on the line shapes of the interband transitions.

The effect of the I_o and $dI_o/d\lambda$ terms on the interband transitions depends, primarily, on the light source used in that particular region of the spectrum. Xenon arc lamps are commonly used for the ultraviolet region of spectra. The derivative of its spectrum,[8] shown in Fig. 4, contains sharp structures and therefore poses a serious problem in this region. Tungsten

light sources, in the visible region of spectra, also have structures as reported in the literature.[19] The structures in the $dI_0/d\lambda$ spectrum at longer wavelength are primarily due to the atmospheric absorption as discussed before.

The structure in the spectra of the transmittance $T(\lambda)$ and its derivative $dT/d\lambda$ are caused by the spectral changes of the optical constants in the metal and the insulating layers and the reflection coefficient of the semiconductor, as well as the interference patterns generated because of the interfaces [see Eqs. (4)-(7)]. These factors are separately discussed below:

a) The spectral changes of the reflectivity of gold $R(\lambda)$ as well as its logarithmic derivative $dR/d\lambda$,[20] are shown in Fig. 5. These spectral changes occur in the 2.0 - 5.0 eV region of the spectra and are primarily due to the d-band to Fermi level transitions. Structural changes in the spectrum of the derivative of its transmission coefficient in the 2.0 - 3.5 eV region have also been observed.[21]

b) The optical constants of the insulating layer, SiO_2, are fairly smooth in the 0.5 - 4.5 eV region of the spectrum,[22] and therefore are not expected to influence the line shapes of the interband transitions.

c) The spectral changes caused by the interference pattern depend on the thickness of the layers, their index of refraction, and the spectral region of interest. Optical interference patterns have been studied for the MIS structures with various thicknesses of Au and SiO_2 layers on silicon substrates.[23] The signatures of such interference patterns have also been observed in the surface photovoltage spectra.[24]

d) Finally, the spectral changes in the $R(\lambda)$ and $dR/d\lambda$ of the semiconductor substrate contribute significantly to the spectra of $T(\lambda)$ and $dT/d\lambda$, and hence to the DSPV spectra. Figure 6 shows the reflectivity of Si and its logarithmic derivative obtained by the wavelength modulation reflectance spectroscopy.[18]

V. COMPARISON OF WAVELENGTH MODULATION PHOTORESPONSE AND WAVELENGTH MODULATION ABSORPTION/REFLECTION SPECTROSCOPIES

It is therefore clear that the spectra of $T(\lambda)$ and $dT/d\lambda$ contain substantial structures that could significantly change the line shapes of the absorption obtained from the wavelength modulation surface photovoltage, as well as other forms of wavelength modulation photoresponse spectroscopies.

In contrast to the wavelength modulation absorption/reflection spectroscopy, removal of the background interferences $I_o(\lambda)$ and $dI_o/d\lambda$ from the DSPV spectra is very difficult. To date no systematic method for its subtraction has been suggested. We present a technique utilizing a double-beam system in combination with a reference optical detector and feedback loops to suppress the spectral changes of $I_o(\lambda)$ and $dI_o/d\lambda$. Its success, hwoever, depends on the relative smoothness of the spectral responsivity of the detector in the spectral region of interest.

To suppress the spectral changes of $I_o(\lambda)$ and $dI_o/d\lambda$, a double-beam system is needed. For this purpose, the light beam from the exit slit of the monochromator in a DSPV spectrometer needs to be split by a beam splitter. Both beams can therefore be wavelength modulated at frequency ω_2. One of the beams can be used to illuminate the DSPV sample while the other beam can be chopped at frequency ω_1 and then incident upon an optical detector. The output of the detector is fed into two lock-in amplifiers. One of the lock-in amplifiers (I) is tuned to ω_1 to measured the light intensity, and the other one is turned to ω_2 to measured $dI_o/d\lambda$. Except for the beam splitter and the DSPV sample, this is similar to the infrared wavelength modulation spectrometer described elsewhere.[1] The output of the lock-in amplifier I can be used in a negative feedback loop to regulate the power supply of the light source. This arrangement will keep the light intensity constant as the

wavelength is scanned. The output of the lock-in amplifier II can be used in another negative feedback loop to regulate an intensity modulator to keep $dI_o/d\lambda$ equal to zero. The intensity modulator can be placed anywhere in the light path before the beam splitter. Its modulation frequency should be the same as the wavelength modulator and its amplitude can be controlled by the negative feedback loop from the lock-in amplifier II. One such intensity modulator has been used in a wavelength modulation reflectance spectrometer for the same purpose.[25] The two feedback loop systems eliminate $dI_o/d\lambda$ and the spectral changes of the background $I_o(\lambda)$ to the extent that it is smooth in the spectra region of interest. This is not possible in the absolute sense nor the entire region of the spectrum. However, what is needed in practice is to have detectors whose spectral responsivity are flat and smooth compared to the line shapes of the optical transitions under investigation.

Finally, in comparing the wavelength modulation techniques, the wavelength modulation absorption/reflection (WMA/R) spectroscopy has several advantages over the wavelength modulation photoresponse spectroscopy (WMPR). Firsty and foremost, the WMA/R method yields unambiguous line shapes for the optical transitions, which are therefore easier to interpret. This is also true of the temperature dependence of the line shapes. Second, the intra-center transitions involving the deep levels can be observed by the WMA but not with the DSPV spectroscopy. Third, in the WMA/R, the only source of spurious signals is the background spectrum which can be completely removed in a systematic way, independent of the spectral responsivity of the detector. Finally, the WMA/R is a nondestructive method which can be applied directly to the bulk of the materials. In contrast, the WMPR measurements often require fabrication of devices in the form of MIC, p-n junction, of Schottky barriers which could result in the introduction of process related impurities or defects into the samples.

VI. CONCLUSIONS

We have shown that contrary to the previous assumptions, the DSPV in general is not proportional to the derivative of the absorption coefficient. A general formulation of the DSPV was derived which revealed the various possible sources of spurious interference spectra. The effects of these interferences on the line shapes of the optical transitions were studied and their impact on the identification of the deep levels and the critical poings in the band structures were discussed. A practical method for removal of the main source of the disortions, i.e., the background, was suggested.

ACKNOWLEDGMENTS

The support of this work by the Air Force Office of Scientific Research under AFOSR-84-0169B, the Army Research Office-Durham under DAAG29-81-K-0164, and the State of Calfiornia-MICRO program is gratefully acknowledged.

REFERENCES

1. R. K. Kim and R. Braunstein, Appl. Opt. 23, 1166 (1984).
2. T. Nishino and Y. Hamakawa, Phys. Stat. Sol. (b) 50, 345 (1972).
3. J. Lagowski, W. Walukiewicz, M. M. G. Slusarczuk, and H. C. Gatos, J. Appl. Phys. 50, 5059 (1979).
4. E. Kamieniecki, J. Lagowski, and H. C. Gatos, J. Appl. Phys. 51, 1863 (1980).
5. M. Cardona, Modulation Spectroscopy (Academic Press, New York, 1969).
6. G. Bonfiglioli, P. Brovetto, G. Busca, S. Levialdi, G. Palmieri, and E. Wanke, Appl. Opt. 6, 447 (1967).
7. R. K. Willardson and A. C. Beer, editors, Semiconductors and Semimetals - Vol. 9, Modulation Techniques (Academic Press, New York, 1977).
8. M. Welkowsky and R. Braunstein, Rev. Sci. Instrum. 43, 399 (1972).
9. R. Stearns, J. Steele, and R. Braunstein, Rev. Sci. Instrum. 54, 984 (1983).
10. S. M. Eetemadi, Ph.D. Thesis, University of California at Los Angeles (1984).
11. A. S. Grove, Physics and Technology of Semiconductor Devices (John Wiley and Sons, New York, 1967).
12. L. L. Jastrzebski and J. Lagowski, RCA Review 41, 181 (1980).
13. D. L. Lile, Surf. Sci. 34, 337 (1973), and reference therein.
14. O. S. Heavens, Optical Properties of Thin Solid Films (Academic Press, New York, 1955).
15. S. M. Ryvkin, Photoelectric Effects in Semiconductors (Consultants Bureau, New York, 1964), Ch. III.
16. M. Jaros, Deep Levels in Semiconductors (Adam Hilger Ltd., Bristol, U.K., 1982).

17. S. M. Eetenmadi and R. Braunstein, to be published.

18. M. Welkowsky and R. Braunstein, Phys. Rev. B 5, 497 (1972).

19. K. L. Shaklee and J. E. Rowe, Appl. Opt. 9, 627 (1970).

20. M. Welkowsky, Ph.D. Thesis, University of California, Los Angeles (1971).

21. R. Rosei, R. Antonangeli, and U. M. Grassano, Surf. Sci. 37, 689 (1973).

22. W. L. Wolfe, in Handbook of Optics, ed. by W. G. Driscol and W. Vaughan (McGraw-Hill, 1973), Ch. 7.

23. R. J. Powell, J. Appl. Phys. 40, S093 (1969).

24. J. Lagowski, L. Jastrzebski, and G. W. Cullen, J. Electrochem. Soc. 128, 2669 (1981).

25. R. Zucca and Y. R. Shen, Appl. Opt. 12, 1293 (1973).

FIGURE CAPTIONS

Fig. 1. (a) The derivative surface photovoltage spectra of silicon (T = 83 K); (b) the derivation of the background spectra in the spectral range of 1.0 - 1.35 eV; amplitude of modulation $(\Delta\lambda/\lambda) = 10^{-2}$.

Fig. 2. (a) The derivative surface photovoltage spectra of silicon (T = 83 K); (b) the derivative of the background spectra in the spectral range of 0.6 - 1.0 eV; amplitude of modulation $(\Delta\lambda/\lambda) = 10^{-2}$.

Fig. 3. Derivative of the background spectra in the spectral range of 0.76 - 1.0 eV; amplitude of modulation $(\Delta\lambda/\lambda) = 2\times10^{-3}$.

Fig. 4. Derivative of the background spectra in the spectral range of 4400 - 3400 A using a xenon arc source; derive from reference 8.

Fig. 5. (a) Normal reflectivity spectrum, and (b) logarithmic derivative spectrum of the reflectivity of Au at 80 K; derived from ref. 19.

Fig. 6. Logarithmic derivative spectrum of the reflectivity of silicon at 80 K and 300 K and the normal reflectivity spectrum at 80 K; derived from reference 18.

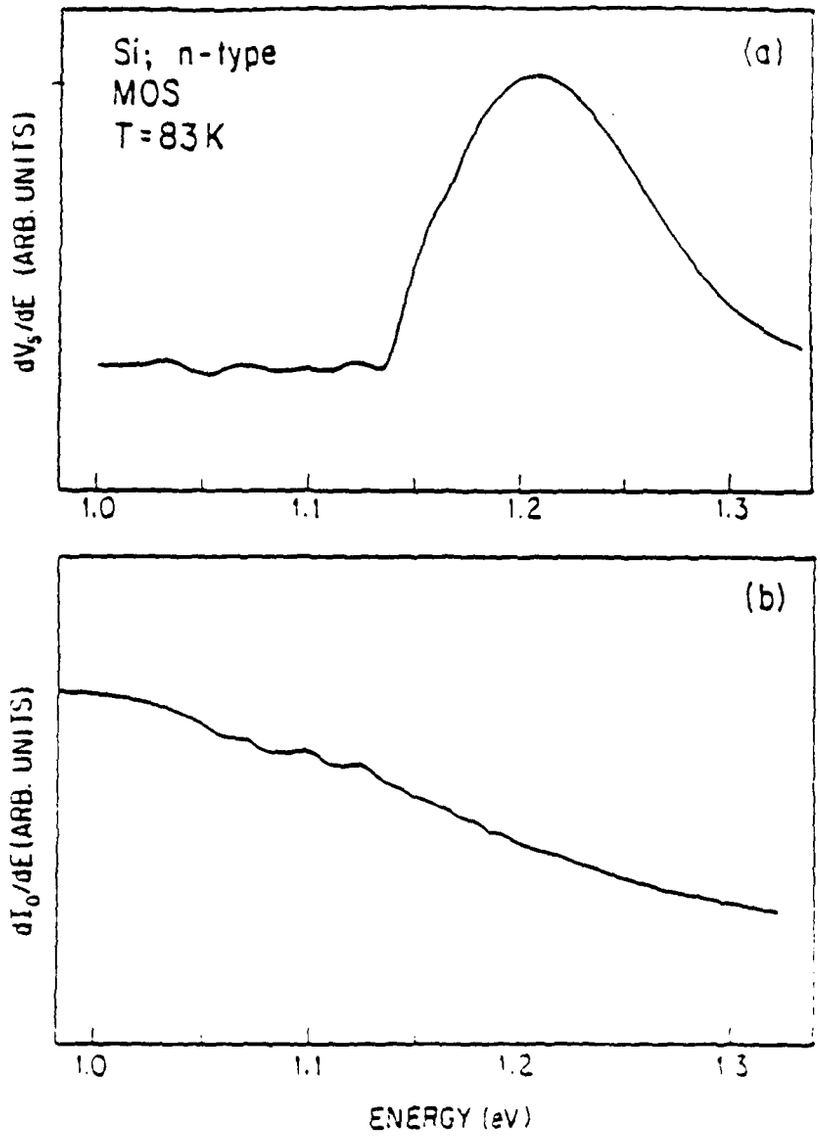
Si; n-type
MOS
T=83K
(a)
dV_s/dE (ARB. UNITS)
1.0
1.1
1.2
1.3
(b)
dI_o/dE (ARB. UNITS)
1.0
1.1
1.2
1.3
ENERGY (eV)

Fig. 1

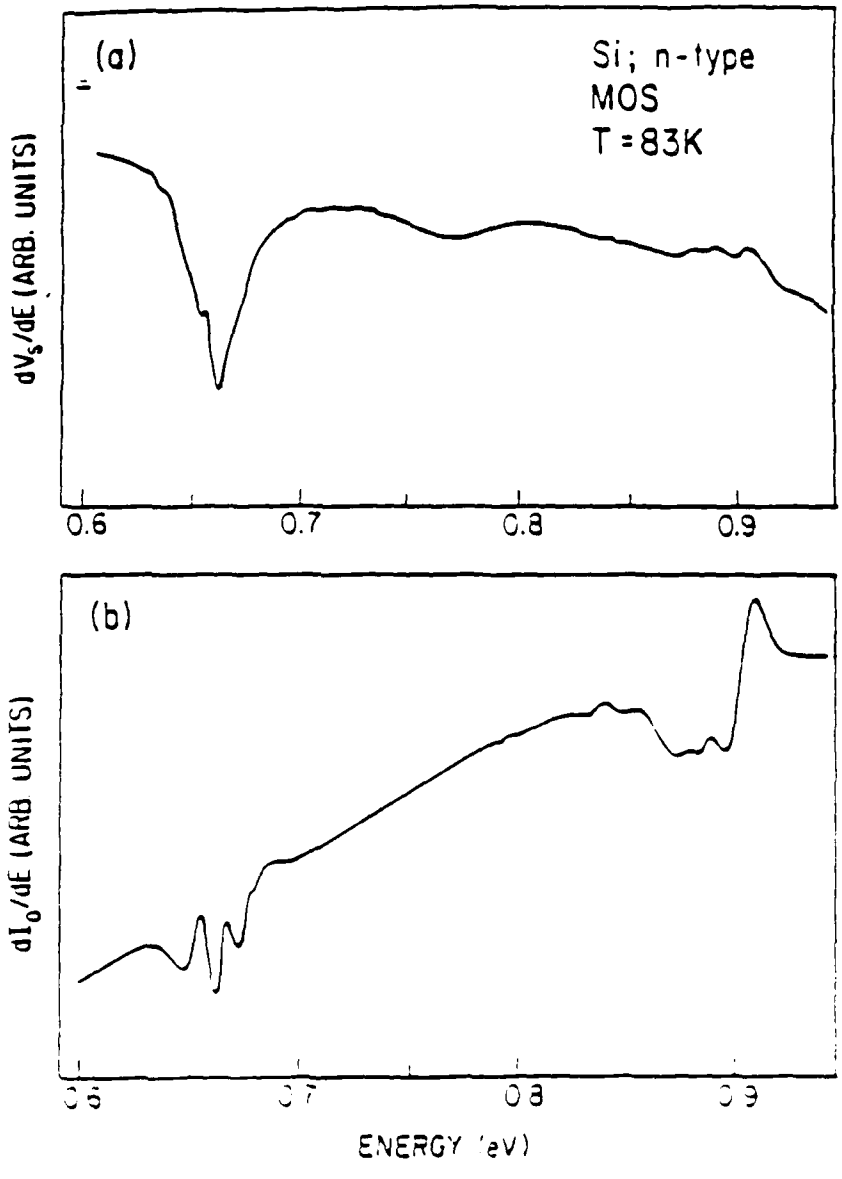
(a)
Si; n-type
MOS
T = 83K
dV_s/dE (ARB. UNITS)
0.6
0.7
0.8
0.9
(b)
dI_0/dE (ARB UNITS)
0.6
0.7
0.8
0.9
ENERGY (eV)

Fig. 2

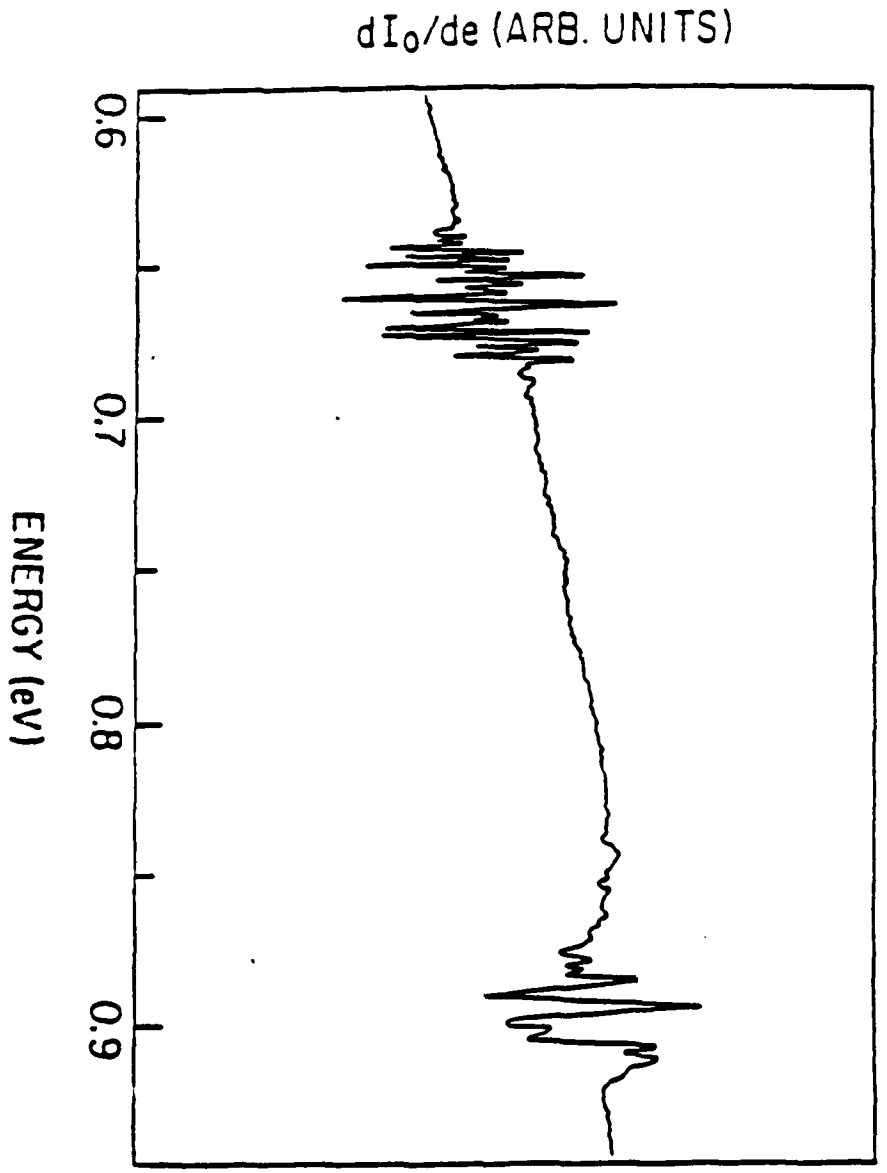

Fig. 3

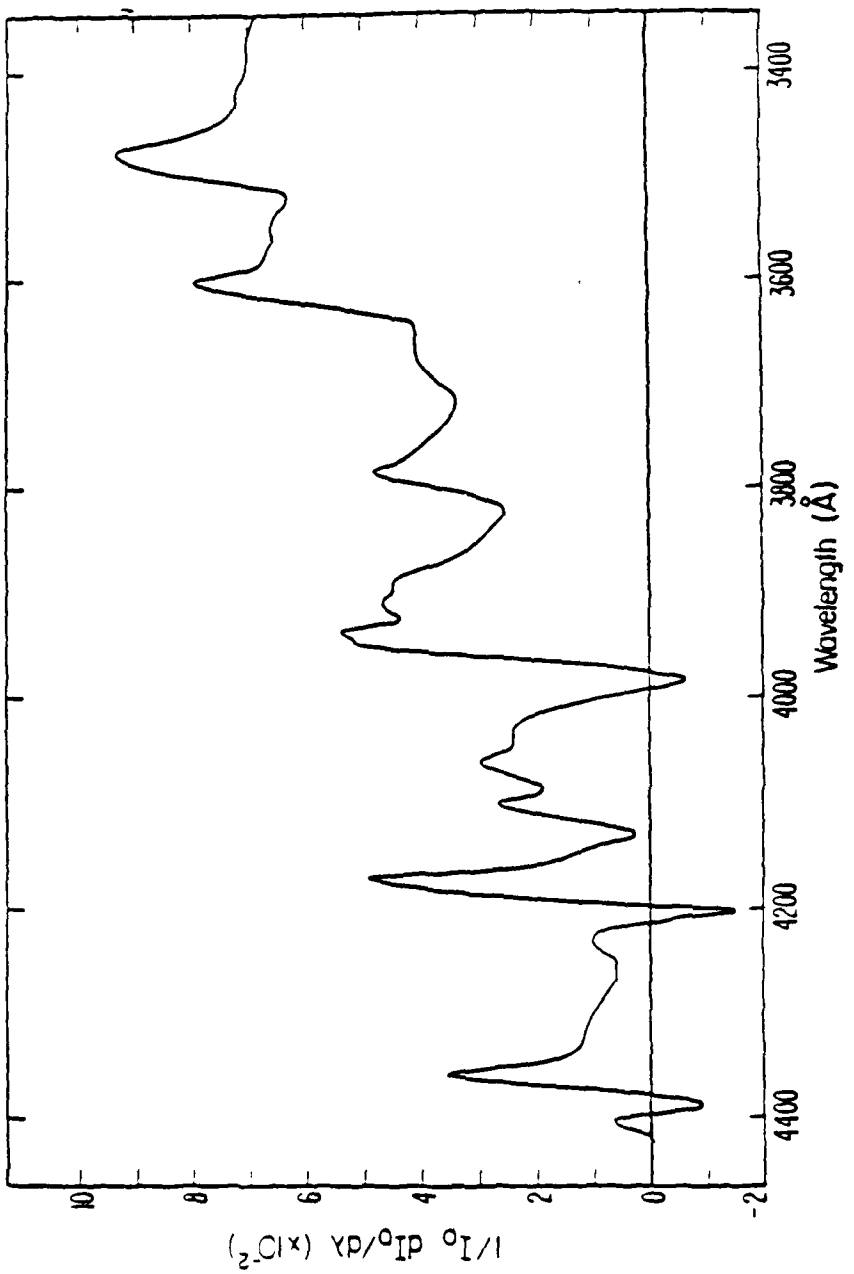
$1/I_o\ dI_o/d\lambda\ (x10^{-2})$
10
8
6
4
2
0
-2
4400
4200
4000
3800
3600
3400
Wavelength (Å)

Fig. 4

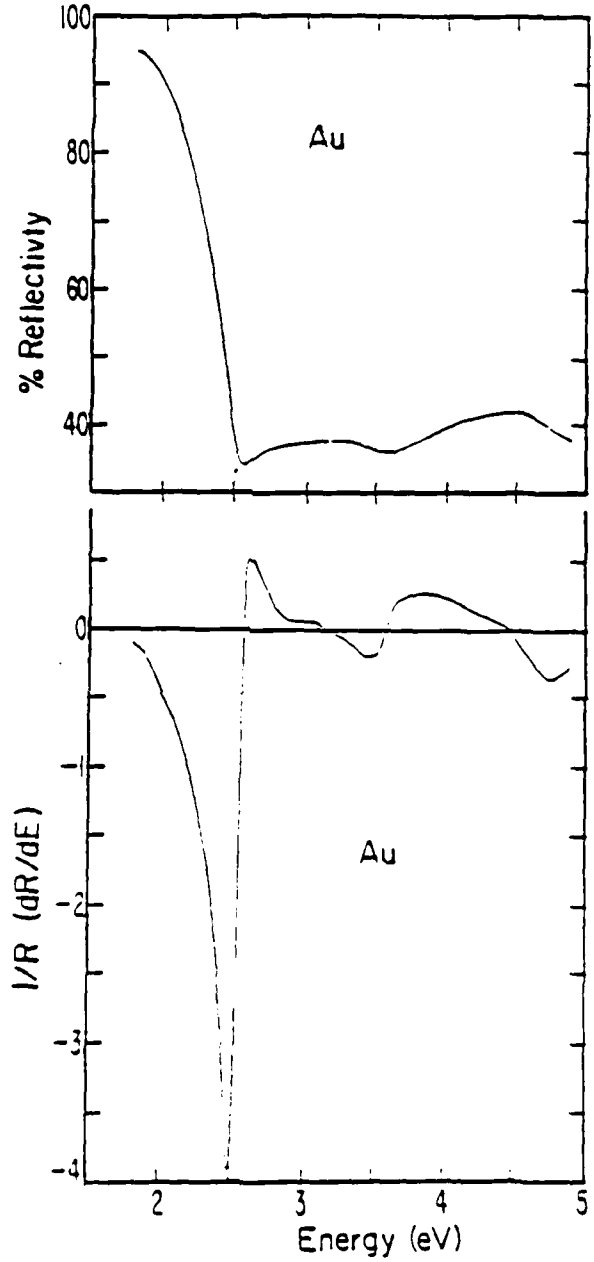

Fig. 5

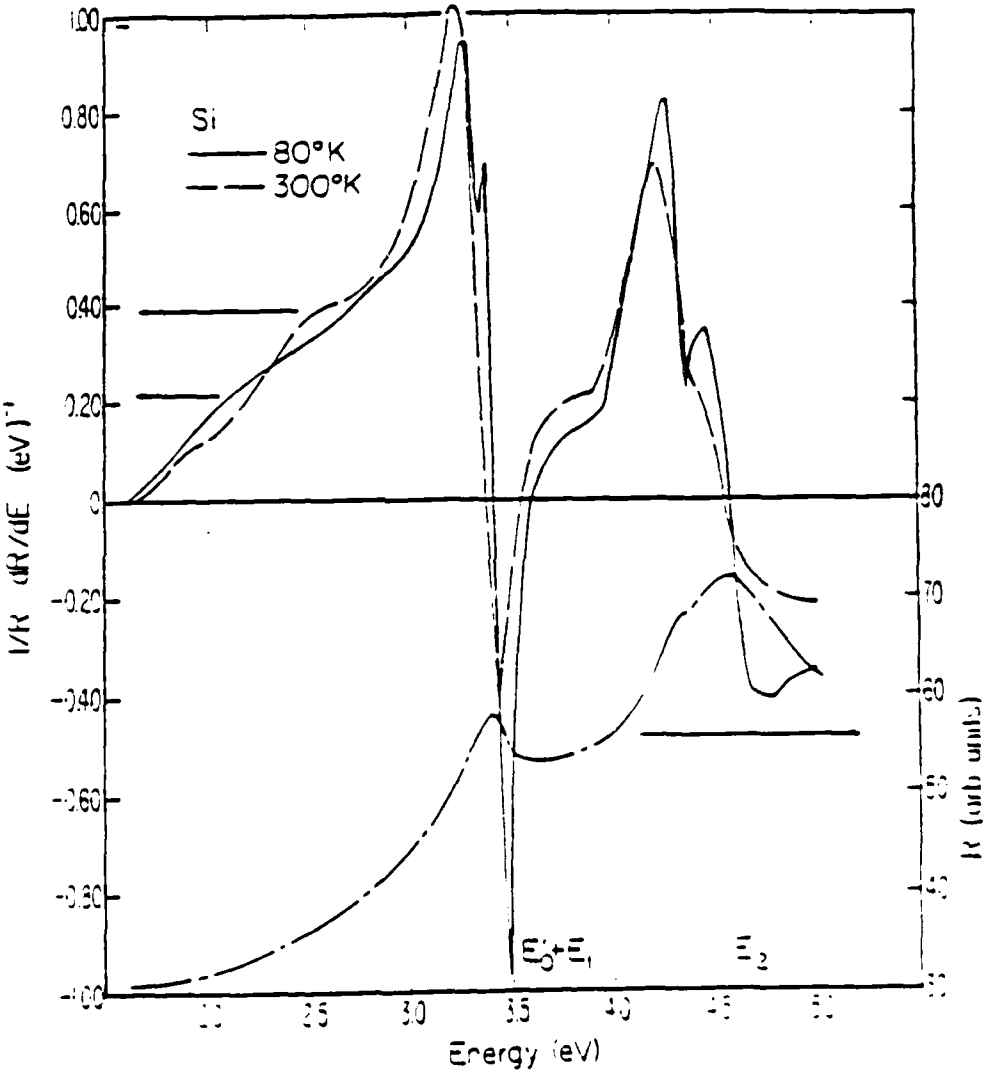

Fig. 6

Deep Levels in Semi-Insulating, Liquid-Encapsulated-Czochralski-Grown GaAs

M.R. Burd and R. Braunstein

Department of Physics, University of California

Los Angeles, California 90024

Abstract

Using photo-induced-transient-spectroscopy on variously heat-treated samples of semi-insulating LEC grow GaAs, we detected seven deep levels. Six of these levels were matched with previously catalogued levels, four of them being hole-like and two being electron-like. The seventh level appears to be associated with a boron-related defect which has previously been seen only as a band in boron-implanted GaAs.

I. Introduction

It is important to fully understand the deep levels present in GaAs samples which have been prepared by various growth techniques. Unfortunately, in many of the studies done on samples produced by a particular growth method the measurement techniques used tended to obscure some of the deep levels which may have been present at the time of growth. For instance, the use of deep level transient spectroscopy (1) requires the construction of a diode structure from the sample to be studied causing the sample to be subjected to relatively high temperature annealing. Such temperature treatment can remove defects that give rise to certain deep levels, thus, making them impossible to study.

The purpose of this study is to investigate the deep levels present in samples of liquid encapsulated Czochralski (LEC) grown, semi-insulating GaAs. To accomplish this, photo-induced-transient spectroscopy was used as the measurement technique for detecting deep levels in the sample. This method was chosen for two reasons: first, it is one of the preferred methods for detecting deep levels in semi-insulating GaAs, and, second, the preparation of the samples for this technique involves only a small amount of heat treatment allowing study of annealable deep levels which may have been introduced during the growth process.

Measurements were made on samples which had been subjected to a variety of heat treatments with the purpose of giving some evidence for possible defect structures which may be causing the deep levels. Using these methods seven deep levels were observed with most of them being readily identified with deep levels seen in other works.

II. Experimental Techniques

All of the samples used in this study were LEC grown (2) GaAs and were semi-insulating because of the deep levels which were caused by the growth process as opposed to being deliberately introduced into the samples by doping with materials such as Cr. One sample, M177, however, did have a layer of GaAs grown on it by molecular beam epitaxy. A summary of the treatment of the samples is presented in Table 1.

Samples M039, M043, and M25-2 had no heat treatment performed on them until they had first been tested for deep levels; then the same samples were annealed and redesignated M039 ann, M043 ann, and M25-2 ann. The annealing process involved raising their temperature in a nitrogen atmosphere over a period of one hour from room temperature to 700K. They were left at this temperature for four hours and then, over a period of one hour, their temperature was lowered back to room temperature. After being tested for deep levels sample M039 ann was given another heat treatment and redesignated M039 que. This particular heat treatment involved raising its temperature to 700K over a period of one hour. The sample was left at this temperature for a period of three hours and then was cooled back down to room temperature in approximately ten seconds.

Samples M25-2I, D9, M025, and M177 had ion-implanted electrical contacts. This process involves masking the samples and implanting Si ions into the surface at extremely high concentrations such that the conductivity becomes very large in the implanted regions. The samples are then given a high temperature anneal to drive in the Si and remove some of the damage caused by the implantation process. The electrical contacts on all of the other samples were made by soldering In to the surfaces of the samples with an ultrasonic soldering iron. The soldering process was

performed as quickly as possible in order to minimize the amount of heating the samples would be subjected to.

The method used to detect the presence of the deep levels in the samples was photo-induced-transient spectroscopy (3). This technique involves pulsing a monochromatic light source at a sample of GaAs which has a bias voltage applied across contacts on its surface. The transient current which follows the termination of the light pulse is then measured. If the trap being seen is an electron-like trap and the intensity of it is such that a saturated condition is achieved for the photo-current then the form of the transient current becomes:

$$\delta i(t) = CN_T\, e_n \exp(-e_n t)$$

where e_n is the emission rate, N_T is the trap concentration, and C is a constant. When this equation is differentiated with respect to temperature the following results:

$$\frac{d\delta i(t)}{dT} = C\, N_T\, (1-e_n) \exp(-e_n t) \frac{de_n}{dT}$$

It can be seen that an extremum occurs when $t=1/e_n$. Therefore, by choosing a time after the termination of the light pulse and plotting the magnitude of the transient current as a function of temperature, a series of peaks are obtained. Each peak corresponds to a different deep level with the position of the peak occurring at a temperature, T_m, where the level's emission rate is equal to the reciprocal of the time chosen. By graphing the transient current's value at different times as a function of temperature, several values of T_m can be obtained for the different values

of the time, t. Assuming the form for e_n is (6):

$$e_n = \gamma_n T^2 (\sigma_{n\infty} g_n \exp(\alpha/k)) \exp(-E_A/kT).$$

where E_A is called the activation energy and $\sigma_{na} = (\sigma_{n\infty} g_n \exp(\alpha/k))$ is the apparant cross-section. A plot of $\log(T^2 t)$ versus $1/T$ will yield a straight line graph. The value for γ_n has been determined to be $(4\sqrt{6}\ \pi^{3/2} h^{-3} m_n^* k^2)$ (11). For electrons this equals 2.28×10^{20} $cm^{-2}s^{-1}K^{-2}$ (6). Putting in the effective mass term for holes yields a value of 1.7×10^{21} $cm^{-2}s^{-1}K^{-2}$ (5). This straight line graph or the combination of E_A and σ_{na} (σ_{pa} for holes) is called the signature of the deep level and is preferred method for identifying a deep level.

The photo-induced-transient spectroscopy (P.I.T.S.) apparatus (4) consisted of a dewar in which the samples could be cooled to liquid nitrogen temperatures. There were windows in the dewar to allow the light pulses from the two light sources used for this experiment to strike the samples. The light sources used were a He-Ne laser and a GaAs light emitting diode which gave light at energies greater than and less than the band gap respectively. The temperatue of the sample was monitored by a thermocouple. The current through the sample was measured as a voltage across a resistor which was placed in series with the sample and the DC power supply which provided the bias voltage to the sample. The apparatus was controlled and the temperature and transient current were read by a CAMAC data acquisition system under the control of an LSI-11/23 computer. A representation of the transient current was obtained at each point in temperature by having the computer read the voltage across the series resistor at several regularly spaced times following each pulse of light. This allowed a complete set of data to be obtained in only one temperature

scan. Figure 1 shows a block diagram of the P.I.T.S. apparatus while Figure 2 shows the flow diagram for the computer program which controls the system.

The signatures of all the deep levels seen in all of the samples tested are compiled in Figure 3, while a tabulation of which level was present in a given sample is diplayed in Table 2. As can be seen there is a rich spectrum of deep levels in the samples which were not subjected to any heat treatment, those being M039, M043, and M25-2. For several of the deep levels definite patterns of behavior can be seen with regard to the heat treatment given the various samples. As can be seen by comparing Figure 4 to Figure 5, the difference between an as-grown sample and the same sample after being subjected to heat treatment is quite significant. Table 3 shows a listing of all the observed deep levels' activation energies and emission sections.

The level with an activation energy of 0.18 eV has a signature which matches that of the deep level designated as EL10 and observed in other studies (6). As can be seen in Table 3 it has a σ_{na} equal to 1.5×10^{-15} cm^2. The best identification for the level with the activation energy of 0.22 eV is EL17 (8). The level being an electron level means σ_{na} is equal to 1.5×10^{-14} cm^2. The best fit to the signature of 0.36 eV level occurs for the deep level designated as HL7 (5). The hole nature of the level means σ_{pa} is equal to 5.6×10^{-13} cm^2.

The deep level listed in Table 3 with an activation energy of 0.56 eV has a signature which is an excellent fit to that of the level designated in other studies as HL3 (5) yielding a σ_{pa} equal to 1.4×10^{-15} cm^2. This particular deep level has been found to correspond to the presence of iron in the samples tested in other works. This is supported here by the fact

that this level appears in all of the samples used in this study which gives greater weight to the level being associated with a chemical impurity rather than just a crystal imperfection. Another feature which supports this identification is the presence of this level in the MBE sample M177. It is known that iron is a fast diffuser in GaAs (7) and tends to migrate toward the surfaces of a sample. The presence of the 0.56 eV deep level in the MBE sample would imply that the iron-associated defect had migrated from the LEC substrate into the MBE layer during either the MBE process or the ion- implantation of the electrical contacts.

The deep level with a signature which most closely matches that of the level with the activation energy of 0.42 eV is HB5 which is believed to be the same level as HL5 (5). This particular level is thought to be associated with a native defect in the crystal. This is supported in this study by the fact that it is readily annealed, as can be seen in Table 2 since it does not appear in any of the heat treated samples except M039 que. The fact that it reappears in the quenched sample means that it can be easily reintroduced by "freezing in" the high temperature concentration of these imperfections.

There is some difficulty in assigning a designation to the 0.27 eV level in that its signature lies almost halfway between the signatures of EL8 and HL12 (5). Assuming it is one of the two and not a newly seen level, the feature which lends more weight toward identifying it as HL12 is that the level appears in all of the samples except the MBE samples. HL12 has been seen in samples which contain zinc, a chemical impurity, and is, therefore, not as likely to be affected by annealing. As can be seen in Table 3 this identification results in σ_{pa} being equal to 3.8×10^{-15}

cm^2.

The best candidate for the identification of the deep level seen at an energy of 0.52 eV is a somewhat unconventional band seen in samples which have undergone ion-implantation using boron as the bombarding ions (9). This boron-implantation produced defect structures which were annealable and the energy band associated with them has a peak at temperatures which agree with those seen for the level in this work. Since there is most likely boron present in the samples used in this study (10), and since the band is associated with boron the evidence for associating the level seen in this work with the so-called U-band seen in (9) seems strong. The reason that this defect produced a clear level in the samples studied here while a band was seen in the samples which were boron-implanted would seem to be due to the difference in the manner in which the boron was introduced into the samples. The associated damage produced in the boron-implantation process might be what caused this level to be broadened into a band. This damage would not be present in the samples where the boron was introduced during the growth process. Since it is not possible to determine whether the level is hole-like or electron-like with P.I.T.S. both a σ_{pa} and a σ_{na} are reported for it in Table 3.

IV. Conclusions

Several deep levels were seen in samples of semi-insulating liquid encapsulated Czochralski grown GaAs by photo-induced transient spectroscopy. Two of the levels one at 0.56 eV and the other at 0.27 eV appear in all of the LEC samples regardless of the heat treatment they received and seem to be related to the presence of iron and zinc impurities respectively. These are most probably due to accidental

introduction during the growth process since there was no intentional doping of the GaAs used in this study. Most of the other deep levels seen were correlated with levels seen by other investigators. Very good agreement between the signatures of the levels made the identifications certain. One particular deep level seen with an energy of 0.52 eV seems to be related to a complex defect involving boron present in the samples. It appears to ba a non-broadened version of the band seen in boron-implanted GaAs and probably appears as a single level rather than a band because the boron was introduced during the growth process instead of being ion-implanted.

The support of this work by the Air Force Office Scientific Research under AFOSR-84--01698, the Army Research Office-Durham under DAAG-29-K-1064 and the State of California-MICRO program is gratefully acknowledged.

References

1. C.T. Sah, L. Forbes, L.L. Rosier, and A.F. Tasch, Jr., Solid State Elect. 13, 759 (1970).

2. R. Thyagarajan, R.C. Narula, and T.R. Parashar, Ind. J. Pure and Appl. Phys. 17, 650 (1979).

3. Ch. Gurtes, M. Boulou, A. Mitonneau, and D. Bois, Appl. Phys. Lett. 32, 821 (1978).

4. M.R. Burd, doctoral thesis, University of California, Los Angeles (1984).

5. A. Mitonneau, G.M. Martin, and A. Mircea, Electron. Lett. 13, 666 (1977).

6. G.M. Martin, A. Mitonneau, and A. Mircea, Electron. Lett. 13, 191 (1977).

7. P.E.R. Nordquist, P.B. Klein, S.G. Bishop, and P.G. Siebenmann, Inst. Phys. Conf. Ser. 56, 569 (1981).

8. A. Mircea and D. Bois, Inst. Phys. Conf. Ser. 46, 82 (1979).

9. G.M. Martin, P. Secordel, and C. Venger, J. Appl. Phys. 53, 8706 (1982).

10. R.N. Thomas, H.M. Hobgood, D.L. Barret, and G. Eldridge, Proceedings of the Conference on Semi-Insulating III-IV Materials, Shiva, Nottingham, p. 76 (1980).

11. A. Mircea, A. Mitonneau, and J. Vannemenus, J. Physique (Lett.) 38, L41 (1977).

Figure Captions

Fig. 1 Block diagram of the photo-induced transient spectroscopy apparatus.

Fig. 2 Flow diagram of the computer program which operates the photo-induced transient spectroscopy apparatus.

Fig. 3 Plots of $\log(T_m^2 t)$ versus $1/T$ for all deep levels seen by photo-induced transient spectroscopy.

Fig. 4 Transient current vs. T for sample M039 t=40 msec, He-Ne laser light source.

Fig. 5 Transient current vs. T for sample M039 ann t=40 msec, He-Ne laser light source.

SAMPLE	DESCRIPTION OF SAMPLE PREPARATION
D9 M025 M25-2I	LEC-grown GaAs with ion-implanted contacts (note: there is extensive annealing as part of the ion-implantation process)
M177	LEC-grown with MBE layer, ion-implanted contacts (note: there is extensive heat treatment during both the MBE and ion-implantation processes)
M039 M043 M25-2	LEC-grown with In soldered contacts
M039 ann M043 ann M25-2 ann	LEC-grown and annealed at 700K for four hours with a one hour cool off, In-soldered contacts
M039 que	LEC-grown and heat treated at 700K for three hours with a fast cool off, In-soldered contacts

Table 1 Description of sample preparations.

SAMPLE	ACTIVATION ENERGY OF THE LEVEL (eV)						
M25-2I	0.57			0.36	0.27		0.18
D9	0.56			0.36	0.28	0.22	
M025	0.55			0.36	0.27	0.22	0.18
M177	0.56						
M25-2	0.56	0.52	0.42	0.36	0.27		0.18
M039	0.56	0.52	0.42	0.36	0.27	0.22	0.18
M043	0.56	0.52	0.42	0.36	0.27		0.18
M25-2 ann	0.56				0.27		0.18
M039 ann	0.56				0.27	0.22	
M043 ann	0.57				0.27		
M039 que	0.56		0.42		0.27	0.22	

Table 2 Activation energies of deep levels detected by photo-induced transient spectrscopy measurements.

LEVEL IDENTIFIED	ACTIVATION ENERGY (eV)	EMISSION SECTION (cm^2)
HL3	0.56	$\sigma_{pa} = 1.4 \times 10^{-15}$
Boron defect	0.52	$\sigma_{pa} = 1.7 \times 10^{-14}$ $\sigma_{na} = 1.3 \times 10^{-13}$
HB5 or HL5	0.42	$\sigma_{pa} = 2.2 \times 10^{-13}$
HL7	0.36	$\sigma_{pa} = 5.6 \times 10^{-13}$
HL12	0.27	$\sigma_{pa} = 3.8 \times 10^{-15}$
EL17	0.22	$\sigma_{na} = 1.5 \times 10^{-14}$
EL10	0.18	$\sigma_{na} = 1.5 \times 10^{-15}$

Table 3 Activation energies and emission sections for the deep levels seen in this study.

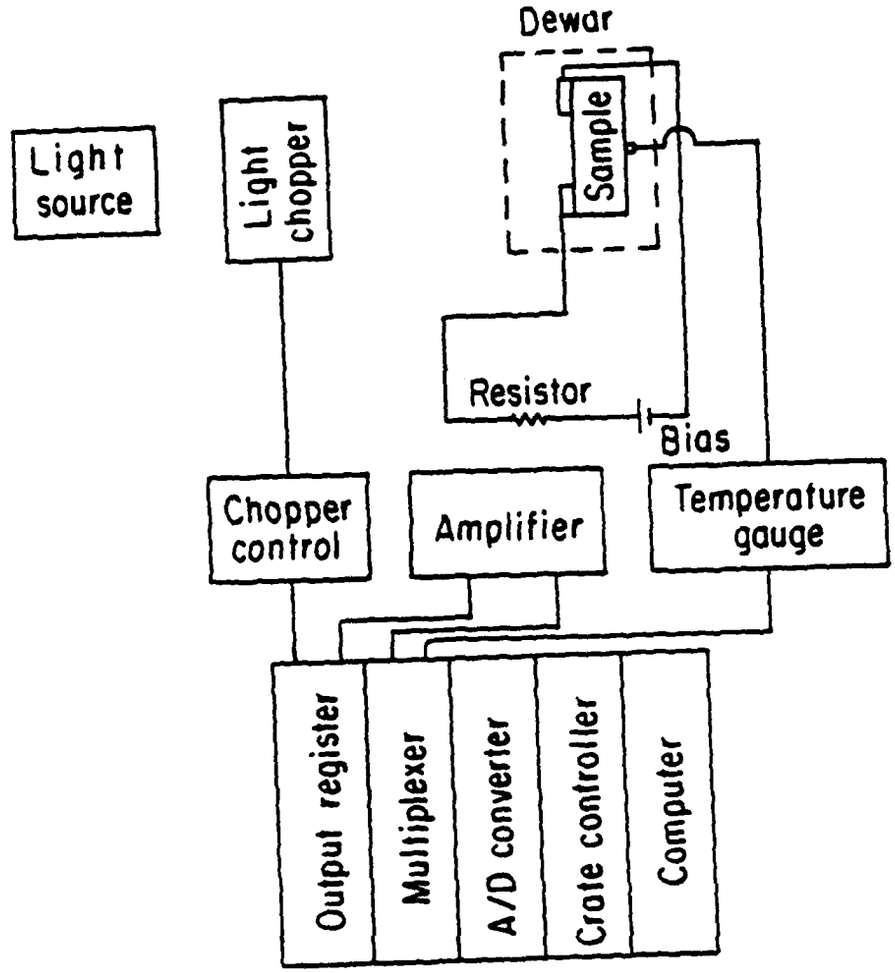
Dewar
Light source
Light chopper
Sample
Resistor
Bias
Chopper control
Amplifier
Temperature gauge
Output register
Multiplexer
A/D converter
Crate controller
Computer

Fig. 1

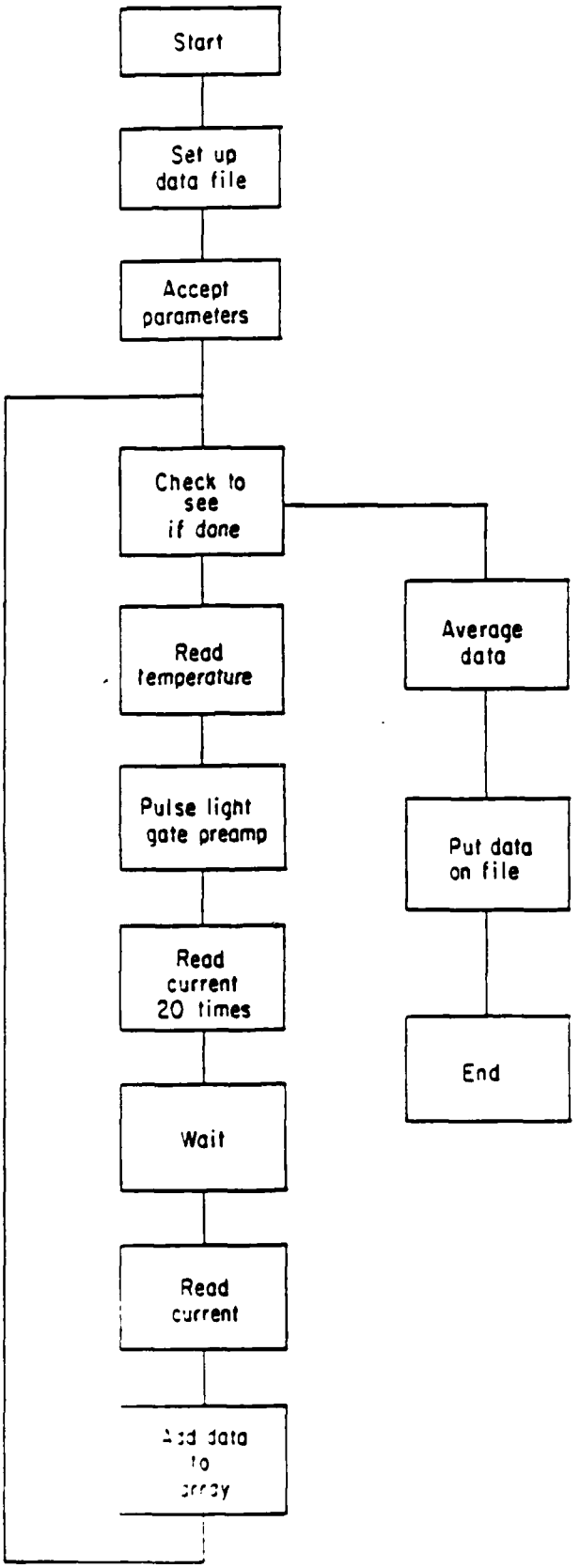
Start
Set up data file
Accept parameters
Check to see if done
Read temperature
Pulse light gate preamp
Read current 20 times
Wait
Read current
Add data to array
Average data
Put data on file
End

Fig. 2

Log ($T_m^2 t$)
10^4
10^3
10^2
3
5
7
9
1/T (x10^{-3}°K)
0.56ev
0.52ev
0.42ev
0.36ev
0.27ev
0.22ev
0.18ev

Fig. 3

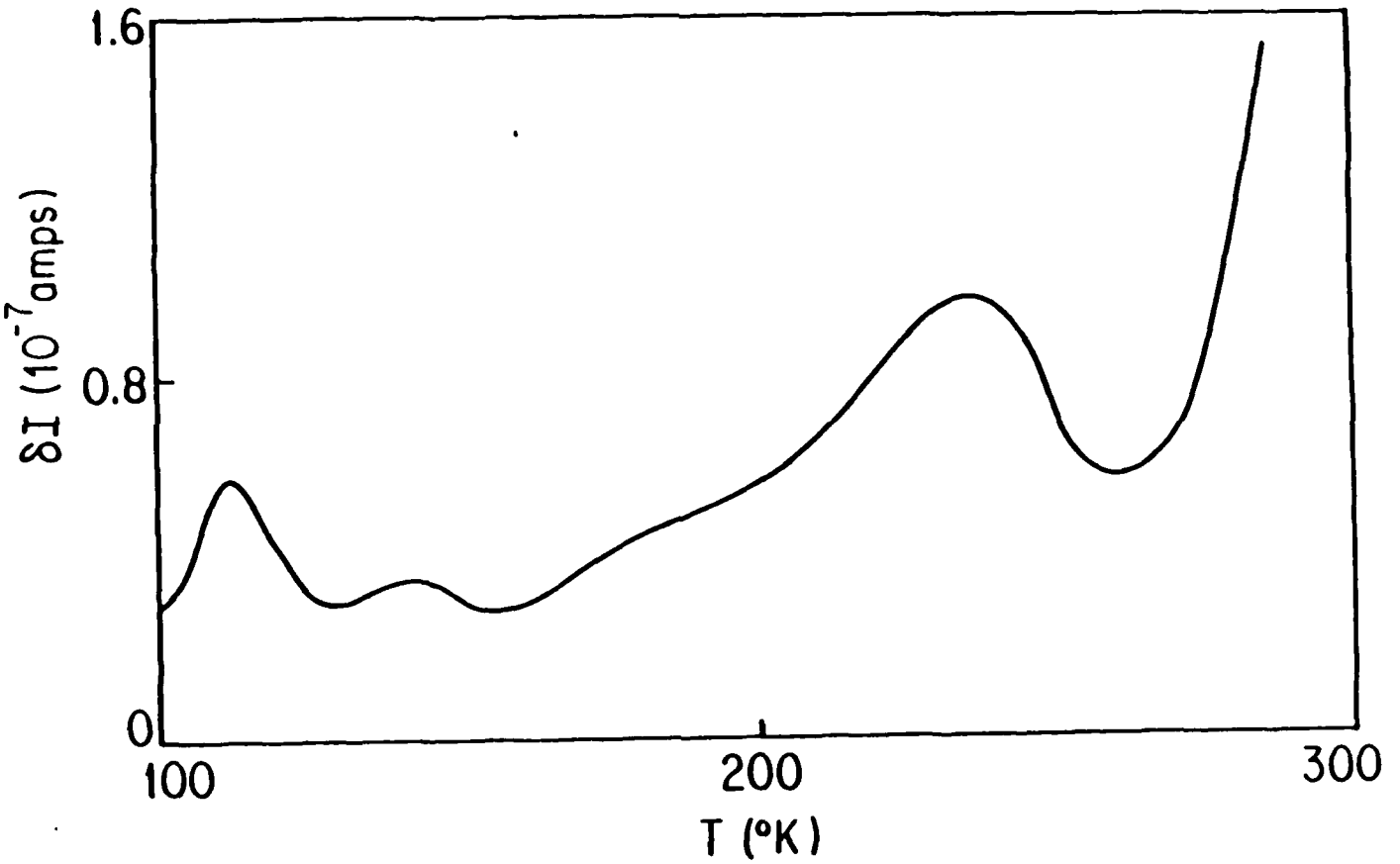
1.6
0.8
0
δI (10^{-7} amps)
100
200
300
T (°K)

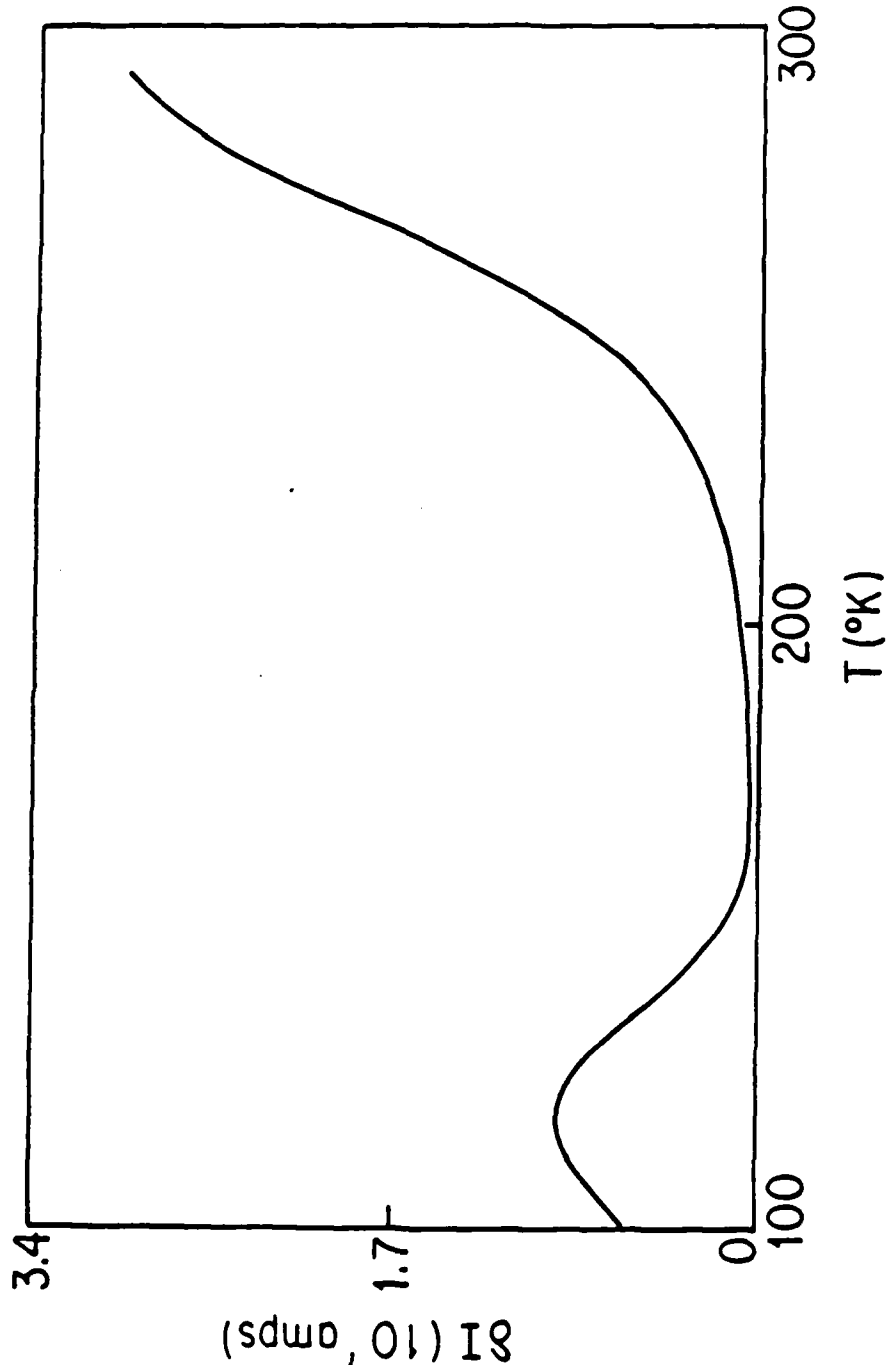

Fig. 5

END

11-86

DTIC